156p

H-6

N63-14679
Code 1

OTS PRICE

XEROX $ 11.50 ph

MICROFILM $ 4.88 mf

MISSILES and SPACE DIVISION

3-17-62-1

Final Report:

A STUDY OF INTERPLANETARY TRANSPORTATION SYSTEMS

2 June 1962

Work carried out under Contract NAS 8-2469

Prepared for
George C. Marshall Space Flight Center
Huntsville, Alabama

LOCKHEED MISSILES & SPACE COMPANY
A Group Division of Lockheed Aircraft Corporation
Sunnyvale, California

FOREWORD

This volume contains a series of investigations covering five areas of current importance in the planning of manned interplanetary missions. Although these studies are closely related to one another, and oriented toward the main problem of flight trajectory selection, each of the sections is self-contained, and may be read separately from the others. While none of the subjects is considered to be closed, it is nevertheless hoped that the material presented herein may be of use in understanding the basic physical concepts involved in scheduling these flights.

Contributors to the present volume were:

S. Ross, Project Leader
N. C. Adams
J. V. Breakwell
R. W. Gillespie
M. A. Krop
D. McKellar
H. F. Michielsen
J. L. Schroedter
L. D. Simmons
Z. A. Taulbee

CONTENTS

Section		Page
4	PRECISE CALCULATIONS AND THE INVESTIGATION OF GUIDANCE SENSITIVITIES	4-1
	4.1 Introduction	4-1
	4.2 Computer Programs	4-2
	4.3 Target-Seeking Techniques	4-3
	4.4 Illustrative Example of Earth-to-Mars Trajectory	4-5
	4.5 Illustrative Example of Venus Nonstop Round Trip Trajectory	4-6
	4.6 Interplanetary Trajectory Program	4-7
	4.7 References	4-10
5	NONSTOP TRIPS PASSING BOTH MARS AND VENUS: THE INTERPLANETARY GRAND TOURS	5-1

ILLUSTRATIONS

Section 1
NONSTOP INTERPLANETARY ROUND TRIPS

1.1 PHILOSOPHY OF APPROACH

The employment of nonstop round trips for early manned or instrumented planetary reconnaissance flights introduces many especially attractive mission possibilities. These trajectories are represented by Sun-centered, free-flight orbits which begin and end at the Earth, and pass near the target planet during the course of each journey. Study shows that many such flights appear feasible, for which the total velocity requirements represent only modest additional fuel penalties beyond those usually quoted for "minimum-energy," one-way trips, while the compensating advantages of short communication distances and capsule recovery possibilities render these round trips worthy indeed of careful consideration.

Using the technique outlined in Ref. 1-1, an orderly method of approach to the study of such missions is described, affording the analyst not only a qualitative insight into the general nature of the solutions, but also a guarantee that all possible classes of round-trip flights are taken into account in the analysis.

The method proceeds by increasing stages of complexity. For preliminary purposes, the planets are first assumed to be traveling in coplanar circles about the Sun. The dynamical model is thereby rendered strictly periodic, permitting convenient generalizations to be drawn for all qualitative phenomena characterizing these trips. A modified form of Lambert's Theorem (Ref. 1-2) is applied to the present study by incorporating the relationship between transfer angle and trip time for each mission.

By the proof outlined in Ref. 1-2, this stipulation of both transfer angle and trip time immediately determines the precise number of orbital solutions which can fulfill the specified mission. All possible families of Keplerian round-trip orbits are thus categorically produced and graphically displayed. The output data are studied at length, noting for further investigation the promising areas of solutions, while less feasible groups of orbits may be summarily rejected.

These solutions are to be regarded as nominal orbits, idealized in the sense that planetary perturbations during the encounter phases have thus far been neglected. By then extending the analysis to include gravitational effects resulting from close-approach maneuvers, many neighboring groups of solutions are introduced, all of which may be interpreted as having evolved from the nominal orbit families through a process of continuous perturbation, considering the periplanet distance as the generating parameter. In this intermediate phase of the study, the circular coplanar model is still retained for the planetary motions so that the close-approach effects may be isolated from additional complications due to planetary orbit inclinations and eccentricities. Although the absolute values of the numerical results obtained may therefore be subject to possible inaccuracies (especially for some trips past Mars, whose orbit eccentricity is comparatively large), nevertheless the relative effects will remain valid. Since the planetary geometry remains periodic, the results from this phase of the study retain their generality. The qualitative phenomena may be thoroughly explored and further undesirable areas eliminated from future consideration.

Finally, after cases of interest have been located by the method described above, the cases still remaining may be subjected to refinement by the adoption of a more realistic model for the planetary motions, which accounts for their orbital eccentricities and inclinations. We expect the data for this more sophisticated analysis to lie reasonably near those predicted by the

preliminary study. Accordingly, the three-dimensional, one-way trip tables computed in connection with the studies of Ref. 1-2 are searched near the dates indicated, and the proper pairs of one-way orbits thus found are joined to fabricate the more accurate round-trip estimates. Where desired, these latter data may be used to form the basis for precise calculations in advanced vehicle navigation and guidance studies, employing highly accurate numerical integration procedures.

1.2 GENERAL DISCUSSION

The idealized study of nonstop round trips seems to divide itself naturally into consideration of the two basic orbit types illustrated in Fig. 1-1.

Nonsymmetric trips leave and encounter the Earth at times when it occupies one and the same position in space. Such journeys are thereby limited to Sun-centered missions whose flight durations span integral numbers of years. The probe may circle the Sun several times before the planetary encounter; further, it may circle the Sun several more times before returning to Earth.

Vehicles on the symmetric trips return to Earth in fractions of complete years. By geometrical considerations it can be seen that the transfer orbit's major axis must bisect the angle formed by the Earth's position vectors at the times of departure and arrival. Also, from considerations of symmetry it is evident that at the halfway point of each symmetric trip, the Earth, Sun, and vehicle are always in strict alignment. Each symmetric orbit will, in actual practice, require a midcourse plane change to achieve rendezvous at the points of departure, encounter, and arrival, since these points are normally noncoplanar with the Sun.

The nonsymmetric round trips, however, require no such corrections, since the departure and arrival points coincide. In these cases, the orbit plane

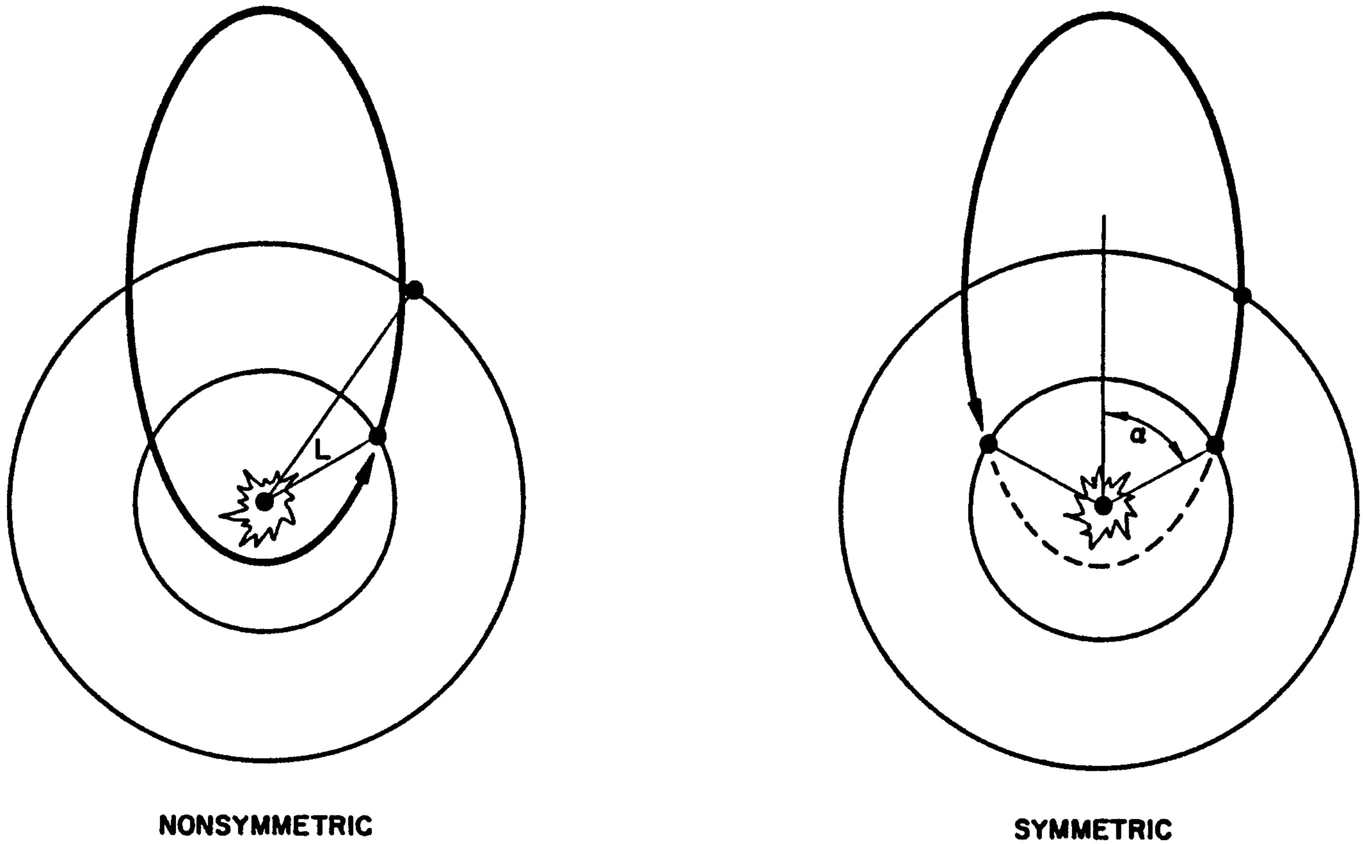

Fig. 1-1 Types of Nonstop Round-Trip Orbits

must contain only three distinct points, Sun, Earth, and planet, which is always possible.

For any orbit-plane changes which may be required in practical cases, either an impulsive velocity correction may be applied, or else a close approach to the planet may be utilized to modify the local asymtote direction. In fact, combinations of both types of maneuvers may be incorporated into trips which involve planetary reconnaissance operations as mission objectives.

Although total trip times exceeding 2 years appear most unsuitable for serious practical study, it is perhaps instructive, from a heuristic point of view, to enlarge the scope of this preliminary survey to encompass journeys of up to, say, 4 years' duration. Included in the study are not only all orbits whose periods are integral numbers of years, but also those orbits having periods expressible as rational fractions whose numerators do not exceed the maximum trip time under consideration. Thus, on an orbit whose period is expressible as p/m years, a vehicle will negotiate m complete solar circuits in p years.

For missions past Mars, the aphelion distance $r_A = a(1 + e)$ must never fall short of 1.52369 AU, Mars' orbital radius. From this we infer that

$$2 P^{2/3} > P^{2/3} (1 + e) > 1.52369$$

or

$$P > 0.664 \text{ yrs}$$

That is, no orbit whose period is less then 0.664 years will ever reach Mars' orbit.

Similarly, for trips past Venus, the vehicle's aphelion distance must never fall short of Earth's orbital radius of 1.0 AU. For this case, $P > 0.354$ defines the lower limit for this class of orbits.

1.3 NONSYMMETRIC ROUND TRIPS

These trips, whose durations are expressible as integral numbers of years, are quite easily calculable, even by hand. Given an orbit period of P years, then the quantity $a = P^{2/3}$ specifies a semimajor axis length in AU. Corresponding to this value of a, a complete set of orbits may be generated by considering various values of eccentricity. Actually, any other quantity independent of a may be employed as the generator for each class of P-year orbits. In particular, let us choose L, the heliocentric angle swept out by the probe while travelling from Earth to the planet. (See Fig. 1-1.) Then s, the semiperimeter of the triangle whose vertices are occupied by the Sun, the Earth at the departure date, and the planet at the pass date, is readily found. Using $E = -s/2a$, the form of Lambert's theorem described in Ref. 1-2* is employed to find T, the modified first-leg trip time:

$$T = (-E)^{-3/2} \left[2m\pi + (f - \sin f) - (g - \sin g) \right] \tag{1.1}$$

where

$$\sin^2 \frac{f}{2} = -E$$

$$\sin^2 \frac{g}{2} = -E \left(1 - \frac{c}{s} \right)$$

m represents the number of complete orbital circuits traversed before the planetary encounter, and c is the chord connecting Earth at the departure

*Ref. 1-2 discusses the various subcases of Eq. (1.1).

date with the planet on the pass date. The actual first-leg trip time Δt is then obtained from the relation

$$\Delta t = \frac{T}{n}\left(\frac{s}{2}\right)^{3/2}$$

where n is the Earth's mean motion [see Ref. 1-2, Eq. (A-2)].

The time Δt having been found, it merely remains to calculate the launch date, D_o, measured from the time of planetary alignment, using the expression

$$D_o = \frac{N\Delta t - L}{n - N} \tag{1.2}$$

where N is the mean motion of the pass planet. Complete information concerning the orbital parameters and the relative velocities involved at each terminal may now be derived using the equations cited in the Appendix of Ref. 1-2.* Strictly speading, the above calculation for D_o is dispensable. A simple alternate determination of the departure date, useful in hand calculations, may be pursued as follows: It has been remarked in Ref. 1-2 that any line having a slope of $(n/N)-1$ represents an infinitude of constant-angle transfers between the two planets. A preliminary grid of parallel lines having this common slope may be drawn on the $(D_o, \Delta t)$ plane; the angle L associated with any particular line may be obtained by noting D_o^*, the date at which a given line intersects the x-axis, and writing $L = (n - N) D_o^*$. Now, if the angle L is used as the orbit-generating parameter in the manner described above, then a knowledge of any particular pair $(L, \Delta t)$ will suffice to locate that orbit on the graph.

*See Fig. A-2 of Ref. 1-2.

The heliocentric departure speed V_1 for any mission is given by

$$V_1 = \sqrt{2 - \frac{1}{a}}$$

where a is the semimajor axis of the transfer orbit. For each family of constant-period trips, therefore, V_1 remains unchanged, since $a = P^{2/3}$ is also constant. Further, ν_1, the hyperbolic excess departure speed from Earth, is given by

$$\nu_1 = \sqrt{\left[V_1 \sin\psi_1 - 1\right]^2 + \left[V_1 \cos\psi_1\right]^2}$$

where ψ_1 is the heliocentric departure angle, measured clockwise from the Sun-to-Earth radius vector at the time of departure. Then it follows from inspection that $\left(\psi_1\right)_{max} \leq \pi/2$ minimizes not only ν_1, the hyperbolic excess departure speed, but also ν_2, the return speed, by symmetry. That is, for any family of constant-period, nonsymmetric round trips, the trajectory most economical of fuel is that one which leaves most nearly tangent to the Earth's orbit.

In Figs. 1-2 and 1-3, dashed-line contours of constant orbital period are plotted for all nonsymmetric round-trip missions passing Venus and Mars, respectively, on which the associated total trip times do not exceed 4 years. These curves are overlaid on the contours of constant hyperbolic excess departure speeds described in Ref. 1-2.* In one figure, therefore, the analyst may infer all of the following quantities of preliminary interest: departure date, first-leg trip time, total trip time, date of passage,** departure speed, and return speed to Earth, the latter being equal in magnitude to the departure speed, by symmetry.

*Only first-circuit passages have been recorded in the figures.

**Pass a straight line having slope -1.0 through any point on the graph. The place at which it crosses the x-axis is the date of planetary passage (Ref. 1-2).

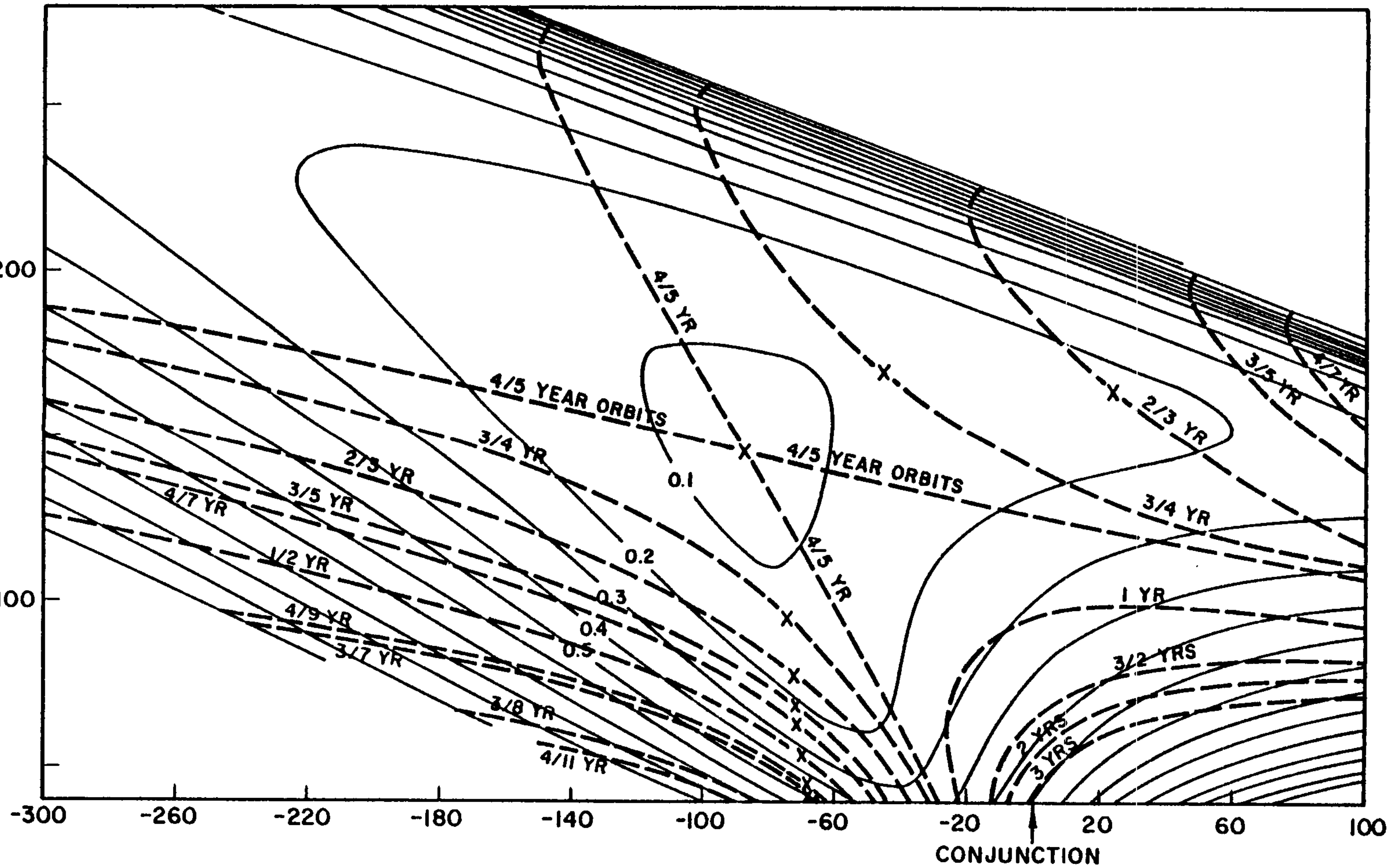

Fig. 1-2 Nonsymmetric Round Trips Past Venus, Overlaid on Contours of Constant Hyperbolic Excess Departure Speed

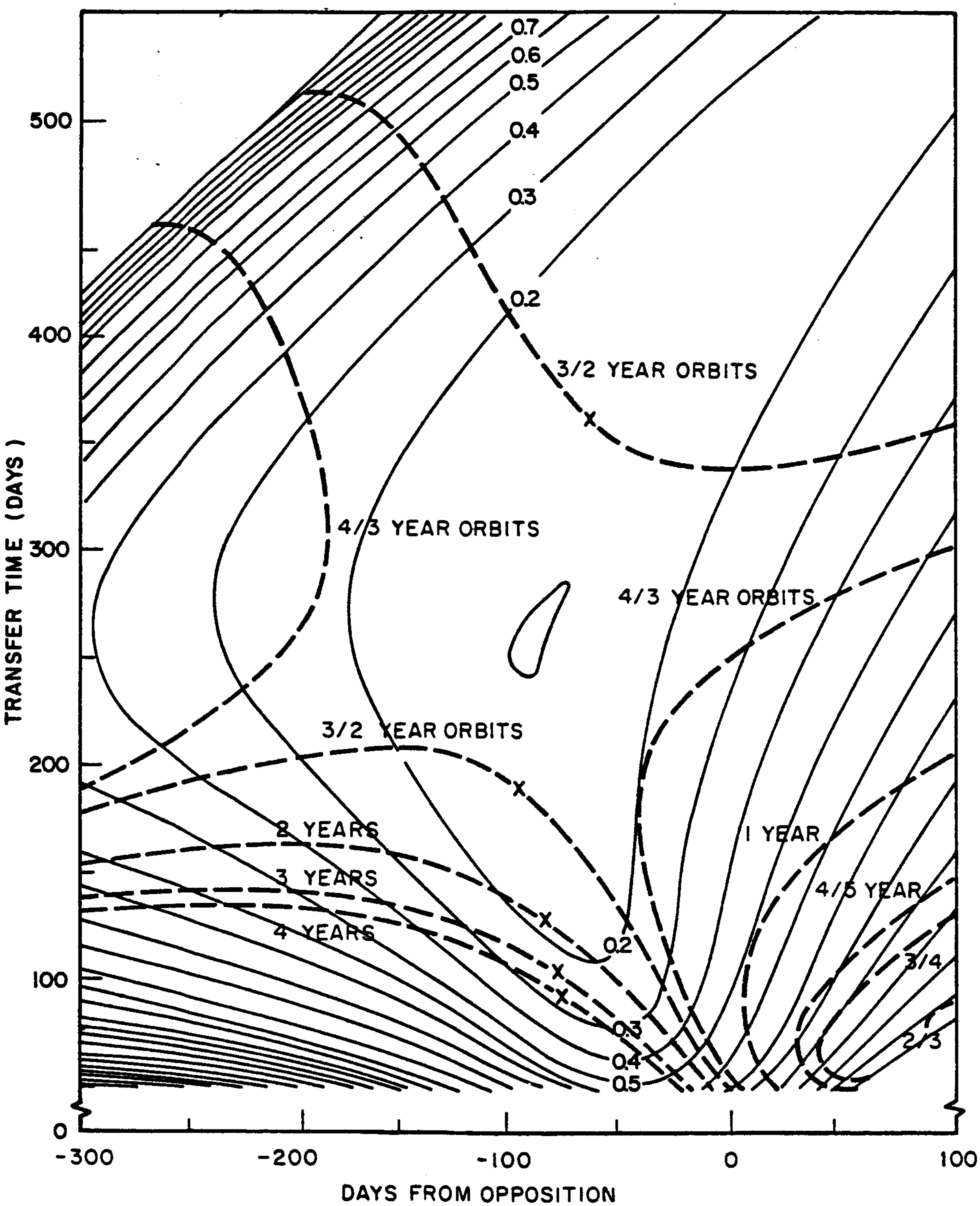

Fig. 1-3 Nonsymmetric Round Trips Past Mars, Overlaid on Contours of Constant Hyperbolic Excess Departure Speed

The time for a Hohmann round trip to Venus is almost exactly 4/5 year (i.e., the vehicle executes five circuits in 4 years). Contours for all nominal orbits having this period may be observed to subdivide Fig. 1-2 into four principal quadrants. These Hohmann contours serve as separatrices between those orbits having periods exceeding 4/5 year, which recede downward to the right and upward to the left from the Hohmann point, and those orbits having periods of less than 4/5 year, which recede into the remaining two quadrants.

For orbits having greater than 4/5-year periods, only the inbound Venusian intercepts fall within the scope of Fig. 1-2. However, analogous considerations apply to trips past Mars, for which curves are visible in Fig. 1-3 representing intercepts on both outbound and inbound phases of the missions.

1.4 SYMMETRIC ROUND TRIPS

Symmetric orbits may also be obtained by employing Eq. (1.1). In this case, however, Lambert's Equation must be inverted for the solution, and the use of a digital computer is dictated. To ensure contact with the Earth at the trip's conclusion, the total mission duration must be written as $\Delta t = 2(p\pi + \alpha)$, where 2α is the total transfer angle, mod (2π), from start to finish of the mission and p represents the number of complete years involved in the trip. Furthermore, the semiperimeter s, in the triangle formed by the Earth's positions at both the start and conclusion of the mission, and the Sun,* is equal to $1 + \sin\alpha$. Then Eq. (1.1) assumes the form:

$$\frac{2(p\pi + \alpha)}{\left(\frac{1 + \sin\alpha}{2}\right)^{3/2}} = (-E)^{-3/2}\left[m\pi + (f - \sin f) - (g - \sin g)\right] \quad (1.3)$$

*Note that the basic Lambert triangles for the symmetric cases are not the same as those for the nonsymmetric cases.

the nomenclature being that of Eq. (1.1). Here, we have the additional relationship $c = 2 \sin\alpha$, from Fig. 1-1, for the chord length between the Earth's positions on the two dates considered.

Given values for p, the number of complete years elapsing, and m, the number of complete circuits negotiated on the orbit, then a complete family of symmetric trips may be generated by allowing α to vary from 0 through π, and inverting Eq. (1.2) for E in each case. The remaining orbital parameters, as well as the relative velocities at each terminal, are again available from the formulas cited in Ref. 1.2.

Figures 1-4 and 1-5 summarize the results obtained by applying Lambert's Theorem to the study of symmetric flights passing Venus and Mars, respectively. Round trips identified by the points marked "X" in these figures pass through heliocentric angles which are integral multiples of 2π. For such trips, the symmetric round trips are identical with the nonsymmetric, and these points, therefore, are common to both sets of curves associated with a given planet.

1.5 RECIPROCITY PROPERTIES OF INTERPLANETARY ROUND TRIPS

From Eq. (1.2) we may immediately deduce the following useful theorem:

Theorem: If the planetary orbits are treated as coplanar circles, then for each and every round trip orbit (either nonstop or stopover), there always exists a reciprocal orbit for which the departure and arrival speeds are interchanged with those of the former, while the departure and arrival dates for the one are negatives of the interchanged values of the other, all dates being measured from the time of planetary alignment.

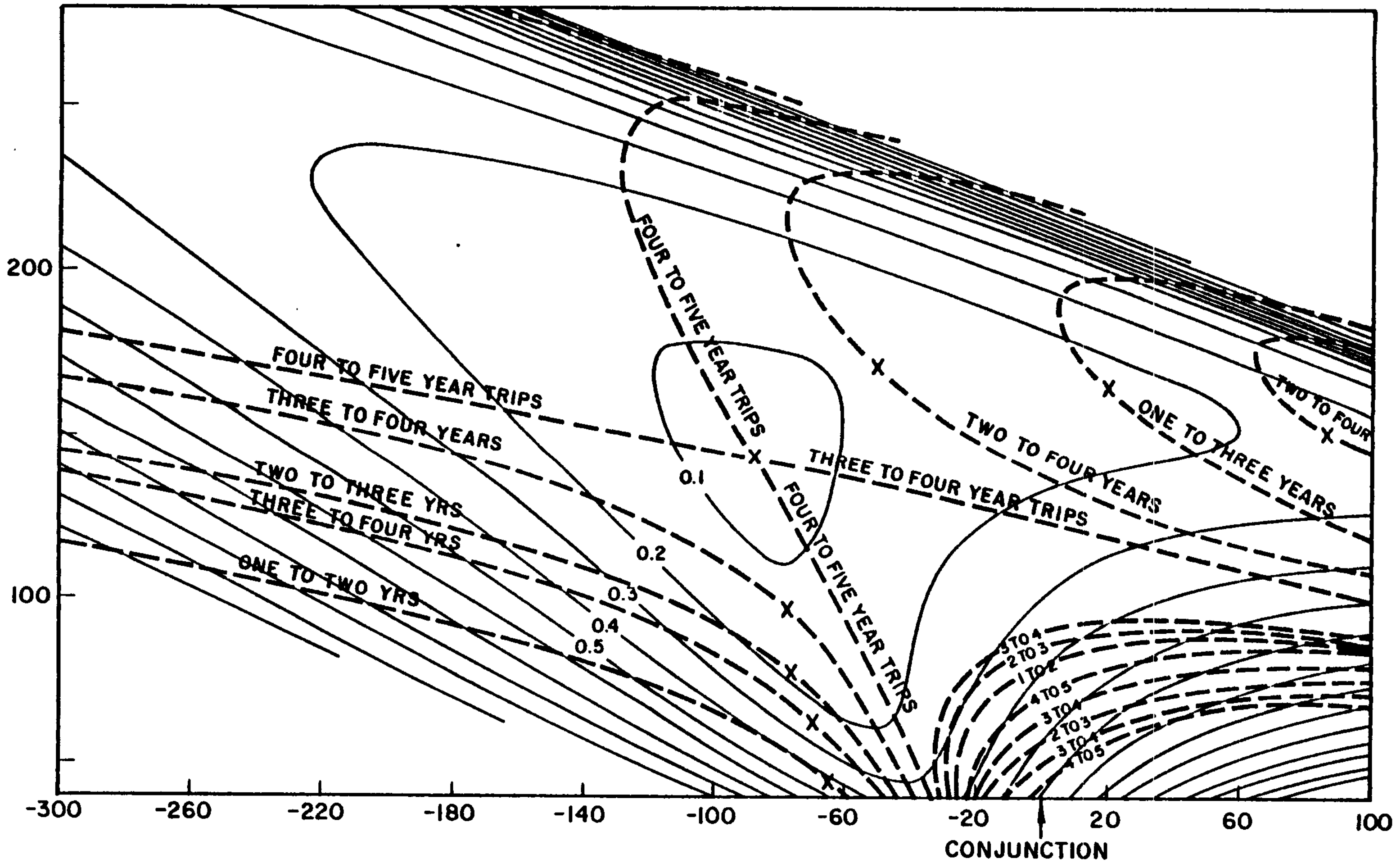

Fig. 1-4 Symmetric Round Trips Past Venus, Overlaid on Contours of Constant Hyperbolic Excess Departure Speed

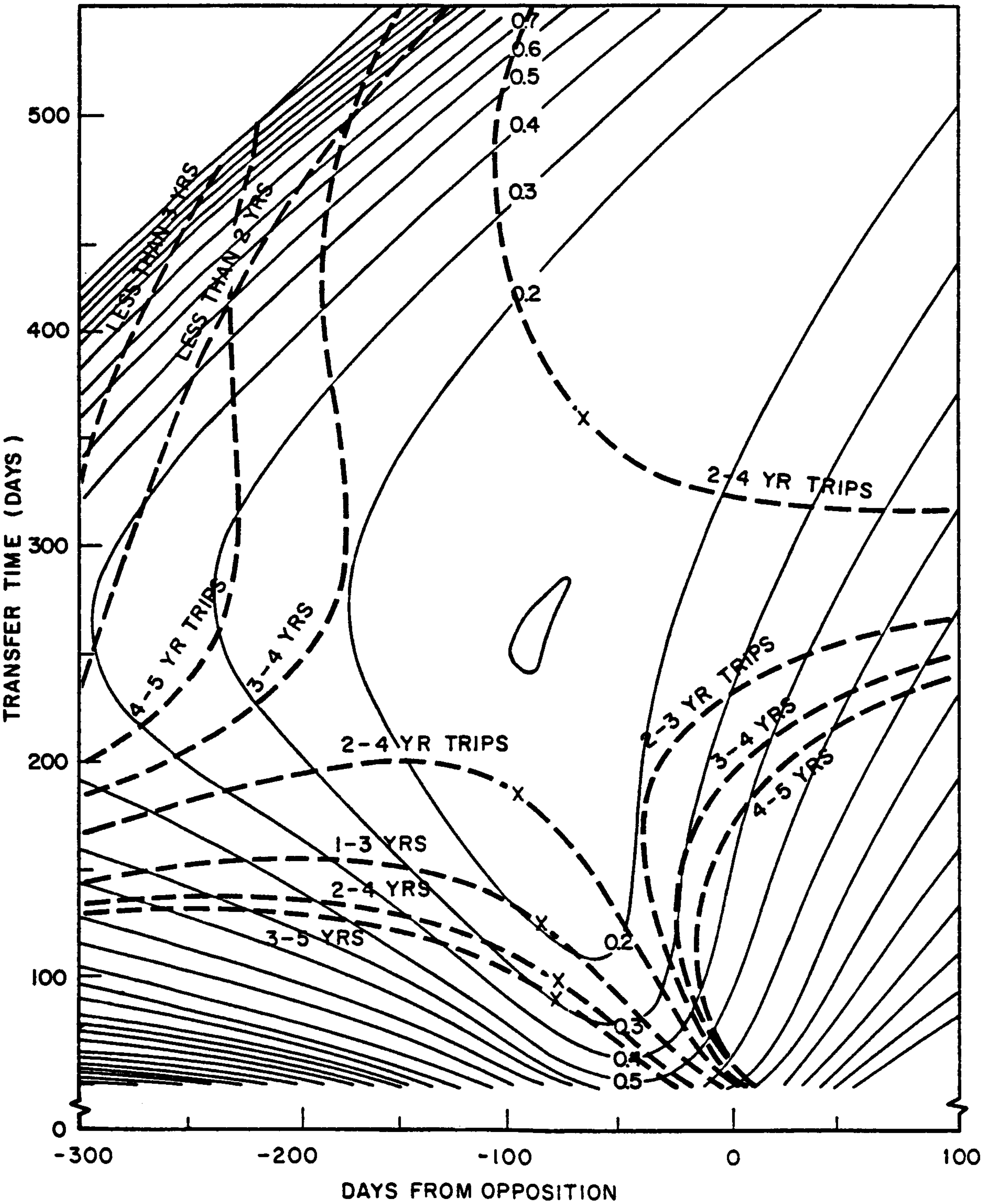

Fig. 1-5 Symmetric Round Trips Past Mars, Overlaid on Contours of Constant Hyperbolic Excess Departure Speed

Proof: (See Fig. 1-6). Let

L = first-leg trip angle
θ = total trip angle
Δt_1 = first-leg trip time
τ = stopover time ≥ 0
n = Earth's mean motion
N = pass planet's mean motion
D_o = launch date from Earth, measured from date of planetary alignment
D_1 = arrival date at Earth, measured from date of planetary alignment

From Eq. (1.2),

$$D_o = \frac{N \Delta t_1 - L}{n - N}$$

so that

$$D_1 = D_o + \Delta t_1 + \tau + \Delta t_2 = \frac{[\theta - (L + N\tau)] - N\Delta t_2}{n - N}$$

or

$$-D_1 = \frac{N \Delta t_2 - [\theta - (L + N\tau)]}{n - N} = \bar{D}_o \tag{1.4}$$

Thus, to perform a mission whose first-leg trip time is Δt_2 , and whose first-leg trip angle is $[\theta - (L + N\tau)]$, Eq. (1.4) shows $\bar{D}_o = -D_1$ to be the launch date for the trip. This new first-leg segment represents a reverse circuit of the original trip's final leg. Analogous arguments regarding the

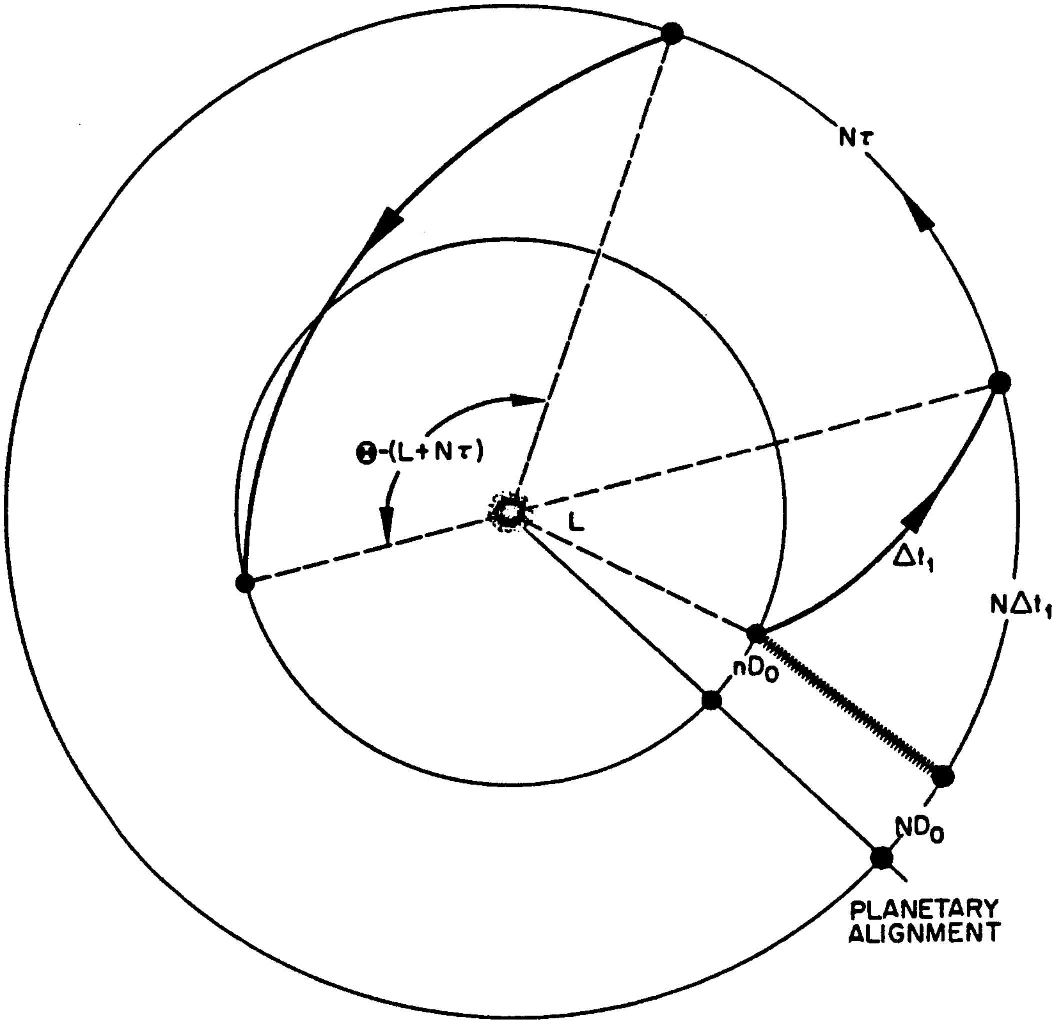

Fig. 1-6 Nomenclature for Reciprocity Theorem

other segments complete the remainder of the proof. Note that the interchange of dates and relative speeds occurs at the pass planet as well as the Earth, and that the entire proof remains valid even for nonstop trips which employ close planetary approaches.

The Theorem is of importance in locating attractive round trips in cases where orbits have been found for which high entry speeds at one end can profitably be interchanged with low departure speeds at the other end, or vice-versa.

In more realistic cases, which include planetary orbit eccentricity and inclination effects, we may be assured of finding almost-reciprocal solutions which exhibit the desired properties.

1.6 SELECTION OF ACCEPTABLE NOMINAL ORBIT FAMILIES

Strictly speaking, any one-way flight may also be considered a round trip, since it must eventually encounter the Earth again at some future time. The orbit analyst really seeks, however, the most acceptable flights whose durations do not exceed some maximum length. This upper limit having once been specified, Figs. 1-2 through 1-5 may be scanned to select, among all contours encompassing nominal trips of sufficient brevity, those segments which indicate favorable mission possibilities. Many of the areas shown will correspond to flights unacceptable under any circumstance; these may be disregarded forthwith, and primary emphasis shifted to the relatively limited trajectory groups remaining for further detailed study.

From Figs. 1-2 to 1-5, then, we immediately eliminate from consideration all nominal families which correspond to trip durations of over 2 years. This choice is dictated first by the desire for flights of reasonable length, especially in view of the ecology requirements for human occupants, and

second because such journeys may easily be negotiated, even under the most pessimistic assumptions of propulsion availability, during the next several years. Trips of longer span are therefore of questionable value, except for possible employment in special missions.

Five local regions remain to be considered as bona fide mission possibilities. General characteristics* of the nominal trips in these areas are summarized in Table 1-1.

For flights past Venus, we have the following regions:

(1) Nominally low-energy trips having durations of 2 years or more. Both symmetric and nonsymmetric groups exist, the former involving trips of 2 to 3 years, and the latter exactly 2 years. The vehicle executes between three and four solar circuits during each mission. Planetary passage may occur during either of two crossings of Venus' orbit on any of the three circuits, although only first-circuit passages are recorded in Figs. 1-2 and 1-4. Contours extend in both directions from the common points located at (-72, 78) and (+24, 164) in the figures. These points represent local departure and arrival velocity minima for the present orbit families. Perihelion distances occur nominally at about 0.5 AU, or less, a factor which must be evaluated in terms of heat and shielding requirements for human occupants as well as cargo. It appears fruitless to investigate this area much beyond the 0.2 speed contour since the 1-year family observed in the lower right-hand sector of the graphs will replace the present group at speeds in excess of 0.28.

*Attention is called to the fact that these nominal trips may in some cases undergo considerable modification through close-approach and/or propulsion maneuvers. However, Table 1-1 provides a heuristic introduction to the various possibilities available.

Table 1-1

FOUR BASIC CLASSES OF NOMINAL NONSTOP ROUND TRIPS
(All worthwhile flights of less than two years' duration are minor variants of these.)

Planet	Trip Type, Nominal Duration, and Time Reduction, if Feasible	Approximate Departure Date	Hyperbolic Excess Departure and Arrival Speed	First-Leg Travel Time	Date of Planetary Passage	Hyperbolic Excess Speed of Passage	Communication Distance to Earth During Pass	Heliocentric Direction of Approach to Pass Planet**	Time Spent in Pass Planet's Sphere of Influence***	Aphelion and Perihelion	Trip Time Reduction, Using Close Planetary Approach
VENUS	<u>Low Energy</u>: 2 years. A local minimum of both trip time and speed of departure	− 72 days from conjunction	0.176 EMOS* (4.3 km/sec)	78 days	+ 6 days from conjunction	0.364 EMOS (7.7 km/sec)	0.28 AU (42×10^6 km)	250°; Approach from dark side	53 hr	1.0 AU 0.53 AU	30 days
	<u>High Energy</u>: 1 year. Nonsymmetric trip family; no time reduction possible	− 24 days from conjunction	0.280 EMOS (6.0 km/sec)	75 days	+ 51 days from conjunction	0.160 EMOS (4.1 km/sec)	0.63 AU (94×10^6 km)	180°; Vehicle overtakes planet	115 hr	1.28 AU 0.72 AU	70 days
MARS	<u>Low Energy</u>: 2 years. As low as 875 days if launch speed is increased to 0.200	− 55 to − 85 days from opposition	0.177 to 0.200 EMOS (4.5 to 4.7 km/sec)	102 to 126 days	+ 42 to + 47 days from opposition	0.30 to 0.32 EMOS (6.3 km/sec)	0.70 AU (105×10^6 km)	155 to 160°; Approach from illuminated side	15 to 17 hr	2.38 AU 1.0 AU	30 to 60 days; order of magnitude
	<u>High Energy</u>: Favorable Opposition (e.g., 1970–2) 545 days, a local minimum	− 273 days from opposition	0.274 EMOS (5.9 km/sec)	273 days	0 days from opposition	0.12 EMOS (3.8 km/sec)	0.38 AU (57×10^6 km)	180°; Planet overtakes vehicle	41 hr	1.38 AU 0.79 AU	40 days
	Unfavorable Opposition (e.g., 1962–4) 570 days, a local minimum	− 285 days from opposition	0.464 EMOS (10.1 km/sec)	285 days	0 days from opposition	0.23 EMOS (5.1 km/sec)	0.67 AU (100×10^6 km)	180°; Planet overtakes vehicle	23 hr	1.67 AU 0.62 AU	40 days
	<u>Very High Energy</u> Favorable Opposition (e.g., 1969–70) 1 year. Nonsymmetric trip family; no time reduction possible	+ 4 days from opposition	0.391 EMOS (8.3 km/sec)	113 days	+ 117 days from opposition	0.202 EMOS (4.9 km/sec)	1.14 AU (170.5×10^6 km)	180°; Planet overtakes vehicle	24 hr	1.38 AU 0.62 AU	
	Unfavorable Opposition (e.g., 1960–1) 1 year. Nonsymmetric trip family; no time reduction possible	+ 22 days from opposition	0.713 EMOS (16.0 km/sec)	130 days	+ 152 days from opposition	0.327 EMOS (6.8 km/sec)	1.63 AU (244.0×10^6 km)	180°; Planet overtakes vehicle	17 hr	1.67 AU 0.33 AU	

*EMOS = Earth's Mean Orbital Speed. Numbers in parentheses refer to launch from 250 km circular orbit.
**Measured counterclockwise from planet's velocity vector.
***For definition of sphere of influence, see K. A. Ehricke, <u>Space Flight, Environment and Celestial Mechanics</u>, 1960, D. Van Nostrand & Co., Vol. 16, Table 3-16, pg. 121.

(2) Nominally high-energy trips, having durations of 1 year or more. Both symmetric and nonsymmetric groups exist, the former involving trips of 1 to 2 years, and the latter exactly 1 year. The vehicle executes between one and two solar circuits during each symmetric mission, and exactly one circuit during the nonsymmetric flights. Generally speaking, the nonsymmetric orbits of this group are preferable to the symmetric in respect to speed and duration. Minimum energy occurs at (-24, 75), the corresponding speed being 0.28; the reciprocal point (second crossing passage) which falls outside the scope of Fig. 1-2, may be found at (-341, 290), by the reciprocity theorem of Subsection 1.5. These orbits, as will be shown later, constitute the most important family of trajectories for missions past Venus.

For flights past Mars, we have the following regions:

(1) Nominally low-energy trips, having durations of 2 years or less. Both symmetric and nonsymmetric groups exist, the former involving trips of 1 to 3 years, and the latter 2 years. The vehicle executes exactly one circuit for the latter, and between zero and two complete circuits for the former. Contours in Figs. 1-3 and 1-5 extend in both directions from the common point at (-86, 126), and its reciprocal at (-140, 604); these points are local speed minima 0.177. Increased launch and arrival speeds associated with the symmetric trips to the right of the lower common point are compensated by shorter resulting trip times, as the total transfer angle is decreased from 2π. Conversely, for symmetric trips to the left of this point, both speeds and durations are increased since the central angle increases from 2π toward 4π. Inverse considerations apply to symmetric trips extending from the upper common point. Particular orbits from this group have been previously studied by a number of authors, including Sternfeld (Ref. 1-4), Vertregt (Ref. 1-5), and Battin (Ref. 1-6).

(2) Nominally high-energy trips, having durations of between 1 and 2 years, illustrated by the curve passing through (-279, 279). Only a symmetric group exists. This curve is self-reciprocal. Its orbits were first studied by Johnson and Smith (Ref. 1-6), and subsequently by Gedeon (Ref. 1-7). Along a brief segment of this contour, the hyperbolic excess launch velocity requirements reach values of below 0.4, experiencing a minimum at about 0.375 (15.7 km/sec equivalent surface launch speed); return velocities are equal, by symmetry. This group of trips is characterized by dates of passage near the planetary opposition, affording comparatively short communication distances.

Although the velocity requirements cited above at first seem to restrict such short flights to vehicles powered by nuclear or highly advanced chemical rockets, the situation is by no means so hopeless: This contour, it should be noted, refers to a family of orbits passing through total trip angles of between 360 and 720 deg. As the trip angle is decreased from 720 deg, the mission ellipses become less and less eccentric, and the departure (and arrival) speeds become correspondingly lower. When some critical value of trip angle (about 560 deg) is reached, the ellipses cease to reach the Mars orbital radius. For this critical value of trip angle, the launch velocity assumes its minimal value of 0.375, as was remarked earlier.

Now, since the mean value, and not the minimum value, of Mars' orbit was employed in the circular planetary orbit model, it becomes clear that there will occur, in practice, times for which the trip angle can be reduced beyond 560 deg, and for which the departure speed requirements, therefore, become somewhat more relaxed. For such cases, the hyperbolic excess speed can be reduced to as low as 0.274 (13.6 km/sec equivalent surface launch speed), a value quite within reason for moderately sophisticated chemical rockets. The next such opportunity occurs in the 1970 — 72 period, and repeats approximately each 15 to 17 years. Conversely, during

relatively poor periods (e.g., 1962 — 64), the minimum launch speed may climb to 0.484 (17.8 km/sec equivalent surface launch speed), rendering this class of trips difficult indeed to negotiate.

No such considerations apply to the low-energy nonsymmetric Mars trips discussed above, since these all extend well beyond the Mars orbital radius. Small adjustments in dates and speeds will, however, cause the low-energy results to differ slightly from one opposition period to the next.

(3) Nominally very high-energy trips, having durations of exactly one year, illustrated by the curve passing through (+13, 122) in Fig. 1-3. Only single circuit nonsymmetric trips exist. At (+13, 122) on which trip the vehicle's orbit reaches just to Mars, the launch hyperbolic and recovery speeds will be 0.55. During favorable opposition periods (e.g., 1969 — 70) this value will dip as low as 0.391. Considering that launch and recovery speeds will necessitate total mission Δv's in the 0.8 range, or greater, while stopover round trips of 330-day-total duration may be scheduled for Δv's in the 0.6 range (see Section 2), this group shows little promise and will be eliminated from further study at the present time.*

1.7 CLOSE-APPROACH MANEUVERS

Having located, in a coarse sense, the main areas of acceptable flights, it now remains to attempt modifications in trip time, terminal speeds, and various other factors by incorporating close approach manuevers** into the flight schedules. These manuevers will no doubt be desirable in most cases

*Even with a close-approach maneuver at Mars, it does not appear that the situation can be much improved.

**The guidance impulse requirements necessary to properly orient the pass hyperbola at the planet are assumed to be insignificant for present planning purposes.

for the performance of reconnaissance operations. In Figs. 1-7 through 1-11, each of the four remaining areas of interest is displayed on a magnified scale, with contours of constant approach distance clearly shown. Since the nominal flights were assumed to be completely unperturbed, the curves of Figs. 1-2 through 1-5 are depicted in the present figures as contours of infinite passage distance.

The close-approach analysis is performed by comparing separate one-way trips to and from each planet, evaluated on a grid of dates in the neighborhood of the nominal flights, still retaining the circular coplanar planetary orbit geometry. By noting the planetary right ascensions and declinations of the vehicle approaching and receding from the pass planet, the asymptote deflection angle can be calculated quite easily, using spherical trigonometry. If we call this deflection angle K , then the periapsis distance of the pass hyperbola is readily shown to be (Ref. 1-4)

$$r_p \text{ (AU)} = \frac{m}{m_\odot}\left[\frac{\csc\frac{K}{2} - 1}{\nu_\infty^2}\right]$$

where $m/m_\odot$ is the pass planet's mass in solar units, and ν_∞ is the hyperbolic excess speed of the pass hyperbola (unchanged by the close-approach maneuver) expressed in EMOS units.

If this calculation is performed for all one-way trip pairs whose relative speeds at the pass planet match exactly, then it is a simple matter to obtain the graphical results shown.

In Fig. 1-7, the region of nonsymmetric low-energy Venus flights described above is presented in detail, with curves of constant approach distance at Venus overlaid on the contours of constant departure speed from Earth.

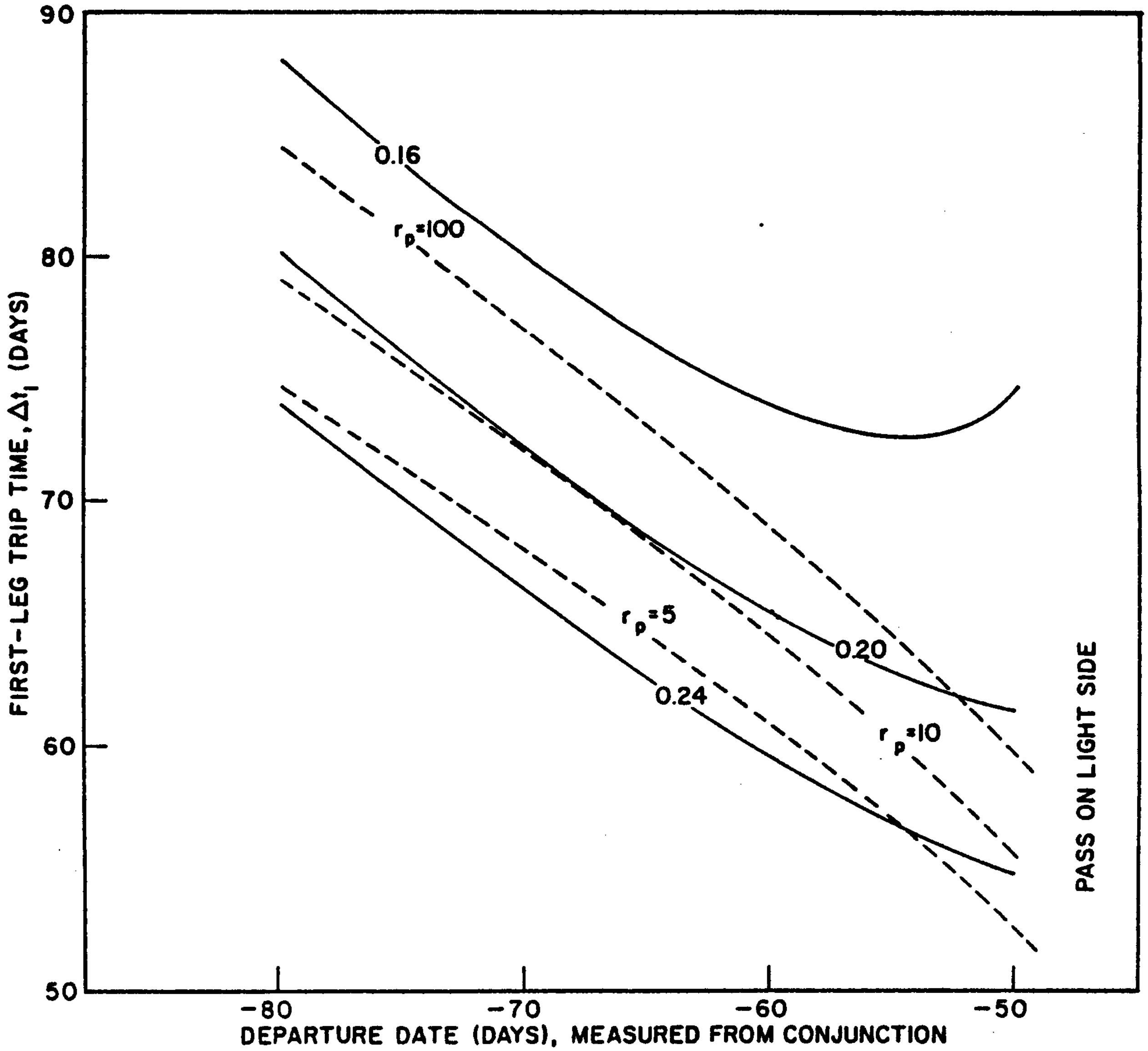

Fig. 1-7 Modified Low-Energy Nonsymmetric Trips Past Venus, Contours of Constant Periplanet Distance, r_p, in Planetary Radii

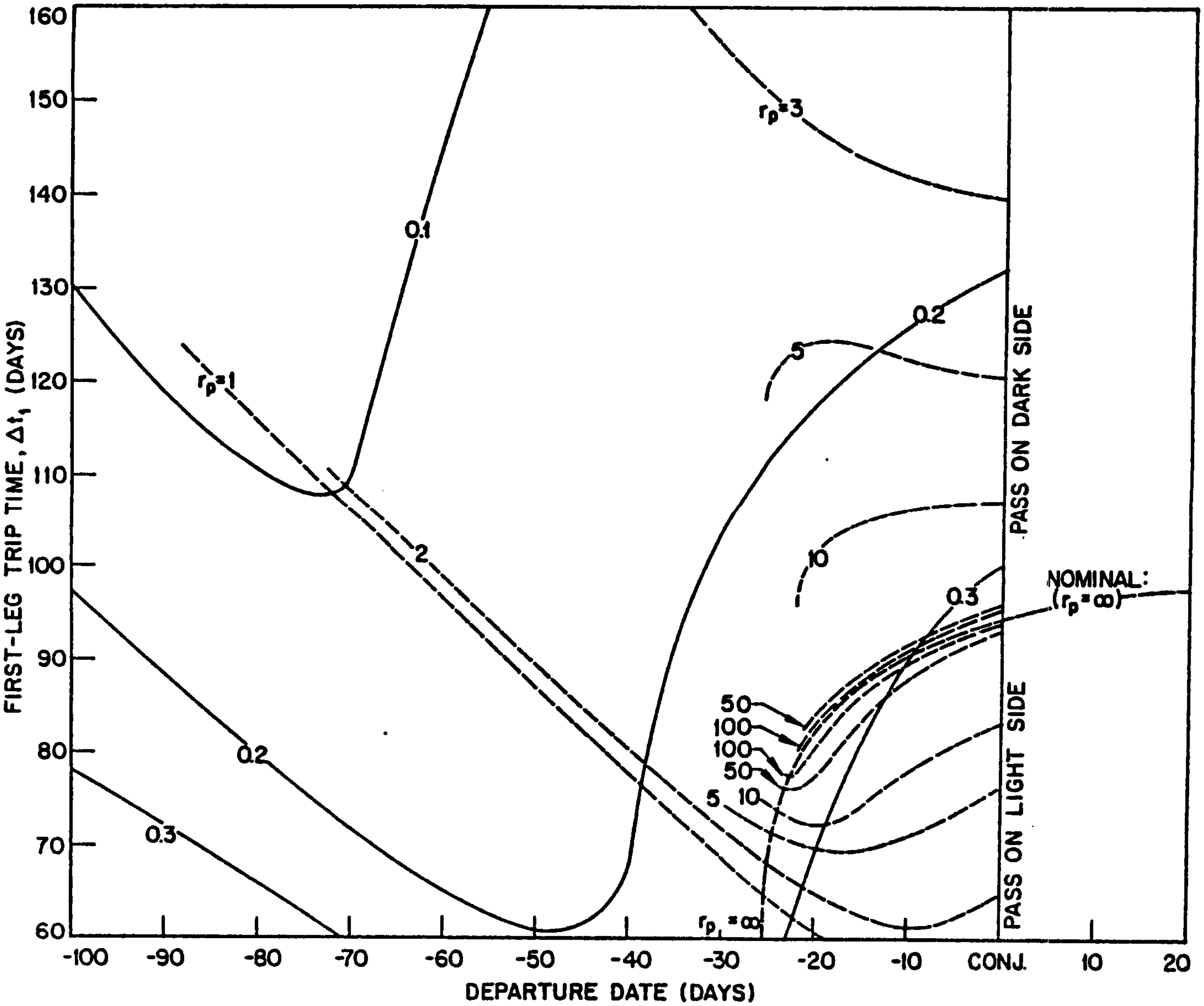

Fig. 1-8 Modified High-Energy Nonsymmetric Trips Past Venus, Contours of Constant Periplanet Distance, r_p, in Planetary Radii

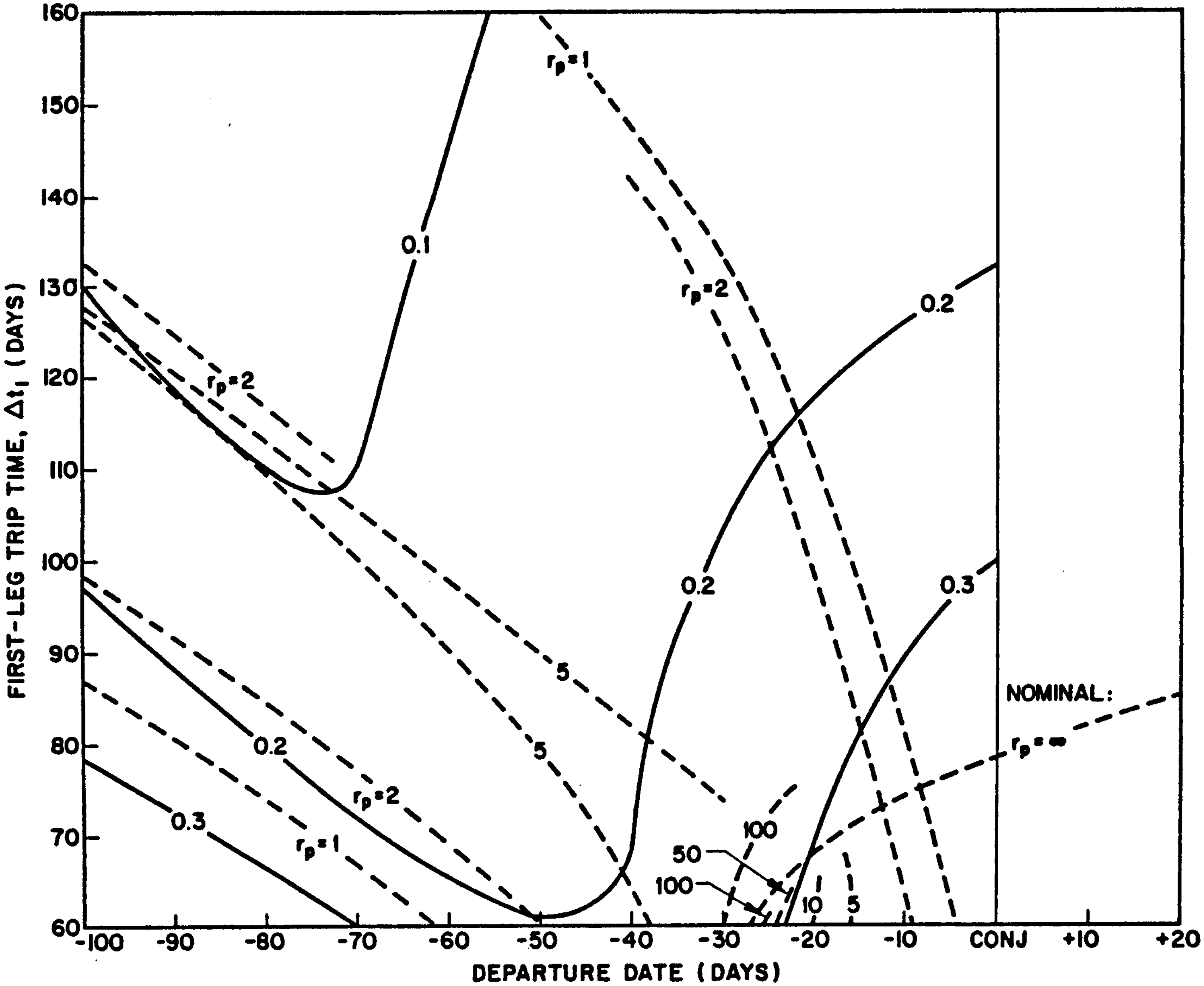

Fig. 1-9 Modified High-Energy Symmetric Trips Past Venus, Contours of Constant Periplanet Distance, r_p, in Planetary Radii

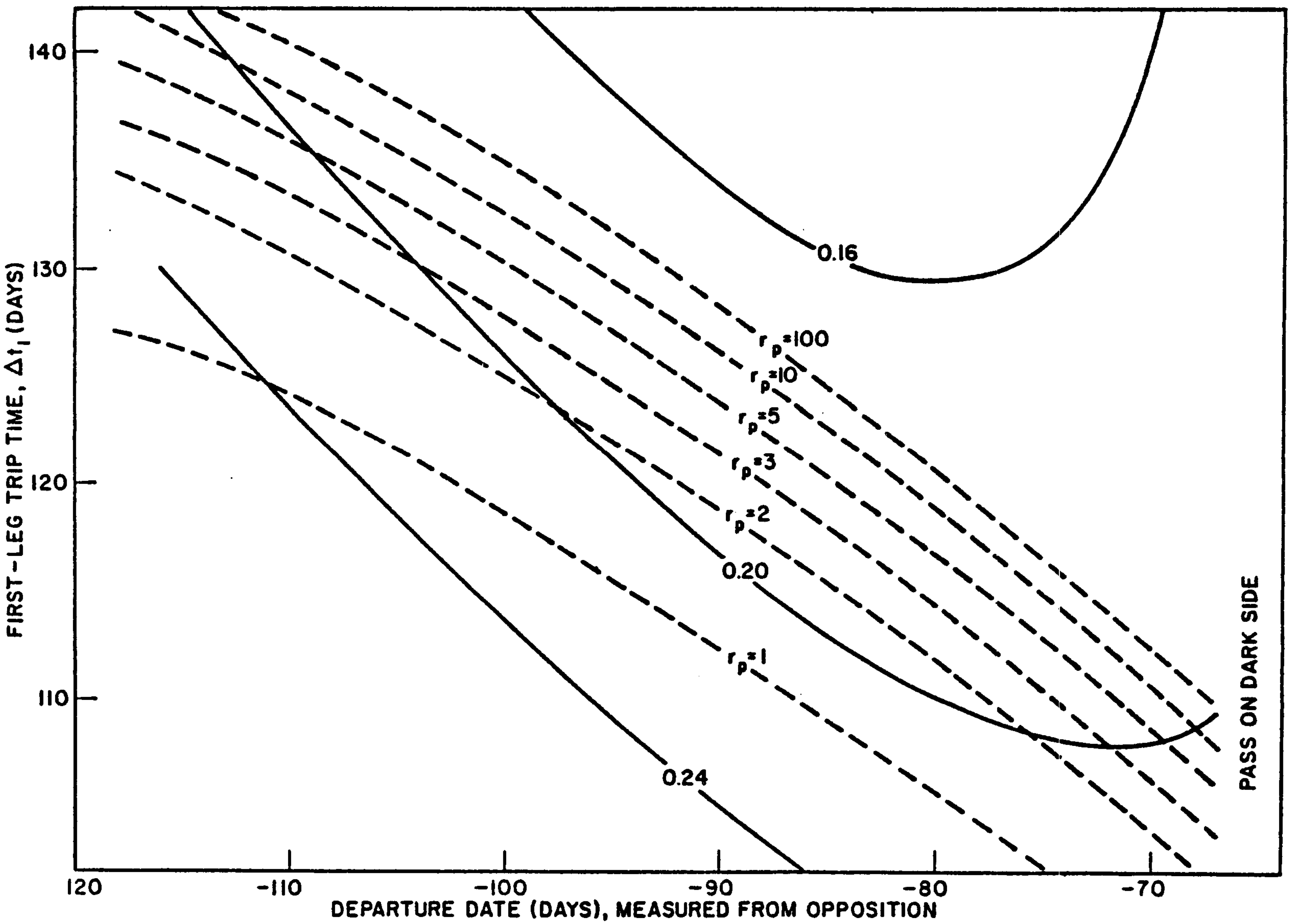

Fig. 1-10 Modified Low-Energy Symmetric Trips Past Mars, Contours of Constant Periplanet Distance, r_p, in Planetary Radii

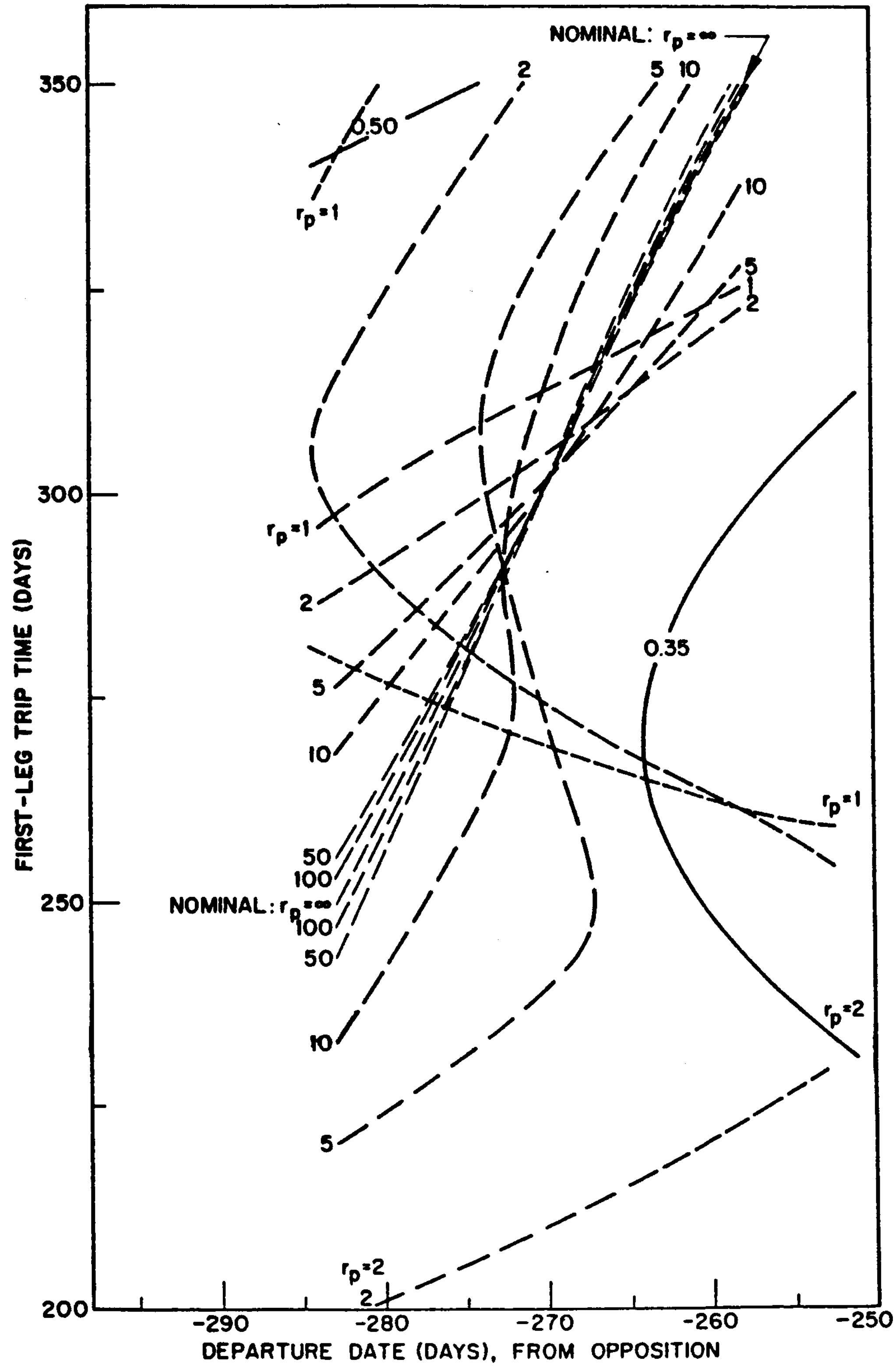

Fig. 1-11 Modified High-Energy Symmetric Trip Past Mars, Contours of Constant Periplanet Distance, r_p, in Planetary Radii

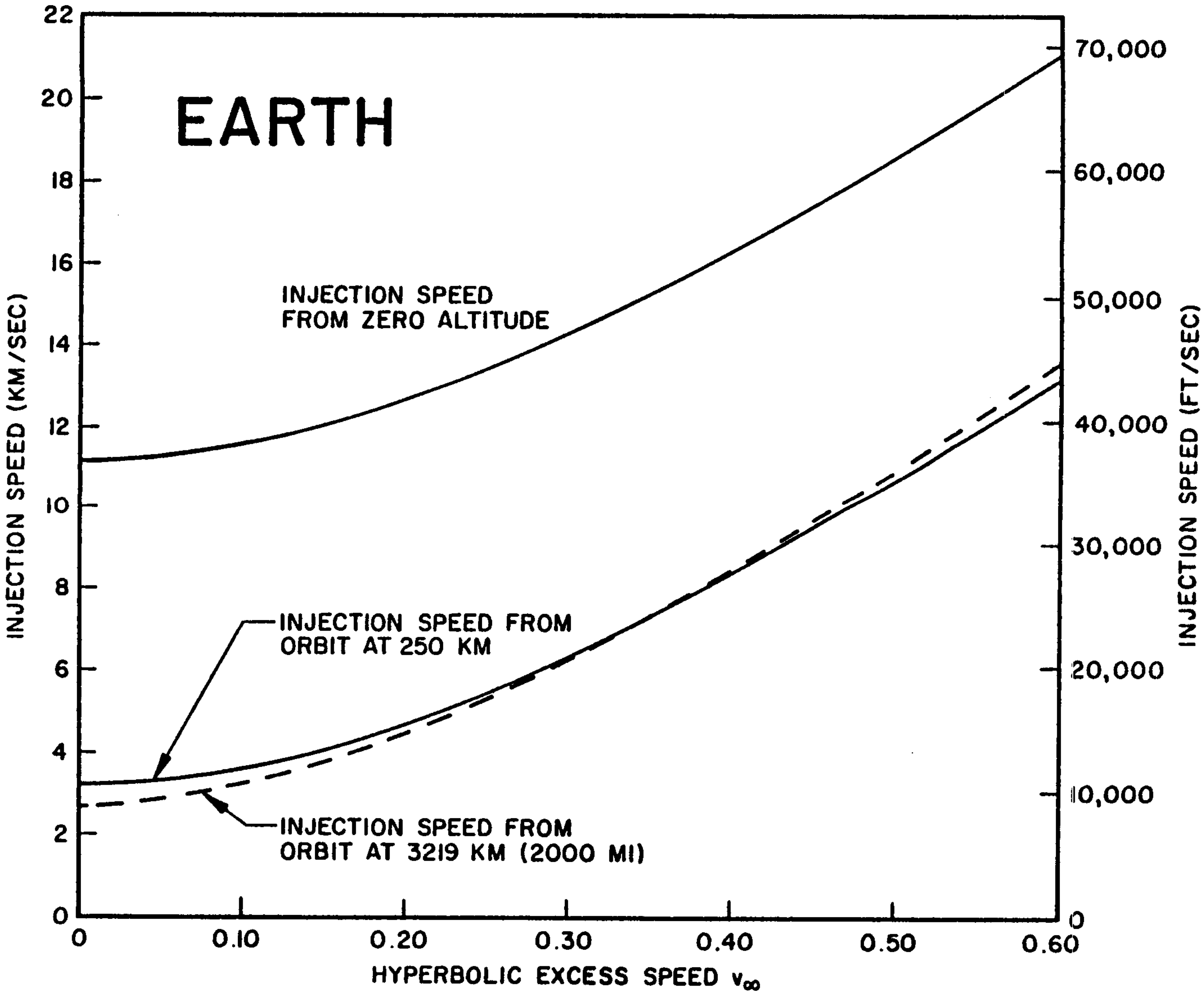

Fig. 1-12a Injection Requirements Onto Departure Hyperbolas, Earth

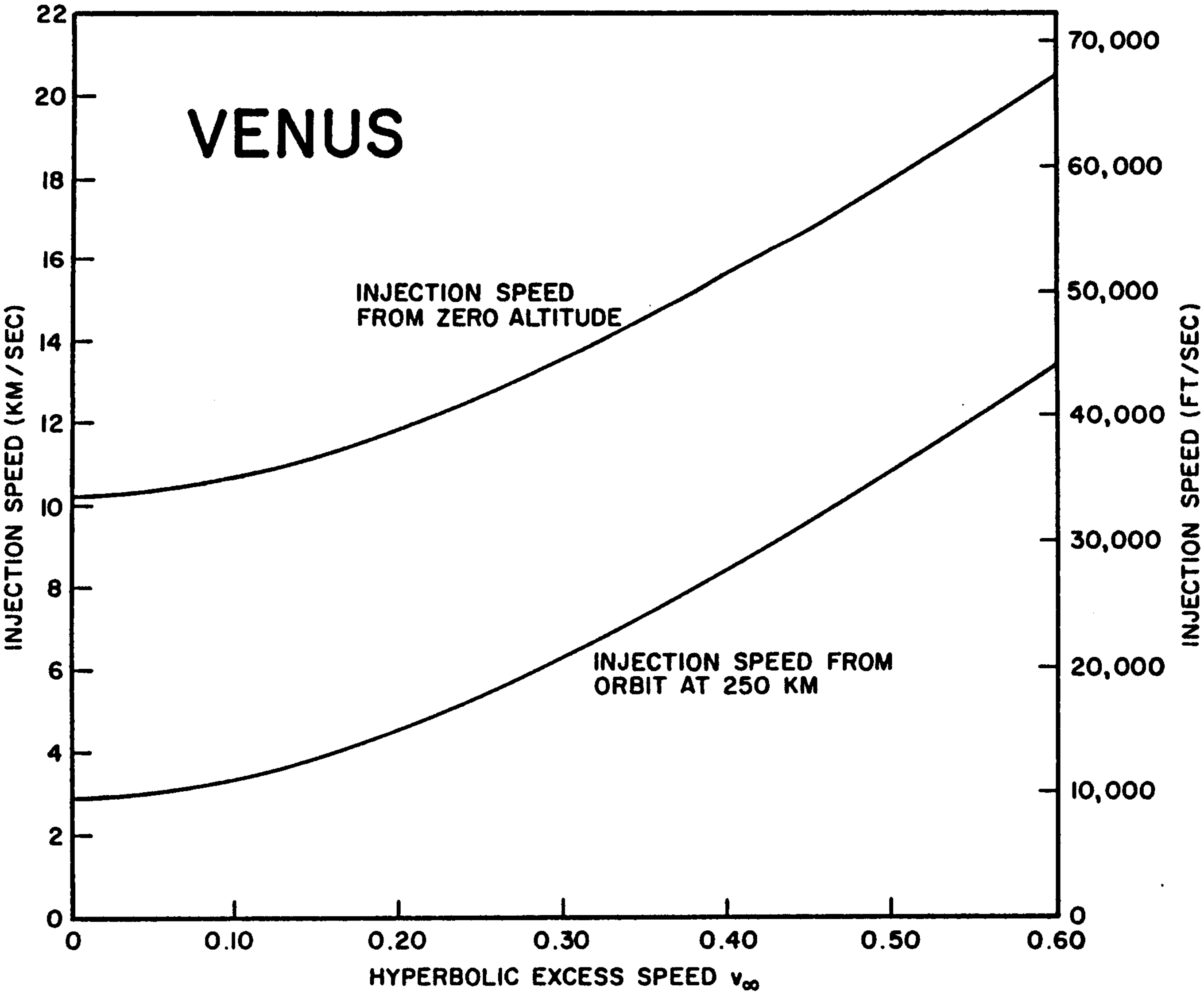

Fig. 1-12b Injection Requirements Onto Departure Hyperbolas, Venus

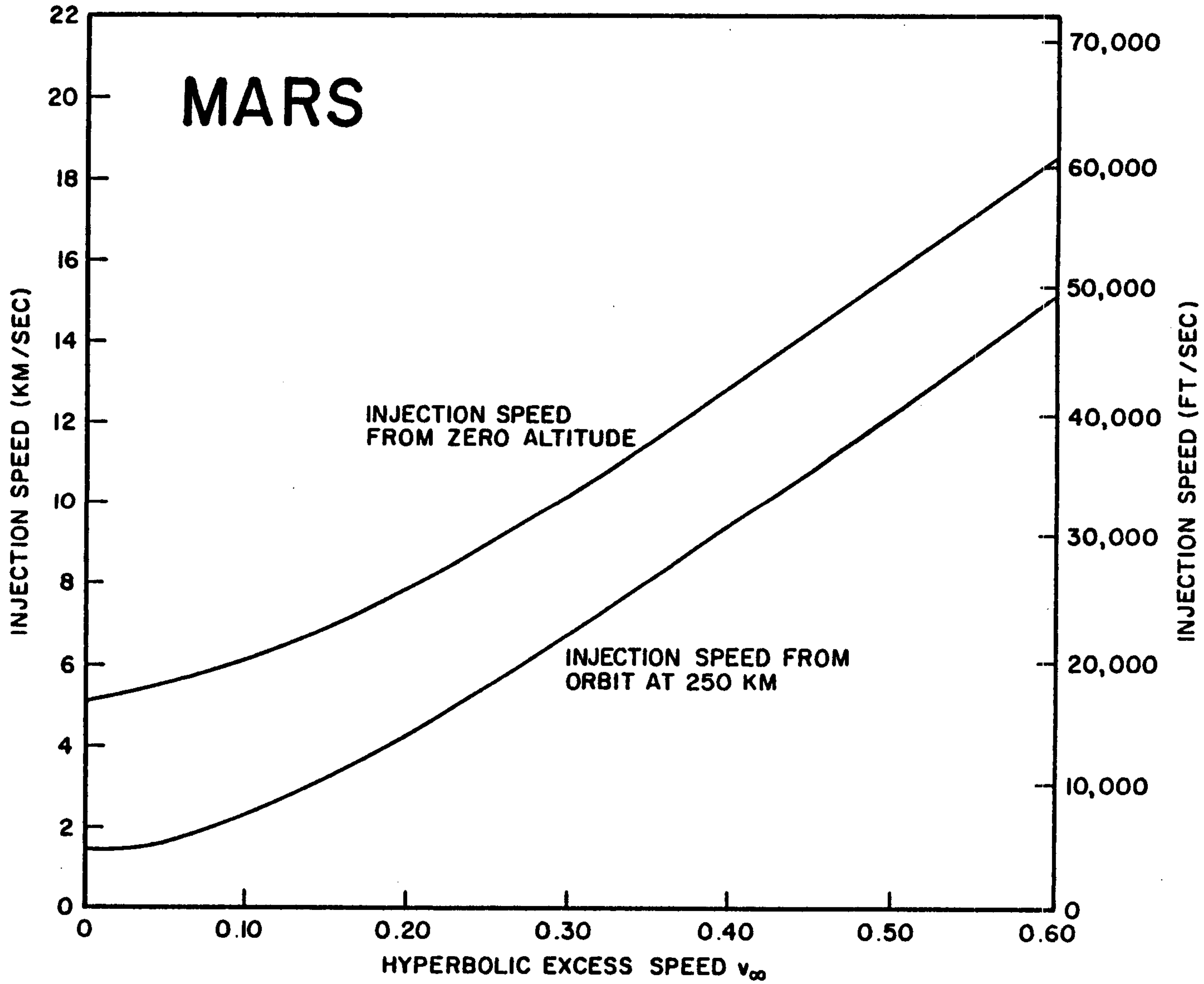

Fig. 1-12c Injection Requirements Onto Departure Hyperbolas, Mars

The diagram underscores the unsuitability of employing this region for planning interplanetary flights. Any appreciable modification of the trajectory by Venus will lead to miss-errors at the time of intersection with the Earth's orbit, which will be greatly aggravated during the course of two additional solar circuits. And while passages of Venus at later crossings of its orbit will mitigate this situation somewhat, the launch sensitivities in such cases will rise accordingly.

Note also that there exist no contours corresponding to approach distances of one to two radii (the most interesting cases); these would be subjected to intolerably large perturbations by Venus.

Figures 1-8 and 1-9 explore the region of nonsymmetric and symmetric high-energy round trips passing Venus. The most surprising feature of these diagrams is the existence of regions of very low departure speed in which the close-approach maneuver causes nominally unsuitable orbits to be modified into acceptable round trips. Several interplanetary trajectories from this area were first found by Bollman (Ref. 1-8) in his study of Mariner probe orbits.

Generally speaking, the nonsymmetric trips of Fig. 1-8 display advantages over the symmetric orbits of Fig. 1-9, in regard to both speed requirements and trip times attainable. This latter point is not surprising, in view of the fact that the symmetric nominals were all of greater duration than the nonsymmetric.

The elongated contours for $r_p = 1$ and $r_p = 2$, extending upwards towards the left in Fig. 1-8 appear to possess especially favorable flight characteristics. Extending to departure speeds almost as low as the Hohmann case, they encompass trip times of between 330 and 380 days, pass on the illuminated side of Venus near the time of opposition, and all possess reasonable return speeds at Earth, in the 0.25 to 0.29 range.

In fact, since future booster capabilities are expected to be in the 0.25 to 0.29 range, it may be even more advantageous to employ the reciprocals to the presently discussed orbits. Return approach speeds in the 0.10 to 0.15 range would thus be produced, and would probably enable pure drag brake recovery at Earth, eliminating the necessity for boosting and carrying retro-propulsion for the return maneuver. These reciprocal orbits may be located by the method of subsection 1.5.

Because of the low eccentricities of Venus' orbit as well as the Earth's orbit, it is to be expected that these results will be generally valid in all practical cases.

In Fig. 1-10, symmetric curves for low-energy trips passing Mars are drawn. Large perturbations of the type exercised by Venus are nowhere evident here. This is due principally to Mars' relatively small mass (about 0.13 that of Venus), and secondarily due to the somewhat higher speeds of passage in the present case. The nonsymmetric orbits, which lead to materially longer trip times, are not considered here.

Trip-time reductions using close-approaches appear to be in the 70 to 90 day range, and it seems possible that missions of perhaps 600-days' duration may be ultimately realized, employing some combinations of higher launch speeds, close planetary approaches, and auxiliary propulsion boost during the planetary maneuver. These possibilities are to be investigated more fully in future studies.

Figure 1-11 treats the high-energy trips passing Mars. Results from study of this area are presently incomplete and will be discussed at a later date.

1.8 SUMMARY AND CONCLUSIONS

Our search for acceptable nonstop interplanetary round trips has been narrowed to the study of three small areas, one for Venus and two for Mars. In the case of Venus, we are assured of finding a series of acceptable trips during any conjunction period of interest. Arising from a nominal high-energy group of orbits, these trajectories nevertheless involve very low energies at each end, and appear most promising for trips in the near future.

For Mars, the high-energy trips are desirable, but are feasible only during two, or at most three periods each 17-year cycle of oppositions. For the remainder of cases, a modified low-energy trip is the only possibility, and a voyage of 100 to 150 days' additional duration is to be expected.

If, on the other hand, the propulsion is available to permit a high-energy nonstop round trip during an unfavorable period, then this capability would be better employed in a short duration stopover journey, such as is described in Section 2 of this Report.

1.9 REFERENCES

1-1 S. Ross, "Researches in Interplanetary Transfer. Part II: Nonstop Round Trips," presented at 1st International Symposium on Analytical Astrodynamics, UCLA, Los Angeles, Jun 1961

1-2 J. V. Breakwell, R. W. Gillespie, and S. Ross, "Researches in Interplanetary Transfer," ARS J., Vol. 31, No. 2, Feb 1961, pp. 201-207

1-3 A. Sternfeld, Introduction to Cosmonautics, 1937, U.S.S.R. Govt. Printing House, (in Russian) [Vvedenyie v kosmonavtiku]

1-4 M. Vertregt, "Een-Jaars Banen voor Kunstmatige Planeten," Ruimtevaart, Vol. 9, No. 5, Jan 1961, pp. 125-132

1-5 R. H. Battin, "The Determination of Round-Trip Planetary Reconnaissance Trajectories," J. Aero/Space Sci., Vol. 26, No. 9, Sep 1959, pp. 545-67

1-6 P. G. Johnson and R. L. Smith, "Round Trip Trajectories for Mars Observation," Advances in the Astronautical Sciences, Vol. 5 Plenum Press

1-7 G. S. Gedeon, "Round Trip Trajectories to Mars and Venus," Am. Astronaut. Soc., Preprint 62-30, 1962

1-8 W. E. Bollman, Preliminary Standard Trajectory; Mariner A, P-37, P-38; Post Injection, JPL Engineering Document No. 38, 24 Jul 1961

Section 2
STOPOVER INTERPLANETARY ROUND TRIPS

2.1 DISCUSSION

Speed contour charts have been prepared for round-trip landing expeditions to Mars and Venus. The charts cover a complete cycle of oppositions of Mars, from 30 December 1960 to 15 December 1975, eight oppositions in all. They cover a complete cycle of conjunctions of Venus, from 11 April 1961 to 29 August 1967, plus the first conjunction from a second cycle, the one which occurs 8 April 1969, making six conjunctions in all.

The chart for each opposition or conjunction displays four sets of speed contours: one for departure from Earth; one for arrival at the destination planet; one for departure from the destination planet; and one for arrival at Earth. The outbound departure and arrival speed contours are superimposed on the left side of the chart, while the homebound departure and arrival contours are superimposed on the right side of the chart. All departure contours are plotted as unbroken lines, while all arrival contours are plotted as broken lines.

The contours represent hyperbolic excess speeds relative to the planet in question. Regardless of the planet in question, the speeds are normalized with respect to Earth's mean orbital speed. The hyperbolic excess speed V_{HE} is computed as if the rocket in the transfer trajectory is passing through the center of a massless planet. The approximate actual speed of the rocket at any given distance γ_0 from the center of the real, massive planet can be found from the expression: -

$$V = \sqrt{(V_{escape})^2 + (V_{HE})^2}$$

where V_{escape} is the escape speed at the distance γ_o.

The contours are plotted on a grid of dates. Dates at Earth are shown on the horizontal coordinate, while dates at the destination planet are shown on the vertical coordinate, at a scale of 1 mm per day. Julian dates are used. The straight diagonal line across the middle of the chart is plotted through points common to both coordinates.

The charts were prepared from a voluminous set of machine printout data (over a quarter of a million transfer trajectories).* By their use, one may simultaneously scan the four terminal speeds of both outbound and homebound trajectories. A rapid, approximate estimate of the "best" selection of trajectory pairs is readily made by scanning the contours; any considerable excursion from this "best" selection results in severe speed penalties at one of the terminations, with only trivial gains at the other terminations. After an approximate choice is made from the chart, exact speeds, angles, etc., can be obtained by refering to the original machine printout sheets. Also, small trade-offs can be made to refine the selection.

The details of the charts do not precisely repeat after a cycle of oppositions of Mars, because the position of corresponding oppositions of the second cycle are displaced about two weeks around the eccentric and inclined orbits. The details of the charts do repeat almost precisely after a cycle of conjunction of Venus. There are almost exactly five conjunctions in 8 years. A chart can be used for a subsequent date by adding 8 years and subtracting 2 days. The error is typically less than 1 day in the positions of contours on the chart. Thus, the Venus charts can be used for the time span from 1960 to 1969, plus 8 years = 1977, and with only a little error, even to 1985.

In addition to the 14 charts already described, two large-scope charts have been included, one covering six conjunctions of Venus and one covering eight

---

*See Ref. 1-2.

oppositions of Mars. The higher speed contours are omitted. Not only have the shorter trips of less than 360 deg at the sun been included, but longer trips of more than 360 deg. These two charts are useful in selecting one-way trips to Mars and Venus, and also for selecting round trips which include departure at the time of one opposition or conjunction, and return at the time of a subsequent opposition conjunction.

It turns out in practice that there is no advantage in selecting trajectories including transfer angles greater than 360 deg, at least for round-trip, stop-over, manned expeditions. This result was not foreseen before the charts were prepared. However, the charts were not revised to omit the greater than 360-deg trajectories, since their inclusion permits anyone to convince himself of their uselessness, or usefulness for special cases.

The long stopover charts include only the 0.2 EMOS* contour and, where one exists, the 0.1 EMOS contour. High-speed contours are unnecessary in all cases. A smaller contour interval was not considered useful after preliminary trials, using the charts with the printout sheets. In case of the Mars chart, when no 0.1 EMOS contour exists, the lowest speed is indicated by a cross or a triangle. In case of the Venus chart, owing to crowding, no such symbols were included.

The short stopover charts included contours to 0.6 EMOS. This includes the highest value appropriate to improved nuclear rockets according to present-day concepts, and exceeds the highest speeds appropriate to chemical rockets using our best engineering knowledge (0.35 EMOS) or using our best presently scheduled hardware (0.2 EMOS).

Comparing the speed contour charts to elevation contour land maps, the low-speed regions are analogous to flat-bottomed sinks with steep slopes around them. Each sink surrounds the so-called Hohmann transfer, which is the

*Earth's mean orbital speed.

point of minimum departure speed, lying on the 180-deg transfer angle for circular, coplanar orbits. However, the orbits are not circular, so that the shape of the sink is distorted; and they are not coplanar, so that there is a ridge across the sink along the 180-deg transfer line. Each sink is therefore distorted, and divided into two separate relative sinks. Owing to the distortion, the dividing ridge does not follow precisely a straight line.

A readout from the charts can be made at any combination of dates which place one on the destination planet in time to come home on a desired date. However, most combinations demand propulsion and drag-brake capabilities which we do not have. It is therefore necessary to select combinations of dates corresponding to local minima of mutually compatible departure and arrival speeds. The selection must be the best compromise among four non-coincident minima. An inspection of the charts reveals four combinations of outbound and homebound trajectories for each shortstopover trip, and four for each longstopover trip. In general, there are these four combinations:

- Long outbound - short homebound
- Short outbound - long homebound
- Short outbound - short homebound
- Long outbound - long homebound

For most of the short stopover trips, the combination which requires the minimum speeds of departure and arrival is the only one which needs to be considered. For most of the long stopover trips, only the short transit times are of practical interest.

A special comment is required about the use of the charts for planning expeditions. All that has been said rests on the assumption of transfer within a single plane inclined to the orbits of both the departure and the destination planets. It is also possible to bend the plane of the transfer trajectory by a midcourse maneuver. Such a maneuver will add to the total energy required for a particular transfer, but may enable one to select more advantageous transfer trajectories. As a first approximation, one can simply fair the contours on the two sides of the 180-deg ridge to eliminate the ridge. Such

a crude procedure will require a midcourse maneuver to bend the trajectory 1.85 deg in the case of an Earth to Mars transfer, and 3.39 deg in the case of the Earth to Venus transfers. The speed increment for the Earth to Mars transfer might be, in an assumed particular case,

$$(1.85 \text{ deg}/57 \text{ deg}) \times 22.8 = 0.74 \text{ mi/sec} = 3907 \text{ ft/sec}$$

The speed increment can be different, depending on the heliocentric speed of the vehicle at the node. In practice, it will be possible to bend the plane through an angle less than that of the inclination of the orbits of the two planets, and at a location removed from the node line, retaining most of the benefits, and eliminating much or most of the propulsion penalties. The present study is being continued to establish suitable methods of planning these maneuvers.

2.2 SUPPLEMENTARY TABLES AND CHARTS

To assist in the use of the charts, some supporting tables and charts have been included. These include a table for comparison of Julian to calendar dates;* tables of dates when Venus and Earth cross through the planes of one another's orbits, and dates when Mars and Earth cross through the planes of one another's orbits; tables of Venus conjunction dates and Mars opposition dates; a chart showing the position of Venus conjunctions, Fig. 2-1, and one showing the position of Mars oppositions, Fig. 2-2; graphs for converting hyperbolic excess speeds to hyperbolic pericenter speeds, Fig. 2-3; and graphs for finding directly the mass fractions for reaching any hyperbolic excess speed starting from specified parking orbits at Earth, Mars, and Venus, Fig. 2-4. A detailed planning study will require additional data, but a first set of selection can be prepared with the use of those which have been included. It should be emphasized that each specific expedition must be uniquely planned before it can actually be engineered.

A special speed contour chart, Fig. 2-5, has been included to illustrate the method of use of all the speed contour charts. The dotted line graphically portrays the selection of the date of departure from Earth, arrival at Mars, departure from Mars, and arrival at Earth. The chart is prepared from the working chart for the Mars opposition of 1971. The particular selection of dates corresponds to the 330-day round trip to Mars in 1971 mentioned in Subsection 2.5.

---

*By the kind permission of the publishers. Planetary Co-ordinates for the Years 1960-1980, prepared by H. M. Nautical Almanac Office. Printed under the authority of Her Majesty's Stationery Office, London, 1958, by William Clowes and Sons, Ltd.

JULIAN DATE—CALENDAR DATE AT 0^h*

Julian Date	Calendar Date	Julian Date	Calendar Date	Julian Date	Calendar Date	Julian Date	Calendar Date
243 6920·5	1959 Dec. 18	243 8840·5	1965 Mar. 21	244 0760·5	1970 June 23	244 2680·5	1975 Sept. 25
6960·5	1960 Jan. 27	8880·5	Apr. 30	0800·5	Aug. 2	2720·5	Nov. 4
7000·5	Mar. 7	8920·5	June 9	0840·5	Sept. 11	2760·5	Dec. 14
7040·5	Apr. 16	8960·5	July 19	0880·5	Oct. 21	2800·5	1976 Jan. 23
243 7080·5	May 26	243 9000·5	Aug. 28	244 0920·5	Nov. 30	244 2840·5	Mar. 3
7120·5	July 5	9040·5	Oct. 7	0960·5	1971 Jan. 9	2880·5	Apr. 12
7160·5	Aug. 14	9080·5	Nov. 16	1000·5	Feb. 18	2920·5	May 22
7200·5	Sept. 23	9120·5	Dec. 26	1040·5	Mar. 30	2960·5	July 1
243 7240·5	Nov. 2	243 9160·5	1966 Feb. 4	244 1080·5	May 9	244 3000·5	Aug. 10
7280·5	Dec. 12	9200·5	Mar. 16	1120·5	June 18	3040·5	Sept. 19
7320·5	1961 Jan. 21	9240·5	Apr. 25	1160·5	July 28	3080·5	Oct. 29
7360·5	Mar. 2	9280·5	June 4	1200·5	Sept. 6	3120·5	Dec. 8
243 7400·5	Apr. 11	243 9320·5	July 14	244 1240·5	Oct. 16	244 3160·5	1977 Jan. 17
7440·5	May 21	9360·5	Aug. 23	1280·5	Nov. 25	3200·5	Feb. 26
7480·5	June 30	9400·5	Oct. 2	1320·5	1972 Jan. 4	3240·5	Apr. 7
7520·5	Aug. 9	9440·5	Nov. 11	1360·5	Feb. 13	3280·5	May 17
243 7560·5	Sept. 18	243 9480·5	Dec. 21	244 1400·5	Mar. 24	244 3320·5	June 26
7600·5	Oct. 28	9520·5	1967 Jan. 30	1440·5	May 3	3360·5	Aug. 5
7640·5	Dec. 7	9560·5	Mar. 11	1480·5	June 12	3400·5	Sept. 14
7680·5	1962 Jan. 16	9600·5	Apr. 20	1520·5	July 22	3440·5	Oct. 24
243 7720·5	Feb. 25	243 9640·5	May 30	244 1560·5	Aug. 31	244 3480·5	Dec. 3
7760·5	Apr. 6	9680·5	July 9	1600·5	Oct. 10	3520·5	1978 Jan. 12
7800·5	May 16	9720·5	Aug. 18	1640·5	Nov. 19	3560·5	Feb. 21
7840·5	June 25	9760·5	Sept. 27	1680·5	Dec. 29	3600·5	Apr. 2
243 7880·5	Aug. 4	243 9800·5	Nov. 6	244 1720·5	1973 Feb. 7	244 3640·5	May 12
7920·5	Sept. 13	9840·5	Dec. 16	1760·5	Mar. 19	3680·5	June 21
7960·5	Oct. 23	9880·5	1968 Jan. 25	1800·5	Apr. 28	3720·5	July 31
8000·5	Dec. 2	9920·5	Mar. 5	1840·5	June 7	3760·5	Sept. 9
243 8040·5	1963 Jan. 11	243 9960·5	Apr. 14	244 1880·5	July 17	244 3800·5	Oct. 19
8080·5	Feb. 20	244 0000·5	May 24	1920·5	Aug. 26	3840·5	Nov. 28
8120·5	Apr. 1	0040·5	July 3	1960·5	Oct. 5	3880·5	1979 Jan. 7
8160·5	May 11	0080·5	Aug. 12	2000·5	Nov. 14	3920·5	Feb. 16
243 8200·5	June 20	244 0120·5	Sept. 21	244 2040·5	Dec. 24	244 3960·5	Mar. 28
8240·5	July 30	0160·5	Oct. 31	2080·5	1974 Feb. 2	4000·5	May 7
8280·5	Sept. 8	0200·5	Dec. 10	2120·5	Mar. 14	4040·5	June 16
8320·5	Oct. 18	0240·5	1969 Jan. 19	2160·5	Apr. 23	4080·5	July 26
243 8360·5	Nov. 27	244 0280·5	Feb. 28	244 2200·5	June 2	244 4120·5	Sept. 4
8400·5	1964 Jan. 6	0320·5	Apr. 9	2240·5	July 12	4160·5	Oct. 14
8440·5	Feb. 15	0360·5	May 19	2280·5	Aug. 21	4200·5	Nov. 23
8480·5	Mar. 26	0400·5	June 28	2320·5	Sept. 30	4240·5	1980 Jan. 2
243 8520·5	May 5	244 0440·5	Aug. 7	244 2360·5	Nov. 9	244 4280·5	Feb. 11
8560·5	June 14	0480·5	Sept. 16	2400·5	Dec. 19	4320·5	Mar. 22
8600·5	July 24	0520·5	Oct. 26	2440·5	1975 Jan. 28	4360·5	May 1
8640·5	Sept. 2	0560·5	Dec. 5	2480·5	Mar. 9	4400·5	June 10
243 8680·5	Oct. 12	244 0600·5	1970 Jan. 14	244 2520·5	Apr. 18	244 4440·5	July 20
8720·5	Nov. 21	0640·5	Feb. 23	2560·5	May 28	4480·5	Aug. 29
8760·5	Dec. 31	0680·5	Apr. 4	2600·5	July 7	4520·5	Oct. 8
243 8800·5	1965 Feb. 9	244 0720·5	May 14	244 2640·5	Aug. 16	244 4560·5	Nov. 17

*See footnote pg. 2-6.

DATES OF NODAL PASSAGES OF VENUS

Ascending	Descending	Ascending	Descending
	2436985.66		2440805.58
2437098.80		2440918.71	
	2437210.36		2441030.28
2437323.50		2441143.42	
	2437435.06		2441254.98
2437548.20		2441368.12	
	2437659.76		2441479.68
2437772.90		2441592.82	
	2437884.47		2441704.38
2437997.60		2441817.52	
	2438109.17		2441929.08
2438222.30		2442042.22	
	2438333.87		2442153.78
2438447.00		2442266.92	
	2438558.57		2442378.49
2438671.70		2442491.62	
	2438783.27		2442603.19
2438896.41		2442716.32	
	2439007.97		2442827.89
2439121.11		2442941.02	
	2439232.67		2443052.59
2439345.81		2443165.73	
	2439457.37		2443277.29
2439570.51		2443390.43	
	2439682.07		2443501.99
2439795.21		2443615.13	
	2439906.77		2443726.69
2440019.91		2443839.83	
	2440131.48		2443951.39
2440244.61		2444064.53	
	2440356.18		2444176.09
2440469.31		2444289.23	
	2440580.88		2444400.79
2440694.01		2444513.93	
			2444625.50

Note: Ascending node 75.95971 deg, descending node 255.95971 deg.

DATES OF NODAL PASSAGES OF EARTH

Earth Descends	Earth Ascends	Heliocentric Longitude (deg)
	2437092.36	
2437275.71		
	2437457.62	
2437640.97		
	2437822.87	
2438006.22		
	2438188.13	
2438371.48		
	2438553.38	
2438736.74		
	2438918.64	
2439101.99		
	2439283.90	
2439467.25		
	2439649.15	
2439832.50		
	2440014.41	
2440197.76		75.95971
	2440379.66	255.95971
2440563.02		
	2440744.92	
2440928.27		
	2441110.18	
2441293.53		
	2441475.43	
2441648.78		
	2441840.69	
2442024.04		
	2442205.94	
2442389.30		
	2442571.20	
2442754.55		
	2442936.46	
2443119.81		
	2443301.71	
2443485.06		
	2443666.97	
2443850.32		
	2444032.22	
2444215.58		
	2444397.48	
2444580.83		

Note: Earth descends at ascending node of Venus, and ascends at descending node of Venus

DATES OF NODAL PASSAGES OF MARS

Ascending Node	Descending Node
2437203.0	
	2437585.6
2437890.0	
	2438272.6
2438576.9	
	2438959.5
2439263.9	
	2439646.5
2439950.9	
	2440333.5
2440637.9	
	2441020.5
2441324.8	
	2441707.4
2442011.8	
	2442394.4
2442698.8	
	2443081.4
2443385.8	
	2443768.4
2444072.7	
	2444455.3 (From ephemeris, 2444455.37)
2444759.7	
	2445142.3

Note: From ephemeris, ascending node = 49.15 deg at 2437203.0, descending node = 229.13 deg at 2437585.6.

DATES OF NODAL PASSAGES OF EARTH

(Earth Versus Orbit of Mars; Earth Descends at Ascending Node of Mars)

Earth Descends	Earth Ascends	Heliocentric Longitude (deg)
	2437064.5	229.15
2437250.2		49.15
	2437429.8	
2437615.5		
	2437795.0	
2437980.7		
	2438160.3	
2438346.0		
	2438525.5	
2438711.2		
	2438890.8	
2439076.5		
	2439256.0	
2439441.7		
	2439621.3	
2439807.0		
	2439986.6	
2440172.3		
	2440351.8	
2440537.5		
	2440717.1	
2440902.8		
	2441082.3	
2441268.0		
	2441447.6	
2441633.3		
	2441812.8	
2441998.5		
	2442178.1	
2442363.8		
	2442543.3	
2442729.0		
	2442908.6	
2443094.3		
	2443273.9	
2443459.6		
	2443639.1	
2443824.8		
	2444004.4	
2444190.1		
	2444369.6	
2444555.5		
	2444734.9	

Note: Siderial year = 365,2564 d.
Earth ascends at descending node of Mars.

PERIHELION PASSAGES OF MARS

Julian Date	Calendar Date	Heliocentric Longitude (deg)
2437080.1	25.6 May 1960	334.586
2437767.1	12.6 Apr 1962	
2438454.0	28.5 Feb 1964	
2439141.0	15.5 Jan 1966	
2439828.0	3.5 Dec 1967	
2440515.0	20.5 Oct 1969	
2441201.9	7.4 Sep 1971	
2441888.9	25.4 Jul 1973	
2442575.9	12.4 Jun 1975	
2443262.9	29.4 Apr 1977	
2443949.8	17.3 Mar 1979	334.564

Note: Period = 1.8808 siderial years = 686.9742 days

CONJUNCTIONS OF VENUS FROM LINEAR GRAPHICAL INTERPOLATION ON BRITISH EPHEMERIS

Julian Date	Calendar Date	Heliocentric Longitude (deg)	Heliocentric Longitude Displacement After 8-yr Cycle (deg)
2437400.50	11.0 Apr 1961	200.72	2.43
2437981.33	12.8 Nov 1962	49.78	2.56
2438566.39	19.9 Jun 1964	268.39	2.24
2439151.79	26.3 Jan 1966	125.63	2.58
2439732.29	29.8 Aug 1967	335.43	2.23
2440320.14	8.6 Apr 1969	198.29	2.40
2440900.82	10.3 Nov 1970	47.22	2.57
2441486.10	17.6 Jun 1972	266.15	2.35
2442071.30	23.8 Jan 1974	123.05	
2442651.97	27.5 Aug 1975	333.20	
2443239.72	6.2 Apr 1977	195.89	
2443820.35	7.9 Nov 1978	44.65	
2444405.73	15.2 Jun 1980	263.80	

OPPOSITIONS OF MARS FROM LINEAR GRAPHICAL INTERPOLATIONS ON BRITISH EPHEMERIS

Julian Date	Calendar Date	Heliocentric Longitude (deg)
2437298.9	30.4 Dec 1960	98.58
2438065.1	4.6 Feb 1963	134.80
2438829.0	9.5 Mar 1965	168.50
2439596.0	15.5 Apr 1967	204.63
2440373.0	1.5 Jun 1969	249.55
2441173.8	10.3 Aug 1971	316.72
2441980.7	25.2 Oct 1973	31.24
2442762.2	15.7 Dec 1975	82.61
2443530.5	22.0 Jan 1978	121.23
2444294.8	25.3 Feb 1980	155.36

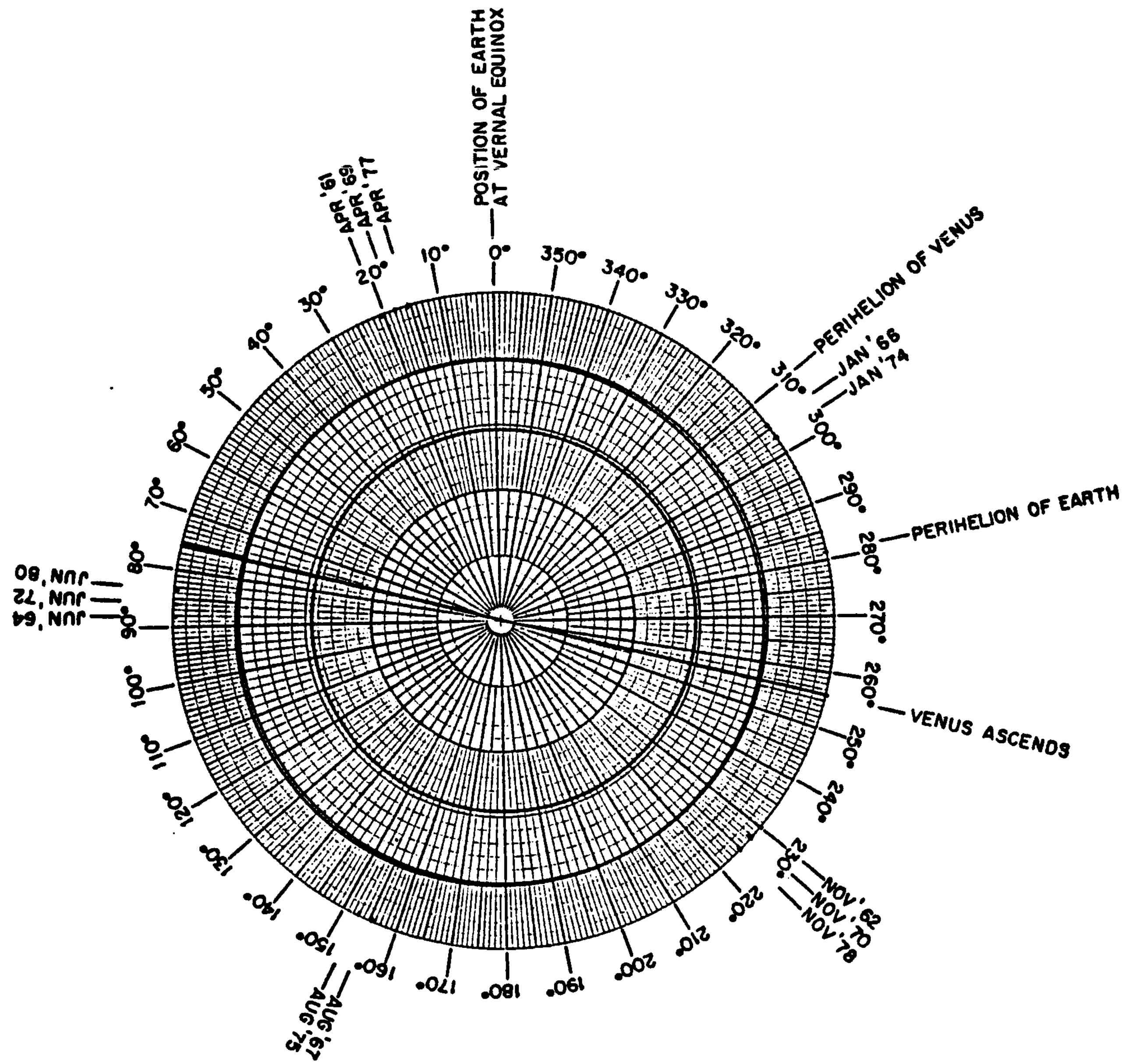

Fig. 2-1 Conjunctions of Venus

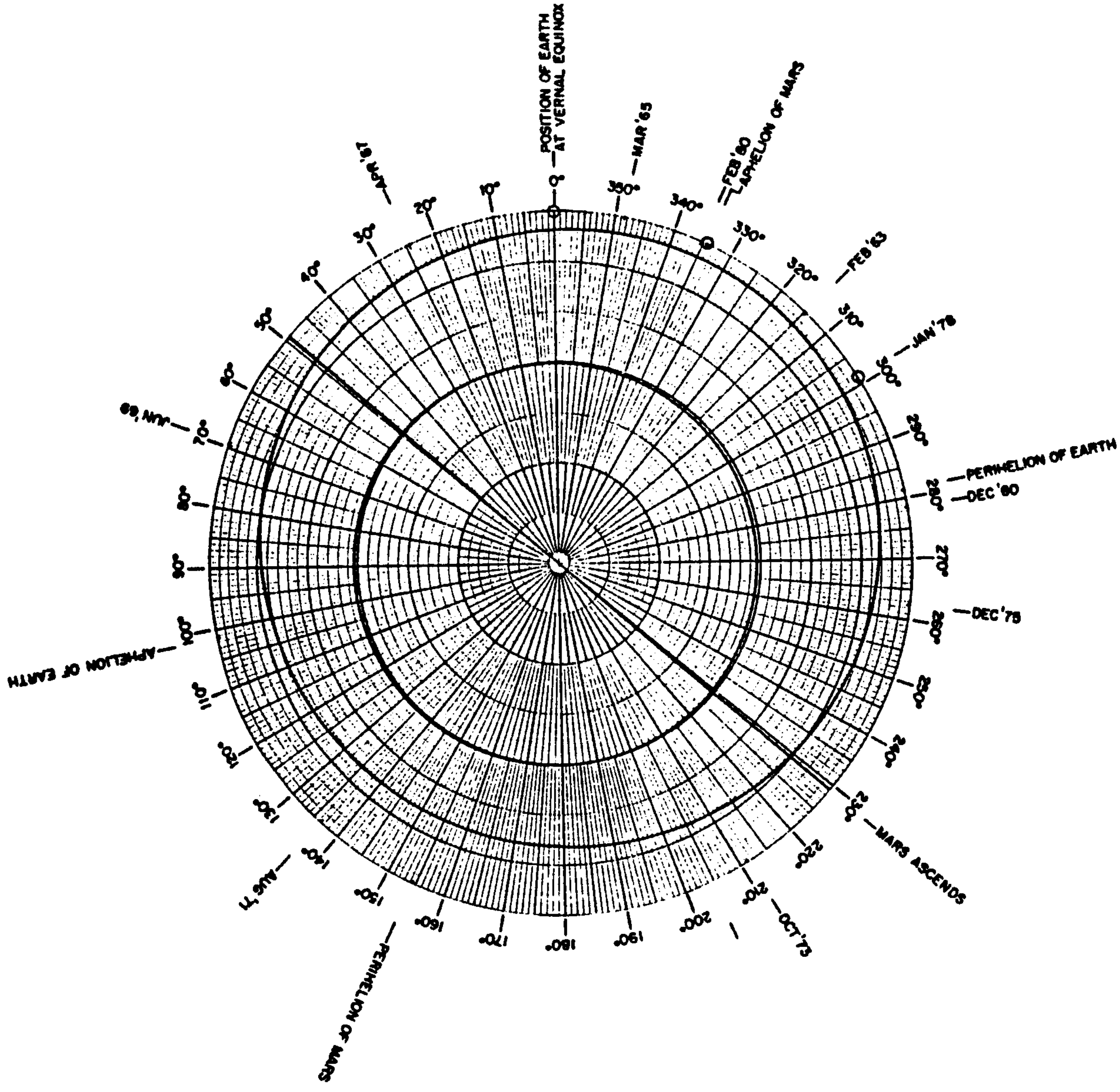

Fig. 2-2 Oppositions of Mars

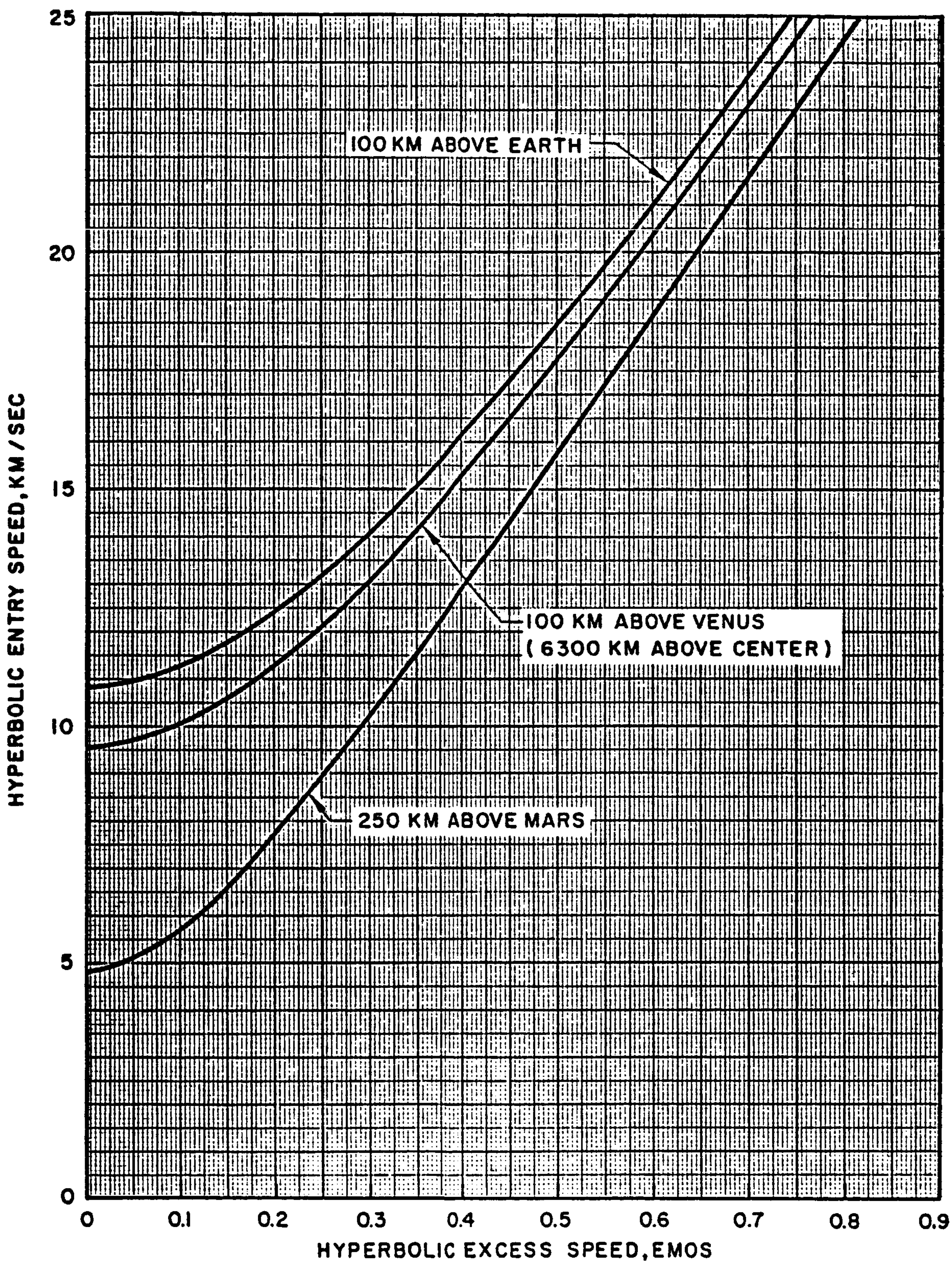

Fig. 2-3 Speed Conversion Chart

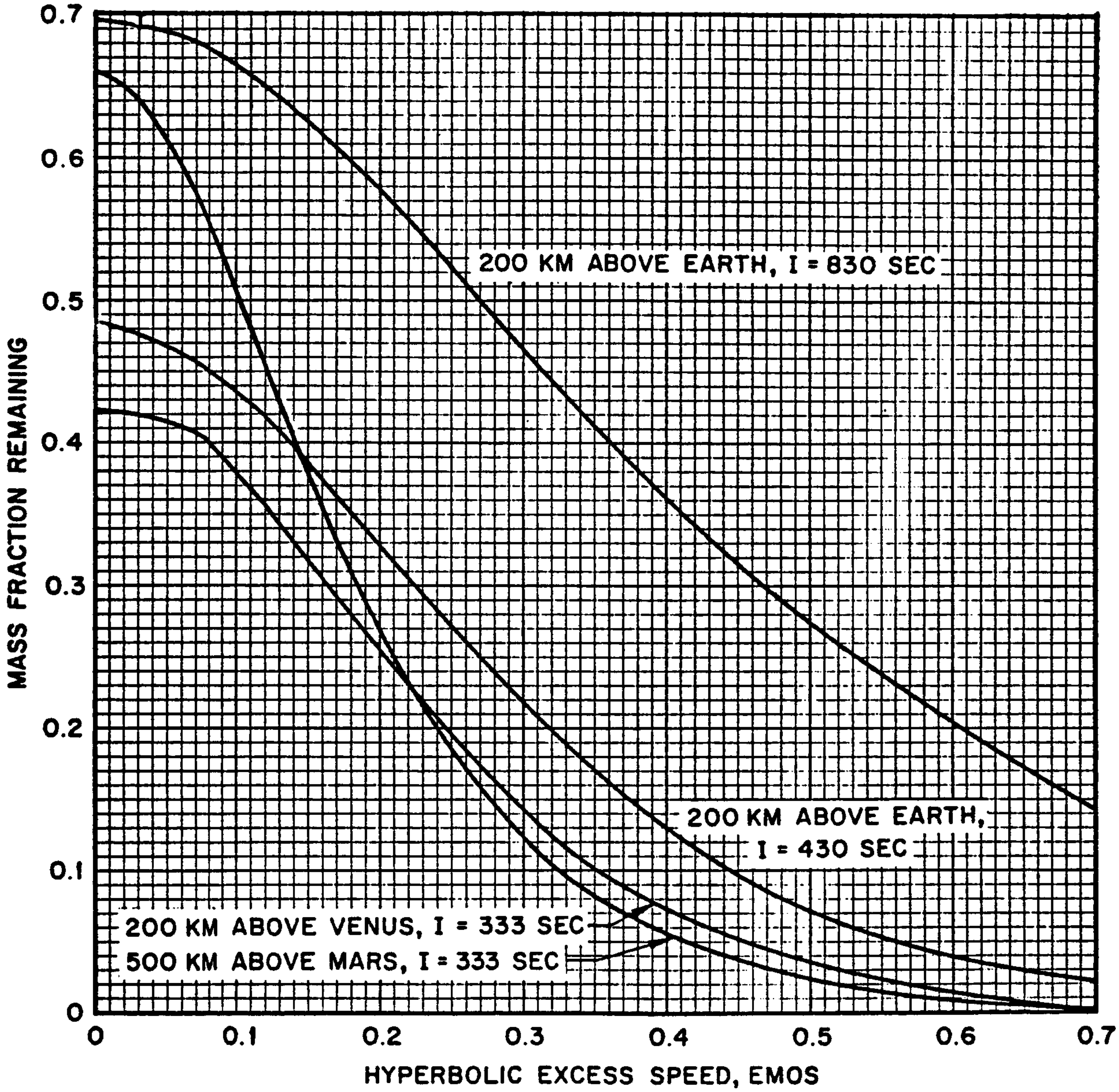

Fig. 2-4 Remaining Mass Fractions Departing From Circular Parking Orbits

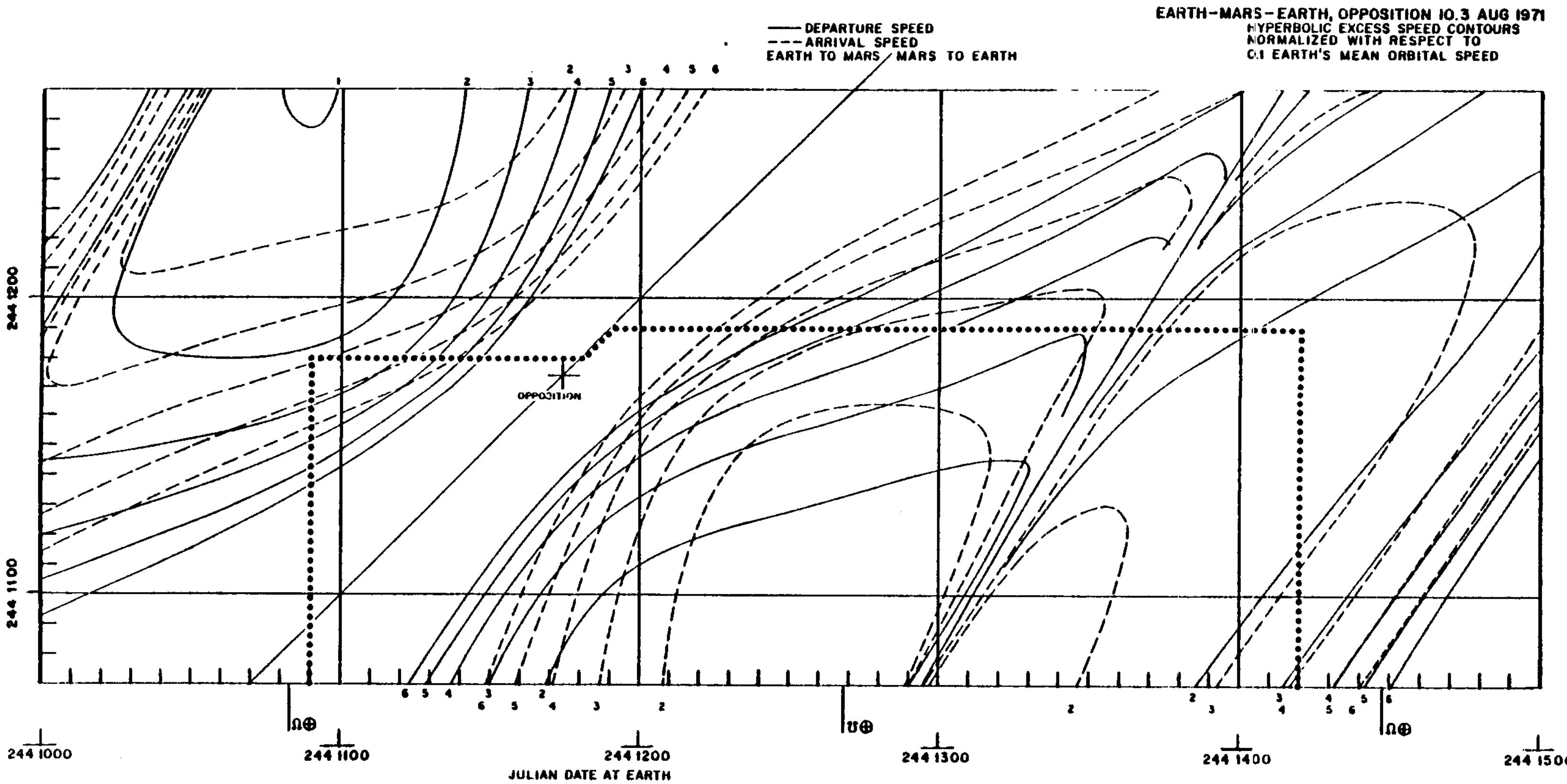

Fig. 2-5 Special Speed Contour Chart Illustrating the Mission Selection Process

2.3 INTERPLANETARY TRANSFER SPEED CONTOUR CHARTS

The following symbols and terms are used on the interplanetary transfer speed contour charts:

⊕	symbol for Earth
♀	symbol for Venus
♂	symbol for Mars
☊	planet crosses south to north through the plane of the orbit of another planet
☋	planet crosses north to south through the plane of the orbit of another planet
conjunction	inferior conjunction; planet crosses Earth's meridian at true solar noon
opposition	planet crosses Earth's meridian at midnight
EMOS	Earth's mean orbital speed
V_{HE}	hyperbolic excess speed of vehicle relative to any planet, but normalized with respect to EMOS
V_P	pericenter speed at a specified altitude, relative to any planet, in km/sec
decl.	declination, in the usual astronomical sense - inclination of plane of orbit relative to the plane of a planet's equator (assumed to be same as the plane of the planet's orbit in case of Venus)
cal. date	legal calendar date
Jul. date	Julian date, universally employed by astronomers, and counted in days since day 1

Fig. 2-6 EARTH-VENUS-EARTH, CONJUNCTION 11.0 APRIL 1961
HYPERBOLIC EXCESS SPEED CONTOURS NORMALIZED WITH RESPECT TO 0.1 EARTH'S MEAN ORBITAL SPEED

Page intentionally left blank

Fig. 2-7 EARTH - VENUS - EARTH, CONJUNCTION 12.8 NOV. 1962

HYPERBOLIC EXCESS SPEED CONTOURS
NORMALIZED WITH RESPECT TO
0.1 EARTH'S MEAN ORBITAL SPEED

Fig. 2-8 EARTH–VENUS–EARTH, CONJUNCTION 19.9 JUNE 1964
HYPERBOLIC EXCESS SPEED CONTOURS
NORMALIZED WITH RESPECT TO
0.1 EARTH'S MEAN ORBITAL SPEED

Page intentionally left blank

Fig. 2-9 EARTH-VENUS-EARTH, CONJUNCTION 26.3 JAN 1966
HYPERBOLIC EXCESS SPEED CONTOURS
NORMALIZED WITH RESPECT TO
0.1 EARTH'S MEAN ORBITAL SPEED

Page intentionally left blank

Fig. 2-10 EARTH-VENUS-EARTH, CONJUNCTION 29.8 AUG 1967
HYPERBOLIC EXCESS SPEED CONTOURS
NORMALIZED WITH RESPECT TO
0.1 EARTH'S MEAN ORBITAL SPEED

Page intentionally left blank

Fig. 2-11 EARTH—VENUS—EARTH, CONJUNCTION 8.6 APRIL 1969
HYPERBOLIC EXCESS SPEED CONTOURS
NORMAL WITH RESPECT TO
0.1 EARTH'S MEAN ORBITAL SPEED

Page intentionally left blank

Fig. 2-12 EARTH-MARS-EARTH, OPPOSITION 30.4 DEC 1960
HYPERBOLIC EXCESS SPEED CONTOURS
NORMALIZED WITH RESPECT TO
0.1 EARTH'S MEAN ORBITAL SPEED

Page intentionally left blank

Fig. 2-13 EARTH–MARS–EARTH, OPPOSITION 4.6 FEB 1963
HYPERBOLIC EXCESS SPEED CONTOURS
NORMALIZED WITH RESPECT TO
0.1 EARTH'S MEAN ORBITAL SPEED

Page intentionally left blank

Page intentionally left blank

Fig. 2-15 EARTH-MARS-EARTH, OPPOSITION 15.5 APRIL 1967
HYPERBOLIC EXCESS SPEED CONTOURS
NORMALIZED WITH RESPECT TO
0.1 EARTH'S MEAN ORBITAL SPEED

Page intentionally left blank

Fig. 2-16 EARTH-MARS-EARTH, OPPOSITION 1.5 JUNE 1969
HYPERBOLIC EXCESS SPEED CONTOURS
NORMALIZED WITH RESPECT TO
0.1 EARTH'S MEAN ORBITAL SPEED

Page intentionally left blank

Fig. 2-17 EARTH–MARS–EARTH, OPPOSITION 10.3 AUG 1971
HYPERBOLIC EXCESS SPEED CONTOURS
NORMALIZED WITH RESPECT TO
0.1 EARTH'S MEAN ORBITAL SPEED

Page intentionally left blank

Fig. 2-18 EARTH–MARS–EARTH, OPPOSITION 25.2 OCT 1973
HYPERBOLIC EXCESS SPEED CONTOURS
NORMALIZED WITH RESPECT TO
0.1 EARTH'S MEAN ORBITAL SPEED

Page intentionally left blank

Fig. 2-19 EARTH-MARS-EARTH, OPPOSITION 15.7 DEC 1975
HYPERBOLIC EXCESS SPEED CONTOURS
NORMALIZED WITH RESPECT TO
0.1 EARTH'S MEAN ORBITAL SPEED

Page intentionally left blank

Fig. 2-20 EARTH-VENUS-EARTH, CONJUNCTIONS 1961–1969

HYPERBOLIC EXCESS SPEED CONTOURS
NORMALIZED WITH RESPECT TO
0.1 EARTH'S MEAN ORBITAL SPEED

MAXIMUM CONTOURS AT 0.2 EMOS
180° TRANSFERS AND NODAL INTERSECTIONS SHOWN

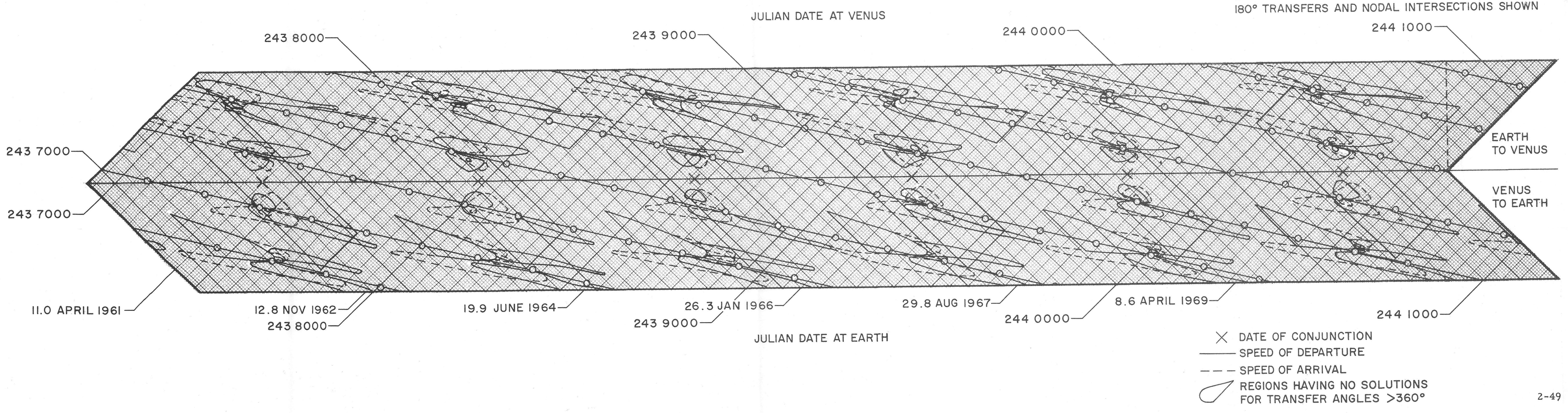

Page intentionally left blank

Fig. 2-21 EARTH-MARS-EARTH, OPPOSITIONS 1960-1975

HYPERBOLIC EXCESS SPEED CONTOURS
NORMALIZED WITH RESPECT TO
0.1 EARTH'S MEAN ORBITAL SPEED

MAXIMUM CONTOURS AT 0.2 EMOS
180° TRANSFERS AND NODAL INTERSECTIONS SHOWN

2.4 READOUT TABLES

A set of readout tables have been made, refined by use of the printout sheets, and tabulated. For practical purposes, the tabulation is complete. It reveals for the first time what is required to make manned, round-trip, landing expeditions to Mars and Venus. The readouts were in many cases modified by assumed limitations of 0.35 EMOS at both ends of the outbound journey to Mars; of 0.20 EMOS at both ends of the homebound journey from Mars; of 0.35 EMOS at departure from Earth to Venus; and of 0.20 EMOS at the other three terminations between Earth and Venus. These limitations correspond approximately to the capabilities of a hydrogen-oxygen, single-stage rocket, and to drag brakes using present design concepts. Higher entry speeds require retrorocket braking, and higher departure speeds require nuclear propulsion or rendezvous of chemical rockets.

VENUS CONJUNCTIONS 12.8 NOV. 1962 — 19.9 JUNE 1964

	JUL. DATE	CAL. DATE	DUR. DAYS	TOTAL DAYS	V_{HE} EMOS	V_P KM/SEC	DECL.	REMAIN MASS
LV ⊕	243 7830	6-15-62	—	—	.1441	11.69	-42.37°	.390
AR ♀	243 8020	12-22-62	190	—	.1069	10.03	9.68°	—
LV ♀	243 8520	5-5-64	500	—	.1073	10.08	-18.56°	.370
AR ⊕	243 8720	11-21-64	200	890	.1592	11.85	2.87°	—
LV ⊕	243 7830	6-15-62	—	—	.1441	11.69	-42.37°	.390
AR ♀	243 8020	12-22-62	190	—	.1069	10.03	9.68°	—
LV ♀	243 8530	5-15-64	510	—	.1766	10.90	27.40°	.235
AR ⊕	243 8630	8-23-64	100	800	.1294	11.52	-42.58°	—
LV ⊕	243 7900	8-24-62	—	—	.0985	11.25	-6.47°	.436
AR ♀	243 8010	12-12-62	110	—	.1960	11.20	-26.62°	—
LV ♀	243 8520	5-5-64	510	—	.1073	10.08	-18.56°	370
AR ⊕	243 8720	11-21-64	200	820	.1592	11.85	2.87°	—
LV ⊕	243 7900	8-24-62	—	—	.0985	11.25	-6.47°	.436
AR ♀	243 8010	12-12-62	110	—	.1960	11.20	-26.62°	—
LV ♀	243 8530	5-15-64	520	—	.1766	10.90	27.40°	.285
AR ⊕	243 8630	8-23-64	100	730	.1294	11.52	-42.58°	—

VENUS CONJUNCTIONS 19.9 JUNE 1964 - 26.3 JAN. 1966

	JUL. DATE	CAL. DATE	DUR. DAYS	TOTAL DAYS	V_{HE} EMOS	V_P KM/SEC	DECL.	REMAIN MASS
LV ⊕	243 8400	1-6-64	–	–	.1774	12.10	45.29°	.354
AR ♀	243 8610	8-3-64	210	–	.1148	10.15	-22.63°	–
LV ♀	243 9110	12-16-65	500	–	.1031	10.01	-10.27°	.372
AR ⊕	243 9290	6-14-66	180	890	.1268	11.51	+1.06°	–
LV ⊕	243 8400	1-6-64	–	–	.1774	12.10	45.29°	.354
AR ♀	243 8610	8-3-64	210	–	.1148	10.15	-22.63°	–
LV ♀	243 9120	12-26-65	510	–	.1582	10.66	-33.82°	.309
AR ⊕	243 9270	5-25-66	150	870	.1078	11.30	26.15°	–
LV ⊕	243 8500	4-15-64	–	–	.1340	11.58	-9.66°	.400
AR ♀	243 8610	8-3-64	110	–	.1543	10.60	31.14°	–
LV ♀	243 9110	12-16-65	500	–	.1031	10.01	-10.27°	.372
AR ⊕	243 9290	6-14-66	180	790	.1268	11.51	1.06°	–
LV ⊕	243 8500	4-15-64	–	–	.1340	11.58	-9.66°	.400
AR ♀	243 8610	8-3-64	110	–	.1543	10.60	31.14°	–
LV ♀	243 9120	12-26-65	510	–	.1582	10.66	-33.82°	.309
AR ⊕	243 9270	5-25-66	150	770	.1078	11.30	26.15°	–

255

VENUS CONJUNCTIONS 26.3 JAN 1966 - 29.8 AUG 1967

	JUL. DATE	CAL. DATE	DUR. DAYS	TOTAL DAYS	V_{HE} EMOS	V_P KM/SEC	DECL.	REMAIN MASS
LV ⊕	243 9080	11-16-65	—	—	.0961	11.22	-2.90°	.437
AR ♀	243 9240	4-25-66	160	—	.1439	10.49	21.64°	—
LV ♀	243 9680	7-9-67	440	—	.1022	10.01	28.22°	.377
AR ⊕	243 9840	12-16-67	160	760	.0995	11.25	-2.59°	—
LV ⊕	243 9080	11-16-65	—	—	.0961	11.22	-2.90°	.437
AR ♀	243 9240	4-25-66	160	—	.1439	10.49	21.64°	—
LV ♀	243 9690	7-19-67	450	—	.1134	10.10	8.92°	.366
AR ⊕	243 9830	12-6-67	140	750	.1032	11.29	10.26°	—
LV ⊕	243 9100	12-6-65	—	—	.1385	11.60	6.44°	.400
AR ♀	243 9220	4-5-66	120	—	.1031	10.02	-7.39°	—
LV ♀	243 9680	7-9-67	460	—	.1022	1001	28.22°	.377
AR ⊕	243 9840	12-16-67	160	740	.0995	11.25	-2.59°	—
LV ⊕	243 9100	12-6-65	—	—	.1385	11.60	6.44°	.400
AR ♀	243 9220	4-5-66	120	—	.1031	10.02	-7.39°	—
LV ♀	243 9690	7-19-67	470	—	.1134	10.10	8.92°	.366
AR ⊕	243 9830	12-6-67	140	730	.1032	11.29	10.26°	—

VENUS CONJUNCTIONS 29.8 AUG 1967 - 8.6 APRIL 1969

	JUL. DATE	CAL. DATE	DUR. DAYS	TOTAL DAYS	V_{HE} EMOS	V_P KM/SEC	DECL	REMAIN. MASS
LV ⊕	243 9640	5-30-67	—	—	.0862	11.15	-9.14°	.444
AR ♀	243 9800	11-6-67	160	—	.1086	10.09	-22.27°	—
LV ♀	244 0250	1-29-69	450	—	.1418	10.45	-41.46°	.329
AR ⊕	244 0420	7-18-69	170	780	.0890	11.20	7.52°	—
LV ⊕	243 9640	5-30-67	—	—	.0862	11.15	-9.14°	.444
AR ♀	243 9800	11-6-67	160	—	.1086	10.09	-22.27°	—
LV ♀	244 0240	1-19-69	440	—	.1264	10.29	-0.42°	.348
AR ⊕	244 0380	6-8-69	140	742	.1176	11.41	-33.49°	—
LV ⊕	243 9660	6-19-67	—	—	.0966	11.21	-0.83°	.435
AR ♀	243 9790	10-27-67	130	—	.1041	10.02	-23.57°	—
LV ♀	244 0250	1-29-69	460	—	.1418	10.45	-41.46°	.329
AR ⊕	244 0420	7-18-69	170	760	.0890	11.20	7.52°	—
LV ⊕	243 9660	6-19-67	—	—	.0966	11.21	-0.83°	.435
AR ♀	243 9790	10-27-67	130	—	.1041	10.02	-23.57°	—
LV ♀	244 0240	1-19-69	450	—	.1264	10.29	-0.42°	.348
AR ⊕	244 0380	6-8-69	140	720	.1176	11.41	-33.49°	—

VENUS CONJUNCTION 11.0 APRIL 1961

	JUL. DATE	CAL. DATE	DUR. DAYS	TOTAL DAYS	V_{HE} EMOS	V_P KM/SEC	DECL.	REMAIN. MASS
LV ⊕	243 7150	8-4-60	—	—	.2350	12.90	-37.20°	.288
AR ♀	243 7390	4-1-61	240	—	.1524	10.61	31.88°	—
LV ♀	243 7400	4-11-61	10	—	.1283	10.30	-1.64°	.346
AR ⊕	243 7640	12-7-61	240	490	.2253	12.77	-8.52°	—
LV ⊕	243 7230	10-23-60	—	—	.2552	13.22	23.90°	.269
AR ♀	243 7390	4-1-61	160	—	.2925	11.94	-24.25°	—
LV ♀	243 7400	4-11-61	10	—	.2987	13.00	24.79°	.146
AR ⊕	243 7550	9-8-61	150	320	.2012	12.40	-28.71°	—

WORK SHEET

LOCKHEED MISSILES & SPACE COMPANY

2-59

VENUS CONJUNCTION 12.8 NOV. 1962

	JUL. DATE	CAL. DATE	DUR. DAYS	TOTAL DAYS	VHE EMOS	VP KM/SEC	DECL.	REMAIN. MASS
LV ⊕	243 7730	3-7-62	—	—	.2252	12.78	24.57°	.300
AR ♀	243 7970	11-2-62	240	—	.1776	10.91	-36.68°	—
LV ♀	243 7980	11-12-62	10	—	.1326	10.34	-10.07°	.339
AR ⊕	243 8200	6-20-63	220	470	.2000	12.40	10.74°	—
LV ⊕	243 7800	5-16-62	—	—	.2327	12.82	-32.20°	.290
AR ♀	243 7970	11-2-62	170	—	.2834	12.70	14.96°	—
LV ♀	243 7980	11-12-62	10	—	.2677	12.40	-29.23°	.178
AR ⊕	243 8130	4-11-63	150	330	.1886	12.21	35.03°	—

VENUS CONJUNCTION 19.9 JUNE 1964

	JUL. DATE	CAL. DATE	DUR. DAYS	TOTAL DAYS	VHE EMOS	Vp KM/SEC	DECL	REMAIN. MASS
LV ⊕	243 8340	11-7-63	—	—	.2271	12.80	10.52°	.299
AR ♀	243 8560	6-14-64	220	—	.1663	10.78	26.66°	—
LV ♀	243 8570	6-24-64	10	—	.1623	10.70	36.25°	.301
AR ⊕	243 8800	2-9-65	230	460	.2241	12.75	−15.22°	—
LV ⊕	243 8380	12-17-63	—	—	.2219	12.70	18.02°	.304
AR ♀	243 8560	6-14-64	180	—	.2436	12.00	20.32°	—
LV ♀	243 8570	6-24-64	10	—	.2393	11.89	−2.34°	[illegible]
AR ⊕	243 8740	12-11-64	174	360	.2161	12.60	−5.97°	—

LOCKHEED MISSILES & SPACE COMPANY

2-60

VENUS CONJUNCTION 26.3 JAN. 1966

		JUL. DATE	CAL. DATE	DUR. DAYS	TOTAL DAYS	V_{HE} EMOS	V_P KM/SEC	DECL.	REMAIN. MASS
LV ⊕		243 8910	5-30-65	—	—	.2129	12.55	-29.59°	.313
AR ♀		243 9140	1-15-66	230	—	.1480	10.50	-7.04°	—
LV ♀		243 9150	1-25-66	10	—	.1667	10.75	-40.61°	.296
AR ⊕		243 9380	9-12-66	230	470	.2060	12.45	11.83°	—
LV ⊕		243 8980	8-8-65	—	—	.2177	12.62	-7.96°	.310
AR ♀		243 9140	1-15-66	160	—	.2998	13.00	-26.02°	—
LV ♀		243 9150	1-25-66	10	—	.2523	12.11	8.42°	.191
AR ⊕		243 9300	6-24-66	150	320	.1906	12.26	-3.50°	—

2-61

LOCKHEED MISSILES & SPACE COMPANY

VENUS CONJUNCTION 29.8 AUG 1967

	JUL. DATE	CAL. DATE	DUR. DAYS	TOTAL DAYS	V_{HE} EMOS	V_P KM/SEC	DECL	REMAIN. MASS
LV ⊕	243 9480	12-21-66	—	—	.2426	13.10	37.99°	.280
AR ♀	243 9720	8-18-67	240	—	.1462	10.50	-8.26°	—
LV ♀	243 9730	8-28-67	10	—	.1384	10.40	25.51°	.333
AR ⊕	243 9970	4-24-68	240	490	.2284	12.80	2.49°	—
LV ⊕	243 9560	3-11-67	—	—	.2431	13.20	-3.68°	.279
AR ♀	243 9720	8-18-67	160	—	.3350	13.75	23.16°	—
LV ♀	243 9730	8-28-67	10	—	.2679	12.39	-14.96°	.177
AR ⊕	243 9870	1-15-68	140	310	.2039	12.42	11.89°	—

LOCKHEED MISSILES & SPACE COMPANY

2-62

VENUS CONJUNCTION 8.6 APRIL 1969

	JUL. DATE	CAL. DATE	DUR. DAYS	TOTAL DAYS	VHE EMOS	VP KM/SEC	DECL.	REMAIN. MASS
LV ⊕	244 0060	7-23-68	–	–	.2385	12.95	-36.90°	.284
AR ♀	244 0310	3-30-69	250	–	.1431	10.47	24.80°	–
LV ♀	244 0320	4-9-69	10	–	.1288	10.30	-3.19°	.346
AR ⊕	244 0560	12-5-69	240	500	.2257	12.79	-8.17°	–
LV ⊕	244 0150	10-21-68	–	–	.2544	13.21	24.47°	.268
AR ♀	244 0310	3-30-69	160	–	.2955	12.91	-26.43°	–
LV ♀	244 0320	4-9-69	10	–	.2997	13.00	24.52°	.145
AR ⊕	244 0470	9-6-69	150	320	.2024	12.41	-28.07°	–

LOCKHEED MISSILES & SPACE COMPANY

MARS OPPOSITIONS 30.4 DEC 1960 – 9.6 FEB 1963

	JUL. DATE	CAL. DATE	DUR. DAYS	TOTAL DAYS	V_{HE} EMOS	V_p KM/SEC	DECL	REMAIN. MASS
LV ⊕	243 7220	10-13-60	—	—	.2034	12.43	34.01°	.326
AR ♂	243 7350	2-20-61	130	—	.3048	10.20	-13.79°	—
LV ♂	243 7900	8-24-62	550	—	.1100	5.83	5.18°	.426
AR ⊕	243 8130	4-11-63	230	910	.1863	12.20	-3.25	—
LV ⊕	243 7220	10-13-60	—	—	.2034	12.43	34.01°	.326
AR ♂	243 7350	2-20-61	130	—	.3048	10.20	-13.79°	—
LV ♂	243 7880	8-4-62	530	—	.0930	5.60	3.68°	.520
AR ⊕	243 8180	5-31-63	300	960	.0963	11.25	-13.51°	—
LV ⊕	243 7230	10-23-60	—	—	.1819	12.13	40.09°	.350
AR ♂	243 7490	7-10-61	260	—	.0795	5.36	-17.66°	—
LV ♂	243 7900	8-24-62	410	—	.1100	5.83	5.18°	.426
AR ⊕	243 8130	4-11-63	230	900	.1863	12.20	-3.25°	—
LV ⊕	243 7230	10-23-60	—	—	.1819	12.13	40.09°	.350
AR ♂	243 7490	7-10-61	260	-	.0795	5.36	-17.66°	—
LV ♂	243 7880	8-4-62	390	—	.0930	5.60	3.68°	.520
AR ⊕	243 8180	5-31-63	300	950	.0963	11.25	-13.51°	—

WORK SHEET

MARS OPPOSITIONS 9.6 FEB 1963 – 9.5 MARCH 1965

	JUL. DATE	CAL. DATE	DUR. DAYS	TOTAL DAYS	V_{HE} EMOS	V_P KM/SEC	DECL.	REMAIN MASS
LV ⊕	243 8000	12-2-62	—	—	.2245	12.74	29.85°	.300
AR ♂	243 8130	4-11-63	130	—	.3141	10.50	-20.63°	—
LV ♂	243 8720	11-21-64	590	—	.1771	7.10	20.77°	.320
AR ⊕	243 8900	5-20-65	180	900	.1891	12.24	-2.77°	—
LV ⊕	243 8000	12-2-62	—	—	.2245	12.74	29.85°	.300
AR ♂	243 8130	4-11-63	130	—	.3141	10.50	-20.63	—
LV ♂	243 8710	11-11-64	580	—	.1552	6.70	28.94°	.368
AR ⊕	243 8930	6-19-65	220	930	.1400	11.63	-23.41°	—
LV ⊕	243 7980	11-12-62	—	—	.1399	11.62	39.89	.397
AR ♂	243 8260	8-19-63	280	—	.0841	5.45	-21.18	—
LV ♂	243 8720	11-21-64	460	—	.1771	7.10	20.77°	.320
AR ⊕	243 8900	5-20-65	180	920	.1891	12.24	-2.77°	—
LV ⊕	243 7980	11-12-62	—	—	.1399	11.62	39.89°	.397
AR ♂	243 8260	8-19-63	280	—	.0841	5.45	-21.18°	
LV ♂	243 8710	11-11-64	450	—	.1552	6.70	28.94°	.368
AR ⊕	243 8930	6-19-65	220	950	.1400	11.63	-23.41°	—

MARS OPPOSITIONS 9.5 MARCH 1965 – 15.5 APRIL 1967

	JUL. DATE	CAL. DATE	DUR. DAYS	TOTAL DAYS	V_{HE} EMOS	V_p KM/SEC	DECL.	REMAIN MASS
LV ⊕	243 8770	1-10-65	—	—	.2281	12.80	18.48°	.298
AR ♂	243 8900	5-20-65	130	—	.3062	10.25	-20.04°	
LV ♂	243 9430	11-1-66	530	—	.0888	5.50	35.10°	.530
AR ⊕	243 9660	6-19-67	230	890	.2001	12.40	5.25°	—
LV ⊕	243 8770	1-10-65	—	—	.2281	12.80	18.48°	.298
AR ♂	243 8900	5-20-65	130	—	.3062	10.25	-20.04°	—
LV ♂	243 9430	11-1-66	530	—	.0931	5.60	50.65°	.440
AR ⊕	243 9680	7-9-67	250	910	.1602	11.88	-11.70°	—
LV ⊕	243 8760	12-31-64	—	—	.1694	11.98	10.35°	.367
AR ♂	243 9000	8-28-65	240	—	.1127	5.90	-5.01°	—
LV ♂	243 9430	11-1-66	430	—	.0888	5.50	35.10°	.530
AR ⊕	243 9660	6-19-67	230	900	.2001	12.40	5.25°	—
LV ⊕	243 8760	12-31-64	—	—	.1694	11.98	10.35°	.367
AR ♂	243 9000	8-28-65	240	—	.1127	5.90	-5.01°	
LV ♂	243 9430	11-1-66	430	—	.0931	5.60	50.65°	.440
AR ⊕	243 9680	7-9-67	250	920	.1602	11.88	-11.70°	—

MARS OPPOSITIONS 15.5 APRIL 1967 – 1.5 JUNE 1969

	JUL. DATE	CAL. DATE	DUR. DAYS	TOTAL DAYS	V_{HE} EMOS	V_P KM/SEC	DECL	REMAIN MASS
LV ⊕	243 9540	2-19-67	—	—	.2128	12.56	-0.79°	.315
AR ♂	243 9660	6-19-67	120	—	.3126	10.44	-13.41°	—
LV ♂	244 0310	3-30-69	650	—	.2054	7.75	19.64°	.260
AR ⊕	244 0430	7-28-69	120	890	.2126	12.55	21.20°	—
LV ⊕	243 9540	2-19-67	—	—	.2128	12.56	-0.79°	.315
AR ♂	243 9660	6-19-67	120	—	.3126	10.44	-13.41°	—
LV ♂	244 0260	2-8-69	600	—	.1034	5.75	30.40°	490
AR ⊕	244 0460	8-27-69	200	920	.1313	11.55	8.66°	—
LV ⊕	243 9530	2-9-67	—	—	.1551	11.80	-12.44°	.380
AR ♂	243 9750	9-17-67	220	—	.1262	6.10	-1.52°	—
LV ♂	244 0310	3-30-69	560	—	.2054	7.75	19.64°	.260
AR ⊕	244 0430	7-28-69	120	900	.2126	12.55	21.20°	—
LV ⊕	243 9530	2-9-67	—	—	.1551	11.80	-12.44°	.380
AR ♂	243 9150	9-17-67	220	—	.1262	6.10	-1.52°	—
LV ♂	244 0260	2-8-69	510	—	.1034	5.75	30.40°	.490
AR ⊕	244 0460	8-27-69	200	930	.1313	11.55	8.66°	---

LOCKHEED MISSILES & SPACE COMPANY

2-68

MARS OPPOSITIONS 15 JUNE 1969 – 10.3 AUG. 1971

	JUL. DATE	CAL. DATE	DUR. DAYS	TOTAL DAYS	V_{HE} EMOS	V_P KM/SEC	DECL.	REMAIN. MASS
LV ⊕	244 0310	3-30-69	—	—	.1646	11.92	−28.80°	.370
AR ♂	244 0420	7-18-69	110	—	.3166	10.52	0.34°	—
LV ♂	244 1120	6-18-71	700	—	.2003	7.65	−9.88°	.270
AR ⊕	244 1220	9-26-71	100	910	.1904	12.25	21.66°	
LV ⊕	244 0310	3-30-69	—	—	.1646	11.92	−28.80°	.370
AR ♂	244 0420	7-18-69	110	—	.3166	10.52	0.34°	—
LV ♂	244 1080	5-9-71	660	—	.1014	5.70	−15.50°	.499
AR ⊕	244 1260	11-5-71	180	950	.1072	11.30	34.34°	—
LV ⊕	244 0310	3-30-69	—	—	.1236	11.45	−41.27°	.413
AR ♂	244 0510	10-16-69	200	—	.1216	6.06	1.04°	—
LV ♂	244 1120	6-18-71	610	—	.2003	7.65	−9.88°	.270
AR ⊕	244 1220	9-26-71	100	910	.1904	12.25	21.66°	
LV ⊕	244 0310	3-30-69	—	—	.1236	11.45	−41.27°	.413
AR ♂	244 0510	10-16-69	200	—	.1216	6.06	1.04°	—
LV ♂	244 1080	5-9-71	570	—	.1014	5.70	−15.50°	.499
AR ⊕	244 1260	11-5-71	180	950	.1072	11.30	34.34°	—

LOCKHEED MISSILES & SPACE COMPANY

2-69

MARS OPPOSITIONS 10.3 AUG. 1971 – 25.2 OCT 1973

	JUL. DATE	CAL. DATE	DUR. DAYS	TOTAL DAYS	V_{HE} EMOS	V_p KM/SEC	DECL.	REMAIN. MASS
LV ⊕	244 1110	6-8-71	—	—	.1812	12.15	−25.89°	.350
AR ♂	244 1200	9-6-71	90	—	.3041	10.24	17.29°	—
LV ♂	244 1870	7-7-73	670	—	.1448	6.55	−19.47°	.390
AR ⊕	244 2010	11-24-73	140	900	.2066	12.50	−8.95°	—
LV ⊕	244 1110	6-8-71	—	—	.1812	12.15	−25.89°	.350
AR ♂	244 1200	9-6-71	90	—	.3041	10.24	17.29°	—
LV ♂	244 1860	6-27-73	660	—	.1207	6.04	−34.66°	.449
AR ⊕	244 2050	1-3-74	190	940	.1090	11.34	15.71°	—
LV ⊕	244 1110	6-8-71	—	—	.1049	11.30	−22.92°	.430
AR ♂	244 1300	12-15-71	190	—	.0970	5.65	3.72°	—
LV ♂	244 1870	7-7-73	570	—	.1448	6.55	−19.47°	.390
AR ⊕	244 2010	11-24-73	140	900	.2066	12.15	−8.95°	—
LV ⊕	244 1110	6-8-71	—	—	.1049	11.30	−22.92°	.430
AR ♂	244 1300	12-15-71	190	—	.0970	5.65	3.72°	—
LV ♂	244 1860	6-27-73	560	—	.1207	6.04	−34.66°	.449
AR ⊕	244 2050	1-3-74	190	940	.1090	11.34	15.71°	—

MARS OPPOSITIONS 25.2 OCT. 1973 – 15.7 DEC. 1975

	JUL. DATE	CAL. DATE	DUR. DAYS	TOTAL DAYS	V_{HE} EMOS	V_P KM/SEC	DECL.	REMAIN. MASS
LV ⊕	244 1900	8-6-73	—	—	.2144	12.60	14.60°	.313
AR ♂	244 2000	11-14-73	100	—	.3098	10.30	12.75°	—
LV ♂	244 2660	9-5-75	660	—	.1759	7.10	-13.50°	.320
AR ⊕	244 2810	2-2-76	150	910	.2084	12.52	-17.05°	—
LV ⊕	244 1900	8-6-73	—	—	.2144	12.60	14.60°	.313
AR ♂	244 2000	11-14-73	100	—	.3098	10.30	12.75°	—
LV ♂	244 2630	8-6-75	630	—	.1331	6.25	-25.73°	.418
AR ⊕	244 2840	3-3-76	210	940	.1210	11.45	3.98°	—
LV ⊕	244 1890	7-27-73	—	—	.1276	11.50	30.77°	.410
AR ♂	244 2090	2-12-74	200	—	.0969	5.60	-5.63°	—
LV ♂	244 2660	9-5-75	570	—	.1759	7.1	-13.50°	.320
AR ⊕	244 2810	2-2-76	150	920	.2084	12.52	-17.05°	—
LV ⊕	244 1890	7-27-73	—	—	.1276	11.50	30.77°	.410
AR ♂	244 2090	2-12-74	200	—	.0969	5.60	-5.63°	—
LV ♂	244 2630	8-6-75	540	—	.1331	6.25	-25.73°	.418
AR ⊕	244 2840	3-3-76	210	950	.1210	11.45	3.98°	—

LOCKHEED MISSILES & SPACE COMPANY

MARS OPPOSITION 30.4 DEC. 1960

	JUL. DATE	CAL. DATE	DUR. DAYS	TOTAL DAYS	V_{HE} EMOS	V_P KM/SEC	DECL.	REMAIN. MASS
LV ⊕	243 7070	5-16-60	–	–	.3477	15.05	11.21°	.175
AR ♂	243 7310	1-11-61	240	–	.1489	6.55	14.20°	–
LV ♂	243 7320	1-21-61	10	–	.2024	7.73	19.33°	.265
AR ⊕	243 7580	10-8-61	260	510	.4369	16.95	7.75°	–
LV ⊕	243 7140	7-25-60	–	–	.3292	14.64	40.33°	.191
AR ♂	243 7310	1-11-61	170	–	.3063	10.30	-14.22°	–
LV ♂	243 7320	1-21-61	10	–	.2024	7.73	19.33°	.265
AR ⊕	243 7580	10-8-61	260	440	.4369	16.95	7.75°	–
LV ⊕	243 7000	3-7-60	–	–	.4437	17.12	-4.27°	.321
AR ♂	243 7200	9-23-60	200	–	.2405	8.65	18.72°	–
LV ♂	243 7210	10-3-60	10	–	.2094	7.92	-9.96°	.254
AR ⊕	243 7400	4-11-61	190	400	.1048	11.30	-23.86°	–

WORK SHEET

LOCKHEED AIRCRAFT CORPORATION

MARS OPPOSITION 9.6 FEB. 1963

	JUL. DATE	CAL. DATE	DUR. DAYS	TOTAL DAYS	V_{HE} EMOS	V_p KM/SEC	DECL.	REMAIN. MASS
LV ⊕	243 7990	11-22-62	–	–	.2085	12.52	28.76°	.320
AR ♂	243 8120	4-1-63	130	–	.3480	11.40	-21.23°	–
LV ♂	243 8130	4-11-63	10	–	.2313	8.48	21.47°	.212
AR ⊕	243 8360	11-27-63	230	370	.5147	18.80	22.85°	–
LV ⊕	243 7800	5-16-62	–	–	.5115	18.75	14.86°	.268
AR ♂	243 7990	11-22-62	190	–	.3124	10.50	6.20°	–
LV ♂	243 8000	12-2-62	10	–	.3044	10.28	10.07°	.120
AR ⊕	243 8160	5-11-63	160	360	.1597	11.86	-27.95°	–
LV ⊕	243 7800	5-16-62	–	–	.5115	18.75	14.86°	.268
AR ♂	243 7990	11-22-62	190	–	.3124	10.50	6.20°	–
LV ♂	243 8000	12-2-62	10	–	.2013	7.70	4.47°	.269
AR ⊕	243 8250	8-9-63	250	450	.2530	13.22	2.74°	–

2-72

LOCKHEED MISSILES & SPACE COMPANY

MARS OPPOSITION 9.5 MARCH 1965

			JUL. DATE	CAL. DATE	DUR. DAYS	TOTAL DAYS	V_{HE} EMOS	V_P KM/SEC	DECL	REMAIN. MASS	
	LV ⊕		243 8610	8-3-64	—	-	.3634	15.35	13.47°	.160	
	AR ♂		243 8840	3-21-65	230	-	.2548	9.00	-14.06°	—	
	LV ♂		243 8850	3-31-65	10	—	.2058	7.82	19.25°	.259	
	AR ⊕		243 9080	11-16-65	230	470	.4217	16.60	23.36°	—	

LOCKHEED MISSILES & SPACE COMPANY

WORK SHEET

LOCKHEED AIRCRAFT CORPORATION

LOCKHEED MISSILES & SPACE COMPANY

MARS OPPOSITION 15.5 APRIL 1967

	JUL. DATE	CAL. DATE	DUR. DAYS	TOTAL DAYS	V_{HE} EMOS	V_P KM/SEC	DECL.	REMAIN. MASS
LV ⊕	243 9400	10-2-66	–	–	.3371	14.85	-4.34°	.183
AR ♂	243 9600	4-20-67	200	–	.3504	11.50	-16.02°	–
LV ♂	243 9610	4-30-67	10	–	.1667	6.95	7.63°	.345
AR ⊕	243 9840	12-16-67	230	440	.3698	15.50	25.47°	–

WORK SHEET

LOCKHEED AIRCRAFT CORPORATION

MARS OPPOSITION 1.5 JUNE 1969

			JUL. DATE	CAL. DATE	DUR. DAYS	TOTAL DAYS	V_{HE} EMOS	V_P KM/SEC	DECL.	REMAIN. MASS	
	LV ⊕		244 0110	9-11-68	–	–	.3496	15.05	5.80°	.174	
	AR ♂		244 0350	5-9-69	240	–	.2520	8.95	-17.54°	–	
	LV ♂		244 0360	5-19-69	10	–	.1469	6.52	1.05°	.388	
	AR ⊕		244 0580	12-25-69	220	470	.2746	13.60	19.15°	–	

MARS OPPOSITION 10.3 AUG. 1971

	JUL. DATE	CAL. DATE	DUR. DAYS	TOTAL DAYS	VHE EMOS	VP KM/SEC	DECL.	REMAIN. MASS
LV ⊕	244 0880	10-21-70	–	–	.3470	15.00	-7.01°	.175
AR ♂	244 1100	5-29-71	220	–	.2828	9.70	-10.64°	–
LV ♂	244 1110	6-8-71	10	–	.1509	6.60	-12.54°	.379
AR ⊕	244 1250	10-26-71	140	370	.1208	11.45	31.12°	–
LV ⊕	244 0880	10-21-70	–	–	.3470	15.00	-7.01°	.175
AR ♂	244 1100	5-29-71	220	–	.2828	9.70	-10.64°	–
LV ♂	244 1130	6-28-71	30	–	.1965	7.60	-14.85°	.278
AR ⊕	244 1260	11-5-71	130	380	.1361	11.57	33.73°	–
LV ⊕	244 1120	6-18-71	–	–	.2111	12.53	-26.30°	.317
AR ♂	244 1200	9-6-71	80	–	.3217	10.70	16.68°	–
LV ♂	244 1210	9-16-71	10	–	.1911	7.48	-13.37°	.289
AR ⊕	244 1450	5-13-72	240	330	.2755	13.63	-24.39°	–
LV ⊕	244 1090	5-19-71	–	–	.2127	12.58	-20.30°	.315
AR ♂	244 1180	8-17-71	90	–	.3885	12.55	17.64°	–
LV ♂	244 1190	8-27-71	10	–	.1337	7.30	-17.85°	.305
AR ⊕	244 14[illegible]	4-13-72	230	330	.2509	13.18	-18.99°	–

MARS OPPOSITION 10.3 AUG. 1971 (CONT'D)

	JUL. DATE	CAL. DATE	DUR. DAYS	TOTAL DAYS	V_{HE} EMOS	V_P KM/SEC	DECL.	REMAIN. MASS
LV ⊕	244 1090	5-19-71	–	–	.2127	12.58	-20.60°	.315
AR ♂	244 1180	8-17-71	90	–	.3885	12.55	17.64°	–
LV ♂	244 1210	9-16-71	30	–	.1911	7.48	-18.37°	.289
AR ⊕	244 1450	5-13-72	240	360	.2755	13.65	-24.69°	–

MARS OPPOSITION 25.2 OCT. 1973

	JUL. DATE	CAL DATE	DUR. DAYS	TOTAL DAYS	V_{HE} EMOS	V_p KM/SEC	DECL.	REMAIN. MASS
LV ⊕	244 1700	1-18-73	—	—	.2990	14.08	−15.66°	.222
AR ♂	244 1930	9-5-73	230	—	.1806	7.25	3.62°	—
LV ♂	244 1940	9-15-73	10	—	.3131	10.50	−26.03°	.111
AR ⊕	244 2050	1-3-74	110	350	.1465	11.75	−2.79°	—
LV ⊕	244 1700	1-18-73	—	—	.2990	14.08	−15.66°	.222
AR ♂	244 1930	9-5-73	230	—	.1806	7.20	3.62°	—
LV ♂	244 1940	9-15-73	10	—	.1922	7.53	−13.89°	.288
AR ⊕	244 2170	5-3-74	230	470	.1955	12.35	−31.17°	—
LV ⊕	244 1700	1-18-73	—	—	.2990	14.08	−15.66°	.222
AR ♂	244 1930	9-5-73	230	—	.1806	7.20	3.62°	—
LV ♂	244 1960	10-5-73	30	—	.2039	7.78	−13.92°	.267
AR ⊕	244 2200	6-2-74	240	500	.2359	12.95	−28.23°	—
LV ⊕	244 1900	8-6-73	—	—	.2144	12.60	14.60°	.312
AR ♂	244 2000	11-14-73	100	—	.3098	10.40	12.75°	—
LV ♂	244 2010	11-24-73	10	—	.2072	7.85	0.03°	.258
AR ⊕	244 2270	8-11-74	260	370	.3559	15.20	−16.44°	—

LOCKHEED MISSILES & SPACE COMPANY

WORK SHEET

LOCKHEED AIRCRAFT CORPORATION

MARS OPPOSITION 15.7 DEC. 1975

	JUL. DATE	CAL. DATE	DUR. DAYS	TOTAL DAYS	V_{HE} EMOS	V_P KM/SEC	DECL	REMAIN. MASS
LV ⊕	244 2610	7-17-75	—	—	.3319	14.7	29.72°	.189
AR ♂	244 2760	12-14-75	150	—	.3324	11.1	-1.02°	—
LV ♂	244 2770	12-24-75	10	—	.2775	9.6	4.53°	.151
AR ⊕	244 3000	8-10-76	230	390	.3567	15.2	-10.00°	—
LV ⊕	244 2500	3-29-75	—	—	.3640	15.4	0.22°	.160
AR ♂	244 2730	11-14-75	230	—	.1616	6.9	17.81°	—
LV ♂	244 2740	11-24-75	10	—	.2216	8.2	2.65°	.230
AR ⊕	244 2990	7-31-76	250	490	.2992	14.5	-13.50°	—

MARS OPPOSITION 25.2 OCT. 1973 (CONT'D)

	JUL. DATE	CAL. DATE	DUR. DAYS	TOTAL DAYS	VHE EMOS	VP KM/SEC	DECL.	REMAIN. MASS
LV ⊕	244 1820	5-18-73	—	—	.2973	14.02	4.76°	.223
AR ♂	244 1960	10-5-73	140	—	.3085	10.30	22.67°	—
LV ♂	244 1970	10-15-73	10	—	.2000	7.67	-11.48°	.270
AR ⊕	244 2220	6-22-74	250	400	.2621	13.32	-26.57°	—

2.5 SAMPLE EXPEDITION PLANS

Representative sample plans of expeditions to Mars and Venus have been prepared for 1969 — 1971. Every short stopover expedition to Mars is a special case. The long stopover trips to Mars are similar to one another. There is relatively little difference from one to another of the short stopover trips to Venus, and almost no difference from one to another long stopover trip to Venus. It can be seen from the plans that they center more on maneuvers than on equipment. Most of the starting cargo is propellant. A plan is a sequence of schedules and maneuvers. Equipment will be designed around the plan more than the plan is designed around the equipment. Even apparently fixed items such as solar-flare radiation shields can be considerably modified by the assumption of open or closed cycle ecology, etc.

1969 VENUS CAPTURE EXPEDITION

Several men, 10 days at Venus, 500 days round trip

Lv ⊕ 244 0060, V_{HE} = 0.2385, V_p = 12.9 km/sec, decl. = -36.95 deg
Ar ♀ 244 0310, V_{HE} = 0.1431, V_p = 10.8 km/sec, duration = 250 days
Stay at Venus 10 days
Lv ♀ 244 0320, V_{HE} = 0.1288, V_p = 10.6 km/sec
Ar ⊕ 244 0560, V_{HE} = 0.2257, V_p = 12.8 km/sec, duration = 240 days

	tons
Launch mass	6,000
Remaining mass on parking orbit	730
Jettison on parking orbit 100 tons	630
Enter hyperbolic orbit, 0.286 × 630	180.18
Midcourse correction, 0.9 × 180.18	162.16
Homing on Venus, 0.96 × 162.16	155.67
Drag brake retardation	155.67
Circularize orbit, 0.99 × 155.67	154.11
Jettison 40 tons, including 10 tons of probes	114.11
Depart from orbit, 0.33 × 114.11	37.66
Midcourse correction, 0.9 × 37.66	33.89
Homing on Earth, 0.96 × 33.89	32.53

Includes 7.5 tons of liquid metabolic waste for four men, more for additional men

1969 MARS CAPTURE EXPEDITION

Two men, 10 days at Mars, 460 days round trip

Lv ⊕ 244 0110, V_{HE} = 0.3496, V_p = 15.0 km/sec, decl. = 5.80 deg
Ar ♂ 244 0350, V_{HE} = 0.2520, V_p = 13.9 km/sec, duration = 240 days
Stay at Mars 10 days
Lv ♂ 244 0360, V_{HE} = 0.1469, V_p = 6.5 km/sec
Ar ⊕ 244 0580, V_{HE} = 0.2746, V_p = 13.6 km/sec

	tons
Launch mass	6,000
Remaining mass on parking orbit	750
Jettison on parking orbit 100 tons	650
Enter hyperbolic orbit, 0.174 × 650	113.30
Midcourse correction, 0.9 × 113.30	101.97
Homing on Mars, 0.96 × 101.97	97.89
Retrorocket retardation, 1.7 km/sec, 0.6 × mass	58.73
Drag brake retardation	58.73
Circularize orbit for remaining mass, 0.99 × mass	58.14
Release 30 tons no longer needed mass	28.14
Enter hyperbolic orbit, 0.388 × 28.14	10.92
Midcourse correction, 0.9 × 10.92	9.83
Homing on Earth, 0.96 × 9.83	9.43
Includes 5 tons liquid metabolic waste	

1969 MARS LANDING EXPEDITION — TWO SPACE VEHICLES

Four men, 10 days at Mars, 460 days round trip

Lv $\oplus$ 244 0110, V_{HE} = 0.3496, V_p = 15.0 km/sec, decl. = 5.80 deg
Ar ♂ 244 0350, V_{HE} = 0.2520, V_p = 13.9 km/sec, duration = 240 days
Stay at Mars 10 days
Lv ♂ 244 0360, V_{HE} = 0.1469, V_p = 6.5 km/sec
Ar $\oplus$ 244 0580, V_{HE} = 0.2746, V_p = 13.6 km/sec, duration = 220 days

	#1 (tons)	#2 (tons)
Launch mass	6,000	6,000
Remaining mass on parking orbit	750	750
Jettison on parking orbit 100 tons	650	650
Enter hyperbolic orbit, 0.174 × 650	113.30	113.30
Midcourse correction, 0.9 × 113.30	101.97	101.97
Transfer surplus propellant from vehicle 2 to 1	134.50	69.44
Homing on Mars, 0.96 × mass	131.12	66.66
Retrorocket retardation, 1.7 km/sec, 0.6 × mass	78.67	40.00
Drag brake retardation	78.67	40.00
Send down two 40 ton landing packages	38.67	00.00
Circularize remaining mass on orbit, 0.99 × mass	38.38	
Rendezvous and reorientation of orbit, 0.9 × mass	34.54	
Enter hyperbolic orbit, 0.388 × 34.54	13.40	
Midcourse correction, 0.9 × 13.40	12.06	
Homing on Earth, 0.96 × 12.06	11.58	
Includes 7.5 tons liquid metabolic waste		

1969 — 1971 MARS LANDING EXPEDITION

Eight men, 570 days at Mars, 950 days round trip

Lv ⊕ 244 0310, V_{HE} = 0.1236, V_p = 11.5 km/sec, decl, = -41.27 deg
Ar ♂ 244 0510, V_{HE} = 0.1216, V_p = 6.1 km/sec, duration = 200 days
Stay at Mars 570 days
Lv ♂ 244 1080, V_{HE} = 0.1014, V_p = 5.7 km/sec
Ar ⊕ 244 1260, V_{HE} = 0.1072, V_p = 11.4 km/sec, duration = 180 days

	tons
Launch mass	6,000
Remaining mass on parking orbit, approx.	730
Jettison on parking orbit 100 tons	630
Enter hyperbolic orbit, 0.413 × 630	260.19
Midcourse correction, 0.9 × 260.19	234.17
Homing on Mars, 0.96 × 234.17	224.80
Drag brake retardation and descent	224.80
Landing retrorocket, 90 m/sec + 10 sec hover, 0.988 × mass	222.10
Includes 30 tons rocket structure used for materials	192.10
Allow 50 tons for 8 men for 570 days residence on Mars	142.10
Launch from surface of Mars to hyperbolic orbit, 0.17 mass	24.14
Midcourse correction, 0.9 × 24.14	21.73
Homing on Earth, 0.96 × 21.73	20.86
Includes 10 tons liquid metabolic waste	

1971 MARS LANDING EXPEDITION — THE VOID VOYAGER

Four men, 10 days at Mars, 330 days round trip

Lv ⊕ 244 1090, V_{HE} = 0.2127, V_p = 12.6 km/sec, decl. = -20.60 deg
Ar ♂ 244 1180, V_{HE} = 0.3885, V_p = 12.5 km/sec, duration 90 days.
Stay at Mars 10 days
Lv ♂ 244 1190, V_{HE} = 0.1837, V_p = 7.3 km/sec,
Ar ⊕ 244 1420, V_{HE} = 0.2509, V_p = 13.2 km/sec, duration 230 days

	tons
Launch mass	6,000
Remaining mass on orbit	750
Jettison on parking orbit 100 tons	650
Enter hyperbolic perigee, 0.315 × 650	204.75
Midcourse correction, 0.9 × 204.75	184.28
Homing on Mars, 0.96 × 184.28	176.91
Drag brake retardation	176.91
Release 40 ton landing package	136.71
Circularize orbit for remaining mass, 0.99 × 136.91	135.51
Rendezvous and reorientation of orbit, 0.9 × 135.51	121.99
Enter hyperbolic orbit, 0.305 × 121.99	37.20
Midcourse correction, 0.9 × 37.20	33.48
Homing on Earth, 0.96 × 33.48	32.19
Retrorocket retardation from 13.2 to 12.2 km/sec, 0.72 mass	23.14
Includes 7.5 tons liquid metabolic waste	

1971 MARS LANDING EXPEDITION—THREE SUPER NOVAS*

Four men, 10 days at Mars, 330 days round trip

Lv ⊕ 244 1090, V_{HE} = 0.2127, V_p = 12.6 km/sec, decl. = -20.60 deg
Ar ♂ 244 1180, V_{HE} = 0.3885, V_p = 12.5 km/sec, duration = 90 days
Stay at Mars 10 days
Lv ♂ 244 1190, V_{HE} = 0.1837, V_p = 7.3 km/sec
Ar ⊕ 244 1420, V_{HE} = 0.2509, V_p = 13.2 km/sec, duration = 230 days

	Pinta (tons)	Nino (tons)	Santa Maria (tons)
Launch 3 Novas	—	—	—
Loaded stages on parking orbit	181.82	181.82	181.82
Enter hyperbolic orbit, 0.315 × 181.82	57.27	57.27	57.27
Midcourse correction, 0.9 × 57.27	51.54	51.54	51.54
Transfer 41.54 tons propellant	10.00	93.08	51.54
Abandon 10 tons empty rocket	00.00	93.08	51.54
Home on Mars, 0.96 × mass		89.35	49.48
Drag brake retardation		89.35	49.48
Land, retrorocket, hover 10 sec., 0.988 × 49.48		89.35	48.88
Circularize orbit, 0.99 × 89.35		88.94	
Jettison 10 tons		78.94	
Rendezvous, reorient, 0.9 × 78.94		71.04	
Enter hyperbolic orbit, 0.305 × 71.04		21.66	
Midcourse correction, 0.9 × 21.66		19.49	
Homing on Earth, 0.96 × 19.49		18.71	
Includes 7.5 tons liquid metabolic waste			

*Novas described in Wall Street Journal, 19 Jan 1962

1971 MARS LANDING EXPEDITION

Four men, 10 days at Mars, 370 days round trip

Lv ⊕ 244 0880, V_{HE} = 0.3470, V_p = 15.0 km/sec, decl. = 7.01 deg
Ar ♂ 244 1100, V_{HE} = 0.2828, V_p = 9.9 km/sec, duration = 220 days
Stay on Mars 10 days
Lv ♂ 244 1110, V_{HE} = 0.1509, V_p = 6.6 km/sec
Ar ⊕ 244 1250, V_{HE} = 0.1208, V_p = 11.48 km/sec, duration = 140 days

	tons
Initial mass	6,000
Remaining mass on parking orbit	750
Jettison on parking orbit 100 tons	650
Enter hyperbolic orbit, 0.175 × 650	113.75
Midcourse correction, 0.9 × 113.75	102.37
Homing on Mars, 0.96 × 102.37	98.28
Drag brake retardation	98.28
Release 40 ton landing package	58.28
Circularize orbit for remaining mass, 0.99 × 58.28	57.70
Rendezvous and reorientation of orbit, 0.9 × 57.70	51.93
Departure from satellite orbit, 0.379 × 51.93	19.68
Midcourse correction, 0.9 × 1968	17.71
Homing on Earth, 0.96 × 17.71	17.00
Includes 7.5 tons liquid metabolic waste	

1973 MARS LANDING EXPEDITION

Four men, 10 days at Mars, 350 days round trip

Lv ⊕ 244 1700, V_{HE} = 0.2990, V_p = 14.0 km/sec, decl. = -15.66 deg
Ar ♂ 244 1930, V_{HE} = 0.1806, V_p = 7.25 km/sec, duration = 230 days
Stay at Mars 10 days
Lv ♂ 244 1940, V_{HE} = 0.3131, V_p = 9.2 km/sec
Ar ⊕ 244 2050, V_{HE} = 0.1465, V_p = 11.7 km/sec, duration = 110 days

	tons
Launch mass	6,000
Remaining mass on orbit	750
Jettison on parking orbit 100 tons	650
Enter hyperbolic orbit, 0.222 × 650	144.30
Midcourse correction, 0.9 × 144.30	129.87
Homing on Mars, 0.96 × 129.87	124.67
Release 40 tons landing package	84.67
Circularize orbit for remaining mass, 0.99 × mass	83.82
Rendezvous and reorientation of orbit, 0.9 × mass	75.44
Enter hyperbolic orbit, 0.288 × 75.44	21.73
Midcourse correction, 0.9 × 21.73	19.56
Homing on Earth, 0.96 × 19.56	18.78
Includes 7.5 tons liquid metabolic waste	

1973 MARS LANDING EXPEDITION—TWO SPACE VEHICLES

Four men, 10 days at Mars, 350 days round trip

Lv ⊕ 244 1700, V_{HE} = 0.2990, V_p = 14.0 km/sec, decl. = -15.66 deg
Ar ♂ 244 1930, V_{HE} = 0.1806, V_p = 7.25 km/sec, duration = 230 days
Lv ♂ 244 1940, V_{HE} = 0.3131, V_p = 9.2 km/sec
Ar ⊕ 244 2050, V_{HE} = 0.1465, V_p = 11.7 km/sec, duration = 110 days

	# 1 (tons)	# 2 (tons)
Launch mass	6,000	6,000
Remaining mass on parking orbit	750	750
Jettison on parking orbit 100 tons	650	650
Enter hyperbolic orbit, 0.222 × 650	144.30	144.30
Midcourse correction, 0.9 × 144.30	129.87	129.87
Transfer 88.21 tons propellant from vehicle 2 to 1	218.08	41.66
Homing on Mars, 0.96 × mass	209.36	40.00
Release two 40-ton landing packages	169.36	00.00
Circularize orbit for remaining mass, 0.99 × mass	167.67	
Rendezvous and reorientation of orbit, 0.9 × mass	150.90	
Departure from orbit, 0.111 × 150.90	16.75	
Midcourse correction, 0.9 × 16.75	15.07	
Homing on Earth, 0.96 × 15.07	14.47	

Includes 7.5 tons of liquid metabolic waste

Section 3
SPACE MISSIONS LAUNCHED NORMAL TO THE ECLIPTIC

3.1 INTRODUCTION

A vehicle launched from the Earth normal to the ecliptic enters a heliocentric orbit which returns to the vicinity of the Earth every 6 months. Except for appreciable hyperbolic excess speeds, however, escape from the Earth is not complete and the vehicle returns to Earth in less than 6 months.

The analysis of the vehicle's trajectory will be based on the supposition that not only does the distance from Earth, measured in astronomical units, remain small, but that also the vehicle's direction from Earth remains approximately perpendicular to the ecliptic plane. More specifically, if a rotating coordinate system is introduced, centered at the Earth as indicated in Fig. 3-1, the coordinates x, y, z are assumed to be such that $x, z << y << 1$. To the extent that $(x/y)^2$ and $(z/y)^2$ may be neglected, the y motion turns out to be uncoupled from the small x and z motions and may be studied separately.

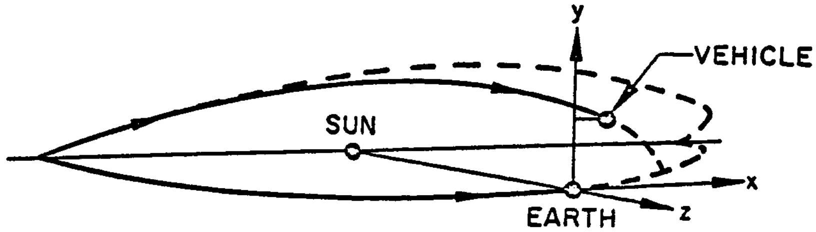

Fig. 3-1 Trajectory Geometry

After the equations of motion have been worked out in general (subsection 3.2), the basic one-dimensional y motion for a zero-eccentricity Earth orbit is investigated in subsection 3. 3. As may be anticipated, this motion, which includes both the Sun's attraction and the Earth's attraction as "restoring" forces tending to reduce y to zero, depends on a single parameter — the one-dimensional total energy. It will be found (Fig. 3-2) that for total energies in the neighborhood of zero, in fact for orbit injection speeds differing from the theoretical escape speed by not more than 100 m/sec, the maximum distance from Earth varies from less than 1/2- to more than 7-1/2-million km, and the trip duration from less than 2 weeks to more than 5-1/2 months.

The linearized equation for the small "off-line" x and z motions are considered in subsection 3-4, wherein y is now regarded as the 1-parameter function of time obtainable from subsection 3-3. The coordinate z contains, not surprisingly, a "driving term" proportional to y^2. The validity of the whole analysis depends, of course, on x/y and z/y remaining small when their "initial" values (i. e., shortly after launch) are small. The solution for the x and z motions will be obtained by variation of four small parameters, namely, the x- and z-direction cosines of the perigee of the geocentric conic and the x and z components of the geocentric angular momentum vector. The form of the equations of variation of parameters, Eqs. (3. 23) and (3. 24) below, suggests that the small parameters do indeed remain small at least for energies not too far in excess of zero (i. e., for values of the energy parameter η of subsection 3-3 not too close to 1), i.e., for trips lasting not too close to 6 months, but the numerical evaluations must be awaited for a better picture of what happens. The linearized x and z motions will provide, in addition, an indication not only of the effect of launch errors but also of the effect of mid-course velocity vector changes.

The perturbations of the previous solutions by the eccentricity of the Earth's orbit will be examined in subsection 3-5, and those by the Moon in subsection 3-6. In the latter case, the Moon is idealized as moving in a circle in

the ecliptic plane, an idealization which may be expected to give a realistic first-order account, since the unperturbed motion is perpendicular to the ecliptic plane while the maximum angular departure of the Moon from this plane is less than 6 deg.

3.2 THE EQUATIONS OF MOTION RELATIVE TO THE EARTH

Let $\vec{r}$ be the position vector of the vehicle relative to Earth, and $\vec{R}$ that of the Earth relative to the Sun. The acceleration of the vehicle relative to Earth is given by

$$\ddot{\vec{r}} = -\frac{GM_E\vec{r}}{r^3} - \left[\frac{GM_S(\vec{R}+\vec{r})}{|\vec{R}+\vec{r}|^3} - \frac{GM_S\vec{R}}{R^3}\right] \tag{3.1}$$

G being the universal gravitational constant and M_E, M_S the masses of Earth and Sun, respectively, and the square bracketed term being the "perturbative" acceleration due to the Sun.

Evaluating $\ddot{\vec{r}}$ in the rotating coordinate system indicated in Fig. 3-1, we have:

$$\ddot{\vec{r}} = \frac{\partial}{\partial t}\dot{\vec{r}} + \vec{\Omega} \times \dot{\vec{r}} = \frac{\partial}{\partial t}\left(\frac{\partial}{\partial t}\vec{r} + \vec{\Omega} \times \vec{r}\right) + \vec{\Omega} \times \left(\frac{\partial}{\partial t}\vec{r} + \vec{\Omega} \times \vec{r}\right)$$

$$= \frac{\partial^2}{\partial t^2}\vec{r} + 2\vec{\Omega} \times \frac{\partial}{\partial t}\vec{r} + \frac{\partial\vec{\Omega}}{\partial t} \times \vec{r} + \vec{\Omega} \times \left(\vec{\Omega} \times \vec{r}\right) \tag{3.2}$$

where $\frac{\partial}{\partial t}$ indicates time differentiation of the respective components, and $\vec{\Omega}$ the angular velocity of the rotating coordinate system. Introducing the components $(a_o x,\ a_o y,\ a_o z)$ of $\vec{r}$, where a_o is the Earth's mean distance from the Sun (=1 astronomical unit), and the components $(o,\ \dot{\theta},\ o)$ of $\vec{\Omega}$, θ being the Earth's heliocentric angular position along its orbit,

measured from some fixed direction, as well as the components (o, o, R) of $\vec{R}$, we obtain from Eqs. (3.1) and (3.2):

$$\ddot{x} - \dot{\theta}^2 x + 2\dot{\theta}\dot{z} + \ddot{\theta} z = -\frac{GM_E x}{a_o^3\left(x^2+y^2+z^2\right)^{3/2}} - \frac{GM_s x}{\left[a_o^2\left(x^2+y^2\right)+\left(R+a_o z\right)^2\right]^{3/2}}$$

$$\ddot{y} = -\frac{GM_E y}{a_o^3\left(x^2+y^2+z^2\right)^{3/2}} - \frac{GM_s y}{\left[a_o^2\left(x^2+y^2\right)+\left(R+a_o z\right)^2\right]^{3/2}}$$

$$\ddot{z} - \dot{\theta}^2 z - 2\dot{\theta}\dot{x} - \ddot{\theta} x = -\frac{GM_E z}{a_o^3\left(x^2+y^2+z^2\right)^{3/2}} - \frac{GM_s (R+a_o z)}{a_o\left[a_o^2\left(x^2+y^2\right)+\left(R+a_o z\right)^2\right]^{3/2}} + \frac{GM_s}{a_o R^2} \qquad (3.3)$$

We now introduce as an independent variable, in place of time, the mean anomaly ϕ of the Earth's motion, so that $R \cong a_o(1-\epsilon_E \cos\phi)$, ϵ_E being the eccentricity of the Earth's orbit, and

$$\frac{d}{d\phi} = \left(\frac{a_o^3}{GM_S}\right)^{1/2} \frac{d}{dt}$$

Expanding in ascending powers of y, $\frac{x}{y}$, $\frac{z}{y}$, the second Eq. (3.3) becomes:

$$\frac{d^2y}{d\phi^2} + y(1+3\epsilon_E \cos\phi) + \frac{\rho}{y^2} = 0 \qquad (3.4)$$

where

$$\rho = \frac{M_E}{M_S} \;(<<1) \qquad (3.5)$$

and where, in accordance with the smallness of ϵ_E and with our underlying assumption: $x, z << y << 1$, we have neglected ϵ_E^2, yz, y^3, $\frac{\rho x^2}{y^2}$, etc. The first and last Eq. (3.3), moreover, linearized with respect to x and z, become:

$$\frac{d^2x}{d\phi^2} + 2\frac{dz}{d\phi} + \frac{\rho x}{y^3} = 0$$

$$\frac{d^2z}{d\phi^2} - 3z - 2\frac{dx}{d\phi} + \frac{\rho z}{y^3} = \frac{3}{2}y^2 \tag{3.6}$$

where we have neglected y^4 and products of ϵ_E or y^2 with the small quantities x and z, which products include the $\ddot{\theta}$ terms in Eq. (3.3).

3.3 BASIC ONE-DIMENSIONAL MOTION

Neglecting ϵ_E in Eq. (3.4) (it will be reintroduced in subsection 3.5), we have:

$$\frac{d^2y}{d\phi^2} + y + \frac{\rho}{y^2} = 0 \tag{3.7}$$

We immediately obtain an "energy" integral:

$$\frac{1}{2}\left(\frac{dy}{d\phi}\right)^2 + \frac{1}{2}y^2 - \frac{\rho}{y} = E \tag{3.8}$$

a constant.

A further quadrature yields the time (through ϕ) as follows:

$$\phi - \phi_o = \int_o^y \frac{\sqrt{y}\,dy}{\sqrt{2\rho + 2Ey - y^3}} \tag{3.9}$$

where the lower limit is taken as zero, rather than some initial $y_o << \rho^{1/3}$ (at which distance the perturbing force due to the Sun is much smaller than the Earth's attraction), so that the contribution to ϕ between o and y_o is unimportant.

A convenient description of the motion, involving essentially one parameter, is obtained if we introduce y_1, the maximum y reached, given by:

$$2\rho + 2Ey_1 - y_1^3 = 0$$

and a nondimensional energy parameter η given by:

$$\eta = \frac{2E}{y_1^2} = 1 - \frac{2\rho}{y_1^3} \tag{3.10}$$

so that

$$y_1 = \left(\frac{2\rho}{1-\eta}\right)^{1/3} \tag{3.11}$$

As the parameter η varies from $-\infty$ to $+1$, the maximum distance y_1 (in astronomical units) varies from 0 to ∞. Our solution, of course, is valid only over the range of values of η for which $y_1 << 1$ (e.g., $y_1 < 0.1$).

The Earth's position during the outward motion of the vehicle is given by:

$$\phi - \phi_o = \int_o^{(y/y_1)} \frac{\sqrt{u}\, du}{\sqrt{(1-u)(1-\eta+u+u^2)}} \tag{3.12}$$

and the total angular travel of the Earth, and hence the total time, by, say,

$$\phi_2 - \phi_o = 2(\phi_1 - \phi_o) = 2\int_o^1 \frac{\sqrt{u}\ du}{\sqrt{(1-u)(1-\eta+u+u^2)}} = f(\eta) \qquad (3.13)$$

In particular, $f\left(\frac{3}{4}\right) = \frac{2\pi}{\sqrt{3}}\left(\sqrt{3}-1\right)$. Other values of $f(\eta)$ may be obtained from tables of elliptic functions. Thus if $\eta < \frac{3}{4}$, $f(\eta)$ may be evaluated according to 3(d) on p. 48 of Gröbner and Hofreiter's Integral Tafeln, Vol 2, while if $\eta > \frac{3}{4}$, $f(\eta)$ may be evaluated by 3(a) on p. 67.

The parameter η, in turn, may be related to the speed v_o at a specified small radial distance r_o from Earth, at which distance the potential energy term $\frac{1}{2}y^2$ due to the Sun's perturbative force may be assumed to be negligible by comparison with the potential energy term $-\rho/y$ due to the Earth's attraction, so that:

$$\frac{1}{2}v_o^2 - \frac{GM_E}{r_o} = \frac{GM_s}{a_o}\left[\frac{1}{2}\left(\frac{dy}{d\phi}\right)^2 - \frac{\rho}{y}\right] \cong \frac{GM_s}{a_o} E$$

(at $y << \rho^{1/3}$)

$$= \frac{GM_s}{a_o}\frac{\eta y_1^2}{2} = \frac{GM_E}{r_o}\cdot\frac{1}{\rho}\frac{r_o}{a_o}\frac{\eta}{2}\left(\frac{2\rho}{1-\eta}\right)^{2/3}$$

and hence, assuming that v_o is close to $\sqrt{\frac{2GM_E}{r_o}}$:

$$v_o \cong \sqrt{\frac{2GM_E}{r_o}}\left\{1 + \frac{\eta}{\left[2(1-\eta)^2\right]^{1/3}}\ \frac{1}{2\rho^{1/3}}\left(\frac{r_o}{a_o}\right)\right\} \qquad (3.14)$$

Equations (3.11), (3.13), and (3.14) may be used to plot the relations between maximum distance, "initial" speed, and flight duration. Thus, in Fig. 3-2, the ordinate is $f(\eta)$, the Earth's angular travel, the lower abscissa is $(1-\eta)^{-1/3}$ (or, rather, its logarithm), and the upper abscissa is $\eta/\left[2(1-\eta)^2\right]^{1/3} = g(\eta)$, say, so that by suitable rescaling we can read the maximum distance $a_o y_1$, in millions of km, $\Delta v_o = v_o - \sqrt{\frac{2GM_E}{r_o}}$ in m/sec, with r_o chosen as 150 km in excess of the Earth's equatorial radius, versus the flight duration in days.

By further rescaling, Fig. 3-2 may be used for trips launched from other planets perpendicular to their heliocentric orbital planes or from the moon perpendicular to its orbital plane, etc. The ordinate rescaling obviously corresponds to the various planetary half-years or the lunar half-month, etc. The scales for the abscissa are determined from the values corresponding to $\eta = -1$ and $g(\eta) = -\frac{1}{2}$, some of which are tabulated in Table 3-1.

The sensitivity of the flight duration and the maximum distance reached to initial speed is apparent from Fig. 3-2. To evaluate the sensitivity of the return time to mid-course changes, small or otherwise, in the velocity in the y-direction, it will be necessary to evaluate the intermediate times by means of Eq. (3.12). These will be evaluated by numerical integration, for both the outward and return journeys, after introduction, in place of u, of the variable $s = \mp\sqrt{1-u}$, according as $\dot{y} \gtrless 0$.

3.4 OFF-LINE MOTIONS

Before attacking the Eq. (3.6) of off-line motion, let us examine the significance of the assumption $x, \; z << y$ in the neighborhood of the Earth.

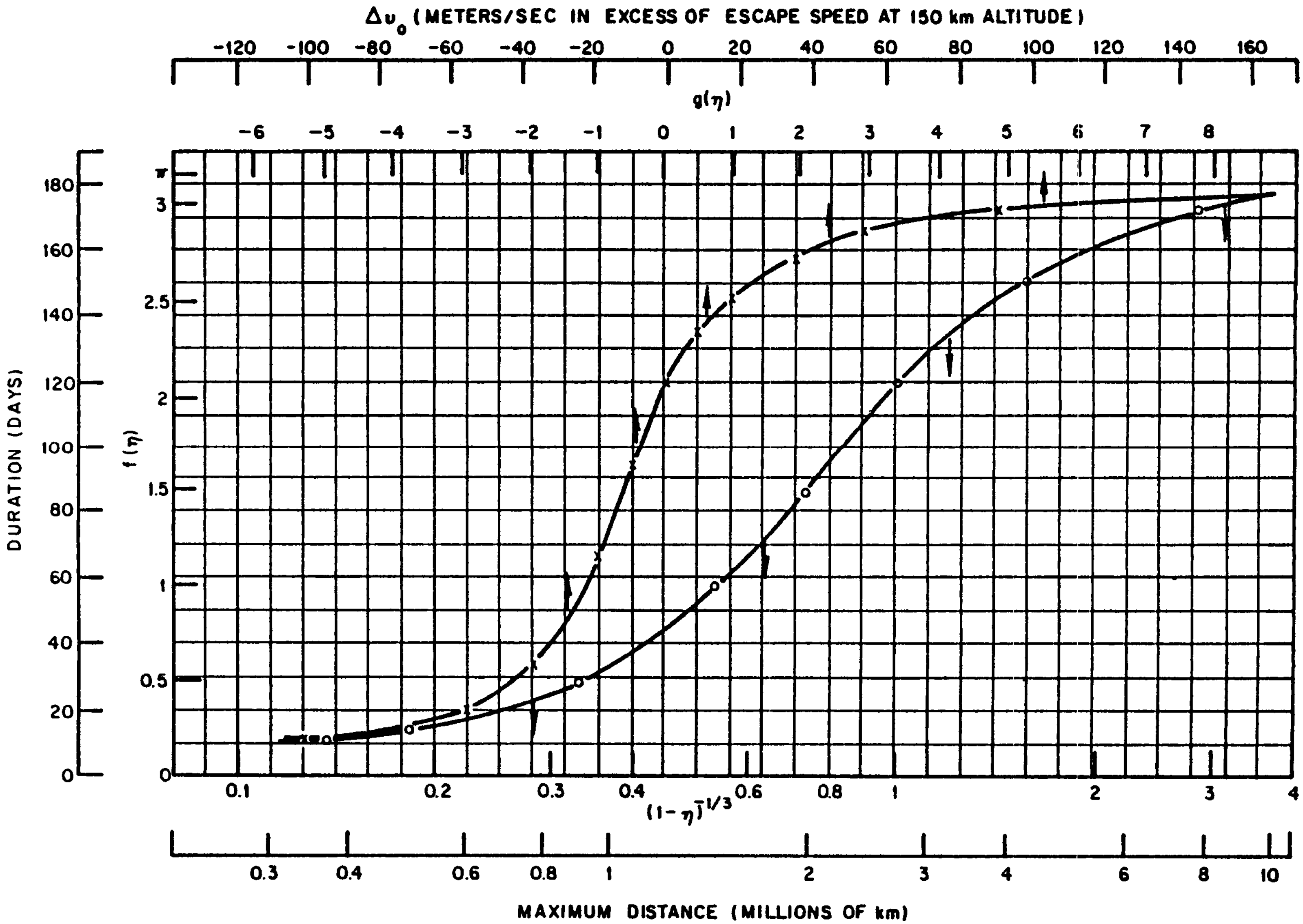

Fig. 3-2 Escape Speed Correction and Maximum Distance Versus Trip Time

Table 3-1

SCALE CHANGES FOR OTHER FLIGHTS

Large Center of Attraction	Small Center of Departure and Return	Mean Distance of Small Center from Large Center a_o (km)	Departure Radius at Altitude 150 km r_o (km)	Escape Speed ν_e (km/sec)	Correction to Escape Speed[(a)] $\Delta\nu_o$(m/sec)	Maximum Distance from Small Center[(a)] (km)	Flight Duration[(a)] (days)
Sun	Mercury	5.7×10^7	2.6×10^3	4.4	-9	3.4×10^5	23
Sun	Venus	1.08×10^8	6.2×10^3	10.8	-12	1.5×10^6	58
Sun	Earth	1.49×10^8	6.5×10^3	11.7	-9	2.1×10^6	94
Sun	Mars	2.3×10^8	3.5×10^3	5.2	-3	1.6×10^6	177
Sun	Jupiter	7.7×10^8	(b) 7.2×10^4	62.5	-16	7.7×10^7	1120
Earth	Moon	3.8×10^5	1.89×10^3	2.4	-12	8.8×10^4	7.6
Mars	(c) Phobos	9.3×10^3	(c) 8	.012	(d) -1	21	1.96 hr
Jupiter	Ganymede	1.06×10^6	2.7×10^3	2.9	(d) -400	4.7×10^3	1.84

(a) For $\eta = -1$, $g(\eta) = -\frac{1}{2}$.
(b) This is 1,100 km above estimated surface.
(c) Phobos is assumed to be a sphere of diameter 16 km and mean density equal to the Moon's; the departure radius is taken equal to the assumed radius of Phobos.
(d) In these cases $|\Delta\nu_o|$ is comparable with the escape speed ν_e so that further increases of $|\Delta\nu_o|$ with $g(\eta)$ are appreciably nonlinear, whereas $\Delta(\nu_o^2)$ remains linear in $g(\eta)$ (see derivation of Eq. (3.14) in the text).

Consider first a conic (Fig. 3-3) in the xy-plane, with semi-latus rectum ℓ , perigee in the (-y)-direction, and eccentricity ϵ close to 1 (it may be more or less than 1). Its equation is:

$$a_o\sqrt{x^2+y^2} = r = \frac{\ell}{1-\epsilon \sin\psi} = \frac{\ell}{1-\epsilon\dfrac{y}{\sqrt{x^1+y^2}}}$$

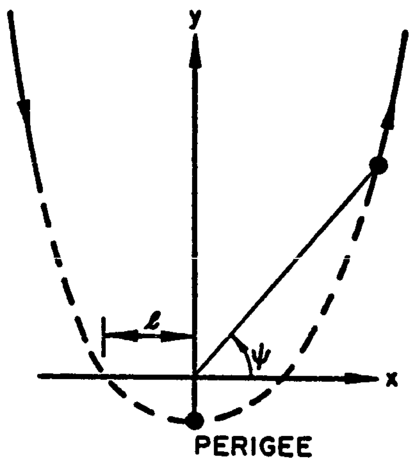

Fig. 3-3 Nearly Parabolic Conic Near the Earth

so that $\sqrt{x^2+y^2} = \epsilon y + \ell/a_o$, and hence:

$$x^2 = \left(\frac{\ell}{a_o}\right)^2 + 2\epsilon\left(\frac{\ell}{a_o}\right)y + \left(\epsilon^2-1\right)y^2 \cong \left(\frac{\ell}{a_o}\right)^2 + 2\left(\frac{\ell}{a_o}\right)y + (\epsilon^2-1)y^2$$

That part of the conic for which $x << y$, and has a $y >> \left(\frac{\ell}{a_o}\right)$ (the full line in Fig. 3-3), thus satisfies:

$$x \cong \pm y\sqrt{\epsilon^2 - 1 + \frac{2\ell}{a_o y}}$$

Furthermore, the velocity along the conic is given by

$$a_o^2\left(\dot{x}^2+\dot{y}^2\right) = v^2 = \frac{2GM_E}{r} + \frac{GM_E\left(\epsilon^2-1\right)}{\ell} = \frac{GM_E}{\ell}\left(\epsilon^2 - 1 + \frac{2\ell}{a_o\sqrt{x^2+y^2}}\right)$$

which becomes, if we neglect x^2 and $\dot{x}^2$

$$\dot{y} = \pm\frac{1}{a_o}\sqrt{\frac{GM_E}{\ell}}\sqrt{\epsilon^2 - 1 + \frac{2\ell}{a_o y}}$$

The part of the conic for which $x << y$ thus satisfies:

$$x \cong a_o \left(\frac{\ell}{GM_E}\right)^{1/2} y\,\dot{y} = \left(\frac{1}{\rho}\frac{\ell}{a_o}\right)^{1/2} y\,\frac{dy}{d\phi}$$

Note that the coefficient here of $y\,\frac{dy}{d\phi}$ is, apart from a fixed scale factor, just the angular momentum $\sqrt{GM_E\,\ell}$ of the geocentric motion.

The generalization to any nearly parabolic conic whose axis nearly coincides with the y-axis is clear; if $x,\ z << y$

$$x = \left(\frac{1}{\rho}\frac{\ell}{a_o}\right)^{1/2} \cos\alpha\ y\,\frac{dy}{d\phi} + Ay$$

$$z = \left(\frac{1}{\rho}\frac{\ell}{a_o}\right)^{1/2} \sin\alpha\ y\,\frac{dy}{d\phi} + By \tag{3.15}$$

where α is the angle which the angular momentum vector makes with the z-axis (measured toward the negative x-axis), and A, B are the (small) direction cosines of the conic's axis in the x-, z directions respectively, i.e., $(-A)$ and $(-B)$ are the x- and z- direction cosines of the conic's perigee direction.

The foregoing discussion of the motion near Earth suggests the following "variation of parameters" description of the entire motion:

$$x = Cy\frac{dy}{d\phi} + Ay \quad , \quad \frac{dx}{d\phi} = C\left[\left(\frac{dy}{d\phi}\right)^2 + y\frac{d^2y}{d\phi^2}\right] + A\frac{dy}{d\phi}$$

$$z = Dy\frac{dy}{d\phi} + By \quad , \quad \frac{dz}{d\phi} = D\left[\left(\frac{dy}{d\phi}\right)^2 + y\frac{d^2y}{d\phi^2}\right] + B\frac{dy}{d\phi} \tag{3.16}$$

where A, B, C, D are now variables which vary, however, very little in passing from launch at perigee, for example, to a near region, as in Fig. 3-3, where x, $z << y$, and where $\frac{d^2y}{d\phi^2}$ is now given by Eq. (3.7), thus including the Sun's perturbative force as well as the Earth's attraction. Note that, accordingly, the rescaled angular momentum components, $x\frac{dy}{d\phi} - y\frac{dx}{d\phi}$ and $z\frac{dy}{d\phi} - y\frac{dz}{d\phi}$, are respectively $C(\rho+y^3)$ and $D(\rho+y^3)$, which can be regarded as fixed multiples of C and D only in the near-Earth region $y << \rho^{1/3}$.

Differentiation of the left Eq. (3.16) in combination with the right equations yields:

$$\frac{dA}{d\phi} = -\frac{dy}{d\phi}\frac{dC}{d\phi} \quad \text{and} \quad \frac{dB}{d\phi} = -\frac{dy}{d\phi}\frac{dD}{d\phi} \tag{3.17}$$

Substitution of Eq. (3.16) into Eq. (3.6), together with Eqs. (3.7), (3.8), and (3.17), yields:

$$\begin{aligned} \frac{dC}{d\phi} &= \frac{y}{\rho+y^3}\left\{2\left(2E+\frac{\rho}{y}-2y^2\right)D + 2\frac{dy}{d\phi}B - 4y\frac{dy}{d\phi}C - yA\right\} \\ \frac{dD}{d\phi} &= \frac{y}{\rho+y^3}\left\{-7y\frac{dy}{d\phi}D - 4yB - 2\left(2E+\frac{\rho}{y}-2y^2\right)C - 2\frac{dy}{d\phi}A - \frac{3}{2}y^2\right\} \end{aligned} \tag{3.18}$$

A convenient renormalization of these equations is obtained by introducing, as at the end of subsection 3.3, a new independent variable:

$$s = \mp\sqrt{1-\frac{y}{y_1}} = \mp\sqrt{1-u} \quad , \text{ according as } \frac{dy}{d\phi} \gtrless 0, \tag{3.19}$$

so that s increases monotonically from -1 to +1 between the time that the vehicle leaves the vicinity of the Earth and the time of return to Earth. From Eq. (3.12) we obtain

$$\frac{ds}{d\phi} = \frac{1}{2\sqrt{u}} \sqrt{1 - \eta + u + u^2} \tag{3.20}$$

At the same time we choose the following variable small parameters:

$$\lambda_1 = \left(\frac{1-\eta}{2}\right)^{1/3} y_1 C = \left(\frac{1}{\rho}\right)^{1/6} \left(\frac{\ell}{a_o}\right)^{1/2} \cos \alpha$$

$$\lambda_2 = A$$

$$\lambda_3 = \left(\frac{1-\eta}{2}\right)^{1/3} y_1 D = \left(\frac{1}{\rho}\right)^{1/6} \left(\frac{\ell}{a_o}\right)^{1/2} \sin \alpha$$

$$\lambda_4 = B \tag{3.21}$$

Substitution of Eq. (3.21) into Eqs. (3.17)and (3.18) together with Eqs. (3.8), (3.10), (3.11), (3.19), and (3.20) yields

$$\frac{d\lambda_1}{ds} = \sqrt{u} \ \Phi_1$$

$$\frac{d\lambda_2}{ds} = \left(\frac{2}{1-\eta}\right)^{1/3} s \sqrt{1 - \eta + u + u^2} \ \Phi_1$$

$$\frac{d\lambda_3}{ds} = \sqrt{u} \ \Phi_2$$

$$\frac{d\lambda_4}{ds} = \left(\frac{2}{1-\eta}\right)^{1/3} s \sqrt{1 - \eta + u + u^2} \ \Phi_2 \tag{3.22}$$

where

$$\Phi_1 = \frac{4s\sqrt{u}}{1-\eta+2u^3}\left[4u\lambda_1 - 2\left(\frac{1-\eta}{2}\right)^{1/3}\lambda_4\right] + \frac{4}{(1-\eta+2u^3)\sqrt{1-\eta+u+u^2}}$$

$$\left[\left(1-\eta+2\eta u-4u^3\right)\lambda_3 - \left(\frac{1-\eta}{2}\right)^{1/3}u^2\lambda_2\right]$$

$$\Phi_2 = \frac{4s\sqrt{u}}{1-\eta+2u^3}\left[7u\lambda_3 - 2\left(\frac{1-\eta}{2}\right)^{1/3}\lambda_2\right] + \frac{4}{(1-\eta+2u^3)\sqrt{1-\eta+u+u^2}}$$

$$\left[\left(1-\eta+2\eta u-4u^3\right)\lambda_1 + 4\left(\frac{1-\eta}{2}\right)^{1/3}u^2\lambda_4\right]$$

$$- \frac{6\rho^{1/3}u^3}{(1-\eta+2u^3)\sqrt{1-\eta+u+u^2}} \qquad (3.23)$$

The solution of Eqs. (3.22) and (3.23), which will be obtained on a digital computer, clearly has the form:

$$\begin{pmatrix} \lambda_1(s) \\ \lambda_2(s) \\ \lambda_3(s) \\ \lambda_4(s) \end{pmatrix} = T(\eta, s)\begin{pmatrix} \lambda_1(-1) \\ \lambda_2(-1) \\ \lambda_3(-1) \\ \lambda_4(-1) \end{pmatrix} + \rho^{1/3} S(\eta, s) \qquad (3.24)$$

Where $T(\eta, s)$ is a 4×4 transition matrix, representing the propagation of initial "errors," with initial value:

$$T(\eta, -1) = \begin{pmatrix} 1 & & & 0 \\ & 1 & & \\ & & 1 & \\ 0 & & & 1 \end{pmatrix}$$

and $S(\eta, s)$ is a 4×1 matrix with initial elements all zero, representing the second-order perturbation due to the Sun [the right member of Eq. (3.6)].

As in subsection 3.3, the results will be applicable to other planetary situations, simply by a change of scale in the definition Eq. (3.20) of the angular momentum parameters λ_1 and λ_3 as well as in the coefficient $\rho^{1/3}$ of $S(\eta, s)$. In particular, the second-order Earth perturbation will probably be quite substantial in the case of trips originating and terminating near the Moon, except for low energies (large negative η).

From Eqs. (3.16) and (3.21), moreover, we can obtain a matrix transformation relating x, $\dot{x}$, z, $\dot{z}$ to λ_1, λ_2, λ_3, λ_4; say.

$$\begin{pmatrix} \lambda_1(s) \\ \lambda_2(s) \\ \lambda_3(s) \\ \lambda_4(s) \end{pmatrix} = \begin{pmatrix} N & O \\ O & N \end{pmatrix} \begin{pmatrix} x \\ \dot{x} \\ z \\ \dot{z} \end{pmatrix} \tag{3.25}$$

Where N is a 2×2 matrix, from which, in particular, the sensitivity of the terminal parameters $\lambda_i(+1)$ to small mid-course changes in off-line velocity components will be obtainable:

$$\begin{pmatrix} \delta\lambda_1(1) \\ \delta\lambda_2(1) \\ \delta\lambda_3(1) \\ \delta\lambda_4(1) \end{pmatrix} = T(\eta, 1) \left[T(\eta, s)\right]^{-1} \begin{pmatrix} N & O \\ O & N \end{pmatrix} \begin{pmatrix} 0 \\ \delta\dot{x} \\ 0 \\ \delta\dot{z} \end{pmatrix} \tag{3.26}$$

The condition for a direct collision with the Earth, of course, is just: $\lambda_1(1) = \lambda_3(1) = 0$.

The inverse of Eq. (3.25) combined with Eq. (3.24) yields the sensitivities of the instantaneous x, $\dot{x}$, z, $\dot{z}$ to changes in the initial small parameters $\lambda_i(-1)$

$$\begin{pmatrix} \delta x \\ \delta \dot{x} \\ \delta z \\ \delta \dot{z} \end{pmatrix} = \begin{pmatrix} N^{-1} & O \\ & \\ O & N^{-1} \end{pmatrix} \quad T(\eta, s) \quad \begin{pmatrix} \delta\lambda_1(-1) \\ \delta\lambda_2(-1) \\ \delta\lambda_3(-1) \\ \delta\lambda_4(-1) \end{pmatrix} \tag{3.27}$$

which, together with the sensitivities of y, $\dot{y}$ to the initial time t_o and energy parameter η, form the basis for a differential-correction of the 6 parameters t_o, η, $\lambda_1(-1)$, $\lambda_2(-1)$, $\lambda_3(-1)$, $\lambda_4(-1)$, to fit observations such as measurements of angles, ranges or range-rates.

3.5 EFFECT OF THE ECCENTRICITY ϵ_E OF THE EARTH'S ORBIT

Returning to Eq. (3.4) for the one-dimensional y-motion, with ϵ_E now included as a small parameter, let ϕ_1 be the eccentric anomaly of the Earth's position at the moment when the vehicle reaches its maximum distance y_1. Then, neglecting ϵ_E^2

$$\left(\frac{dy}{d\phi}\right)^2 = \frac{2\rho}{y} - \frac{2\rho}{y_1} - y^2 + y_1^2 - 6\epsilon_E \int_{y_1}^{y} y \cos\phi \, dy \tag{3.28}$$

in the last term of which ϕ is computed as a function of y from the "unperturbed" motion corresponding to $\epsilon_E = 0$; i.e., according to Eqs. (3.19) and (3.20)

$$\phi - \phi_1 = \int_0^s \frac{2\sqrt{u}\, ds}{\sqrt{1-\eta+u+u^2}} \tag{3.29}$$

in which $u = \frac{y}{y_1} = 1 - s^2$.

The correction in the instantaneous $\left|\frac{dy}{d\phi}\right|$ is thus given by

$$\frac{\delta\left(\left|\frac{dy}{d\phi}\right|\right)}{\left|\frac{dy}{d\phi}\right|} = \nu, \text{ say}, = 6\epsilon_E \cos\phi_1 \frac{u\int_0^s us\cos(\phi-\phi_1)\,ds}{s^2(1-\eta+u+u^2)} - 6\epsilon_E \sin\phi_1 \frac{u\int_0^s us\sin(\phi-\phi_1)\,ds}{s^2(1-\eta+u+u^2)} \tag{3.30}$$

in which $\phi - \phi_1$ is given by Eq. (3.29).

The velocity correction given by Eq. (3.30) integrates to a time correction given by

$$\delta\phi = -2\int_0^s \frac{\nu\sqrt{u}}{\sqrt{1-\eta+u+u^2}}\, ds \tag{3.31}$$

to be added to the ϕ obtainable from Eq. (3.29). The velocity and time corrections ν and $\delta\phi$ will be obtained by numerical integration along with ϕ, $T(\eta, s)$ and $S(\eta, s)$.

3.6 EFFECT OF THE MOON

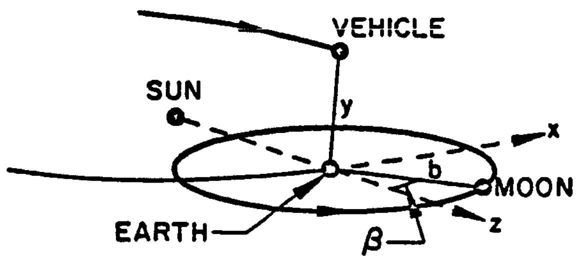

Fig. 3-4 The Presence of the Moon

Idealizing the Moon's orbit as a circle of radius b astronomical units in the x-z plane, and denoting the Moon's "phase," i.e., its angular position east of the midnight position, by β and its mass by M_M, the components of the perturbative force of the moon on the vehicle in its unperturbed one-dimensional motion, $x = z = 0$, are

$$\left.\begin{aligned} F_x^{(M)} &= \frac{GM_M b \sin\beta}{a_o^2\left(b^2+y^2\right)^{3/2}} - \frac{GM_M \sin\beta}{a_o^2 b^2} \\ F_y^{(M)} &= -\frac{GM_M y}{a_o^2\left(b^2+y^2\right)^{3/2}} \\ F_z^{(M)} &= \frac{GM_M b \cos\beta}{a_o^2\left(b^2+y^2\right)^{3/2}} - \frac{GM_M \cos\beta}{a_o^2 b^2} \end{aligned}\right\} \tag{3.32}$$

The y component contributes a term $\frac{-\rho' y}{\left[b^2 + y^2\right]^{3/2}}$ to the right-hand side of eq. (3.4), where ρ' denotes $\frac{M_M}{M_s}$, and this term integrates to an energy correction given by:

$$\delta' \left\{\left(\frac{dy}{d\phi}\right)\right\}^2 = \frac{2\rho'}{\sqrt{b^2 + y^2}} - \frac{2\rho'}{\sqrt{b^2 + y_1^2}}$$

$$= \frac{2\rho'\left(y_1^2 - y^2\right)}{\sqrt{b^2 + y^2}\sqrt{b^2 + y_1^2}\left\{\sqrt{b^2 + y^2} + \sqrt{b^2 + y_1^2}\right\}} \qquad (3.33)$$

and hence a velocity correction

$$\frac{\delta'\left(\left|\frac{dy}{d\phi}\right|\right)}{\left|\frac{dy}{d\phi}\right|} = \nu' = \frac{\rho' u(1+u)}{\left(1-\eta+u+u^2\right)\sqrt{b^2 + y_1^2}\sqrt{b^2 + y_1^2 u^2}\left\{\sqrt{b^2 + y_1^2 u^2} + \sqrt{b^2 + y_1^2}\right\}}$$

(3.34)

yielding, as in subsection 3.5, a time correction given by

$$\delta'\phi = -2\int_o^s \frac{\nu'\sqrt{u}}{\sqrt{1-\eta+u+u^2}}\, ds \qquad (3.35)$$

The x- and z- components of the Moon's perturbative force Eq. (3.32) contribute terms $\rho'\left[\frac{1}{b^2} - \frac{b}{(b^2+y^2)^{3/2}}\right]$ sin β and $\rho'\left[\frac{1}{b^2} - \frac{b}{(b^2+y^2)^{3/2}}\right]$ cos β to the right-hand sides of eq. (3.6), in which β may be replaced by $\beta_o + \frac{n_M}{n_E}(\phi - \phi_o)$, $\frac{n_M}{n_E}$ being the number of lunar months in the year. These perturbative components contribute in turn to the functions Φ_1 and Φ_2 of Eq. (3.23), by amounts:

$$\delta'\Phi_1 = \frac{4\rho^{1/3}\rho u}{y_1^2\left(1-\eta+2u^3\right)\sqrt{1-y+u+u^2}}\left[\frac{1}{b^2} - \frac{b}{\left(b^2+y_1^2u^2\right)^{3/2}}\right]\left\{\sin\beta_o \cos\left[\frac{n_M}{n_E}(\phi-\phi_o)\right]\right.$$

$$\left. + \cos\beta_o \sin\left[\frac{n_M}{n_E}(\phi-\phi_o)\right]\right\}$$

$$\delta'\Phi_2 = \frac{4\rho^{1/3}\rho' u}{y_1^2(1-\eta+2u^3)\sqrt{1-\eta+u+u^2}}\left[\frac{1}{b^2} - \frac{b}{\left(b^2+y_1^2u^2\right)^{3/2}}\right]\left\{- \sin\beta_o \sin\left[\frac{n_M}{n_E}(\phi-\phi_o)\right]\right.$$

$$\left. + \cos\beta_o \cos\left[\frac{n_M}{n_E}(\phi-\phi_o)\right]\right\} \qquad (3.36)$$

The integration of Eq. (3.22) now contributes to the right member of Eq. (3.24) additional terms $\sin\beta_o\ M_1(s) + \cos\beta_o\ M_2(s)$, where the 4×1 matrices $M_1(s)$ and $M_2(s)$ represent the effects of launch at three-quarters and full moon respectively.

In particular, the parameters at return near to earth are given by:

$$\left[\lambda_i(1)\right] = T(\eta, 1)(\lambda_i\ 1) + \rho^{1/3}S(\eta, 1) + \sin\beta_o M_1(1) + \cos\beta_o M_2(1) \qquad (3.37)$$

Assuming that $T(\eta, 1)$ does not have $+1$ as an eigenvalue (for large negative η it does not) we can determine from Eq. (3.37) those initial parameters

$\lambda_i(-1)$ which return to their original values upon return near earth. These "invariant parameters" $\lambda_i^*(\eta)$ will be given by a formula:

$$[\lambda_i^*(\eta)] \quad V_1(\eta) + \sin\beta_o \, V_2(\eta) + \cos\beta_o \, V_3(\eta) \tag{3.38}$$

where the V_i's are certain computable 4×1 matrices.

If the energy parameter η is chosen so that the trip duration is an exact multiple of the lunar month, the initial parameters $\lambda_i^*(\eta)$ will repeat over and over, neglecting the fluctuations in trip duration due to the time of year as described in subsection 3.5, provided at least that $\lambda_1^{*2} + \lambda_3^{*2}$, and hence ℓ is sufficiently large that the trajectory doesn't intersect the Earth or its appreciable atmosphere. Note that the distance of closest approach to the Earth's center is essentially $\ell/2$, since the orbital eccentricity is close to 1. Since the time of month at launch, indicated by the phase β_o, is still at our disposal, it may well be possible for an uncontrolled vehicle to return repeatedly and almost periodically (since $\epsilon_E \neq o$) to a conveniently close distance from Earth.

Section 4

PRECISE CALCULATIONS AND THE INVESTIGATION OF GUIDANCE SENSITIVITIES

4.1 INTRODUCTION

Two objectives of the Interplanetary Transportation Study contract motivated the studies and development concerning the high-accuracy interplanetary trajectory (IPT) program during the current contract period. These objectives were:

- To evaluate the accuracy of the medium-accuracy orbital transfer (MAOT) program that has been employed for the mission studies performed under this contract
- To develop the "target-seeker" techniques needed to determine the correct initial conditions on an interplanetary trajectory in order to impact the target planet

To carry out these objectives most efficiently, it was decided to incorporate that portion of the MAOT program concerned with Lambert's theorem (Ref. 4-1) into the IPT program as part of the input subroutine. The "input subroutine" is that portion of the IPT program that generates from input data specified by the trajectory analyst the starting conditions in inertial Cartesian coordinates. This incorporation greatly facilitated the generation of accurate trajectories and permitted systematic checks to be made on the accuracy of the MAOT program.

The employment of the IPT program and the development of the target-seeker technique produced a series of successive refinements to the MAOT program results leading to an accurate trajectory to the target planet. The series of steps was:

(1) A trajectory determined by the MAOT program
(2) A trajectory determined by the MAOT program, but utilizing the ephemeris routine in the IPT program to determine the positions of the initial and target planets. The IPT ephemeris routine is more accurate than the one in the MAOT program
(3) A trajectory calculated by the IPT program based on initial conditions deduced from Step (2). This trajectory misses the target planet; because of this failing, it is not truly comparable to the other three steps of this series. However, it furnishes the first estimate of the accurate trajectory for the target seeker technique
(4) The accurate direct-hit trajectory determined by the target seeker approach

4.2 COMPUTER PROGRAMS

The characteristics of the MAOT program pertinent to this study are that (1) the program contains an iterative routine for solving Kepler's equation for the heliocentric transfer orbit between the positions of the launch and target planets by use of Lambert's theorem; (2) the program contains a planetary ephemeris routine based on constant mean planetary orbital elements to determine the launch and target planets' position and velocity components; and (3) the program includes a section in which the heliocentric end-point velocities of the transfer orbit are converted to planet-centered hyperbolic excess velocity vectors described in terms of their magnitudes, right ascensions, and declinations.

The IPT program calculates ballistic space trajectories under the gravitational influence of the Sun, the major planets, and the Moon using the method of the Variation of Parameters. The principles upon which the IPT program is based are briefly described in subsection 4.6. Features of interest include: (1) An analytical planetary ephemeris routine, based on time-varying mean planetary orbital elements, with provisions to obtain accurate

planetary positions and velocities by interpolation in a table of corrections to the analytic ephemeris, (2) a subroutine to calculate the relative positions and perturbation accelerations of all the major bodies of the solar system, and (3) an input subroutine that converts input variables and coordinate systems, convenient to the trajectory analyst, to the initial conditions expressed as six components of position and velocity relative to the inertially oriented Cartesian reference system used in the program.

The partial incorporation of the MAOT into the IPT program consisted of taking over the entire Lambert portion intact, calculating in the IPT input subroutine the heliocentric positions and velocities of the launch and target planets and other required input quantities for the Lambert theorem, and converting the end-point transfer-orbit quantities to a set of initial conditions suitable for starting the IPT program integration. Two options on the type of initial conditions were made available to the program user, namely, that the injection into the ballistic interplanetary trajectory could be made from a vertical launch or from a parking orbit. Although the former is not realistic from an operational viewpoint, it greatly simplified the physical treatment of the initial phase of the study by reducing the number of variable parameters without seriously affecting the results and conclusions of the study. Accordingly, most of the high-accuracy trajectories were started from vertical launches. Another input option is that the Lambert calculations could be bypassed if the hyperbolic excess velocity magnitude and direction angles are known from previously obtained runs using the MAOT or other program. The combination of the Lambert and data input conversion subroutines produces a set of initial conditions on a trajectory, which is a good approximation to the desired trajectory. A target-seeking technique was developed to improve this approximation and achieve an impact on the target planet.

4.3 TARGET-SEEKING TECHNIQUES

The two approaches to a target-seeking procedure which have been considered are termed the "general" and the "offset-aiming" techniques. During the

current contract period only the off-set aiming technique has been developed to a useful extent; the general technique is intended to be the subject of future work. It will account for a wide variety of possible constraints on the launch and target conditions; the combinations of constrained variables will be selected as an option by the program user. A number of ways to solve this problem are being studied.

The offset-aiming technique is restricted to one special class of constraints, namely, fixed launch and arrival times. Offset aiming is an iterative technique that takes advantage of the combination of the Lambert routine and the IPT program. The procedure employed is as follows:

(1) The target and launch planets and times having been input, the Lambert routine is used to compute the initial conditions for the trajectory.

(2) An accurate interplanetary trajectory is computed and the miss-distance vector and error in time of arrival at the target planet are noted.

(3) The target planet position and the travel time are offset by the miss-distance and time of arrival errors found in step (2).

(4) The Lambert routine is reentered with the changed target quantities and another set of initial conditions is computed.

(5) The cycle from steps (2) through (4) is repeated until a trajectory resulting in a direct hit on the target planet is obtained.

In both steps (1) and (4), small adjustments are made to the nominal launch and arrival times to eliminate the nonlinear gravitational effects caused by the terminal planets. These corrections are necessary because the Lambert solution ignores these effects.

4.4 ILLUSTRATIVE EXAMPLE OF EARTH-TO-MARS TRAJECTORY

To illustrate the effects of a series of successive refinements to an interplanetary trajectory resulting from applications of the IPT program and offset aiming target seeker technique, four interplanetary trajectories were computed from Earth to Mars. For this trip, the space vehicle left Earth in a vertical launch from an arbitrary radial distance of 22.2×10^6 ft (approximately 6767 Km) at 12:00 hrs Ephemeris Time on 2 April 1969 (Julian Date 2,440,314.0) and arrived at Mars 90 days later. The four trajectories illustrate the steps in the refinement process described in the Introduction to this chapter. Their parameters have been compared in Table 4-1. Distances are expressed in AU; speeds in EMOS; time in days; and angles in degrees.

Table 4-1

TRAJECTORY COMPARISON

Parameter	Type of Trajectory			
	MAOT + Approximate Ephemeris	MAOT + Accurate Ephemeris	MAOT + Accurate Ephemeris + IPT	Target Seeker
Transfer orbit parameters				
Semi-major axis	1.641	1.656	1.668 – 1.657	1.666 – 1.655
Eccentricity	0.407	0.411	0.415 – 0.411	0.414 – 0.410
Launch parameters relative to the Sun				
Velocity	1.1797	1.1818	1.1818	1.1818
Flight path angle	7.09	6.805	6.805	6.765
Launch parameters relative to the Earth				
Hyperbolic excess speed	0.2149	0.2143	0.2143	0.2138
Right Ascension	242.11	244.16	244.16	244.18
Declination	-27.44	-27.88	-27.88	-27.89
Arrival parameters at Mars				
Distance of closest approach	0	0	3.71×10^{-4}	8.21×10^{-8}
Elapsed time from launch	90.0	90.0	90.046	90.0036

Only one iteration was needed to achieve an impact on Mars' surface from the results of the third step. Since Mars' surface radius is 2.269×10^{-5} AU, the trajectory of that step missed the center of Mars by about 16 planet radii and was about one hour late. The iterated trajectory of the fourth step hit about 12 km from Mars' center and only about 5 minutes later than the planned time of arrival.

4.5 ILLUSTRATIVE EXAMPLE OF VENUS NONSTOP ROUND-TRIP TRAJECTORY

A nonstop round-trip trajectory from Earth to Venus and return was selected as another illustrative example. The offset-aiming target seeker technique was also employed effectively in this case to combine the MAOT and IPT programs. The passage around Venus was controlled by so varying the aiming point at Venus for the Earth-to-Venus leg of the trip that the return trajectory passed near the Earth.

The timing for the trip was based on previous approximate studies made with the MAOT and round-trip computer programs. The outbound leg begins on 19 October 1970, at 0:00 hours Ephemeris Time (Julian Date 2,440,878.5) in a vertical launch from an arbitrary radial distance of 22.2×10^6 ft. The Venus transit occurs 60 days later. According to the medium-accuracy results, the return to the Earth follows 250 days after that. Table 4-2 presents a comparison between the MAOT and final IPT results. As may be seen from this table, the agreement between the results obtained from the two programs is reasonably good.

Table 4-2

VENUS ROUND-TRIP TRAJECTORY COMPARISON

Parameters	Type of Trajectory	
	MOAT	IPT
Earth departure		
Hyperbolic excess speed	0.2994	0.3043
Right ascension	211.7	212.16
Declination	-6.8	-6.69
Earth-Venus transfer		
Semi-major axis	1.03	1.032—1.040
Eccentricity	0.304	0.312—0.317
Venus transit		
Hyperbolic excess speed	0.1983	0.1966
Asymptote bend angle	67.9	66.5
Radius of perigee	4.89×10^{-5}	5.27×10^{-5}
Time in periapse, elapsed from Earth launch	60.0	60.08
Venus-Earth transfer		
Semi-Major axis	0.969	0.968—0.963
Eccentricity	0.250	0.267—0.263
Earth return		
Total elapsed time	310.0	311.6
Hyperbolic excess speed	0.2471	0.2567

4.6 INTERPLANETARY TRAJECTORY PROGRAM

The IPT program calculates the unpowered trajectory of a space vehicle of negligible mass under the influence of the gravitational forces of the nine planets, the Moon, and the Sun. The analytical technique employed by this program is the Variation of Parameters; the parameters that are varied are the instantaneous ("osculating") orbit elements. At each place in the trajectory the vehicle is treated as if it were primarily under the influence of only one of the solar system bodies; this body is called the "current dynamic center". From the initial position and velocity components, orbit elements

are calculated and the position and velocity of the vehicle at a later timepoint are computed from these elements using the equations for motion along a conic orbit. If the trajectory analyst elects to account for the perturbations caused by some or all of the other solar system bodies, the initial velocity components are modified, and these modified quantities are employed to determine the orbit elements and from these the position and velocity. Again, the velocity components are varied according to the perturbations acting at the current position and a new set of orbit elements are calculated. This is the manner in which the parameters of the trajectory, the orbit elements, are varied; they are recomputed at each new position; the new set of orbit elements is then used to continue the trajectory until the next timepoint is reached.

The cycle of position-orbit elements-position is repeated until the vehicle approaches so close to another body of the solar system that it is better to use that second body as the dynamic center. Accordingly, a shift in dynamic centers is made. The testing for the shift and its consummation is done automatically by the program. Thus, a trajectory may start with any body as dynamic center and proceed to any number of others, and even return to the original, and the trajectory program will make the proper decisions regarding the choice of new dynamic centers.

The analyst is free to specify whether he wants perturbations or not and which planets he wishes to consider. In order to compute these perturbations and to carry out dynamic center shifts, an ephemeris routine is included to define the positions and velocities of the solar system bodies. This subroutine was developed under an Air Force contract as reported in Reference 4-2. It will generate two types of information, analytic and accurate, and the analyst is free to select which type he wants for each body. The analytic data for the planets are determined from their mean time-varying orbit elements by Kepler's equations of orbital motion; for the Moon, from selected terms in Brown's theory of the Moon. The accurate data, which yield emphemeris

data as precisely as those in Reference 4-3, are obtained by adding small corrections to the analytic values.

All position, velocity, and orbital data are computed with respect to an inertially oriented Cartesian axis system whose origin is at the current dynamic center; for those planets, other than Earth, having natural satellites the origin is located at the mass center of the planet and its satellites. The axis system is oriented as follows:

X and Y	lie in the plane of the Mean Ecliptic of 1950.0
X	lies in the direction of the Vernal Equinox of 1950.0
Y	is 90° in the advance direction from X
Z	is normal to X and Y so as to form a right-hand system XYZ

The unit of distance is the "cosmonautical unit" CU , which is 0.001 AU. The unit of time is the mean solar day. For convenience a number of conversion factors are shown below. They are not claimed to be accurate to the number of digits shown. Rather, they define certain assumptions accurately and thus permit effective evaluation of any discrepancies between calculated and observed positions of space vehicles.

$$1\ \mathrm{CU} = \begin{cases} 10^{-3}\ \mathrm{AU} \\ 149{,}498.5000\ \mathrm{km} \\ 92{,}893.8747\ \mathrm{mi} \\ 80{,}722.7322\ \mathrm{nm} \\ 490{,}479{,}658.2\ \mathrm{ft} \end{cases}$$

$$\left.\begin{array}{lcl} 1\ \mathrm{AU} & = & 10^{3} \\ 1\ \mathrm{km} & = & 0.6689030325.10^{-5} \\ 1\ \mathrm{mi} & = & 0.1076497243.10^{-4} \\ 1\ \mathrm{nm} & = & 0.1238808416.10^{-4} \\ 1\ \mathrm{ft} & = & 0.2038820537.10^{-8} \end{array}\right\}\ \mathrm{CU}$$

$$1\ \mathrm{CU/day} = \begin{cases} 1.730306713\ \mathrm{km/sec} \\ 1.075160586\ \mathrm{mi/sec} \\ 3870.578111\ \mathrm{mi/hr} \\ 3363.447174\ \mathrm{nm/hr} \\ 5676.847896\ \mathrm{ft/sec} \end{cases}$$

Angles are output in degrees and decimal fractions of a degree.

Figure 4-1 is an approximate flow chart of the IPT computer program.

4.7 REFERENCES

4-1 J. V. Breakwell, R. W. Gillespie, and S. E. Ross, "Researches in Interplanetary Transfer," ARS J., Feb 1961, pp. 201-208

4-2 Lockheed Missiles and Space Division, Development of a Computer Subroutine for Planetary and Lunar Positions, by H. F. Michielsen and M. A. Krop, LMSD-311864, WADD TR 60-118, Sunnyvale, Calif., Aug 1960

4-3 The American Ephemeris and Nautical Almanac for the Year 1960, issued by the Nautical Almanac Office, U.S. Naval Observatory, United States Government Printing Office, Washington, 1958.

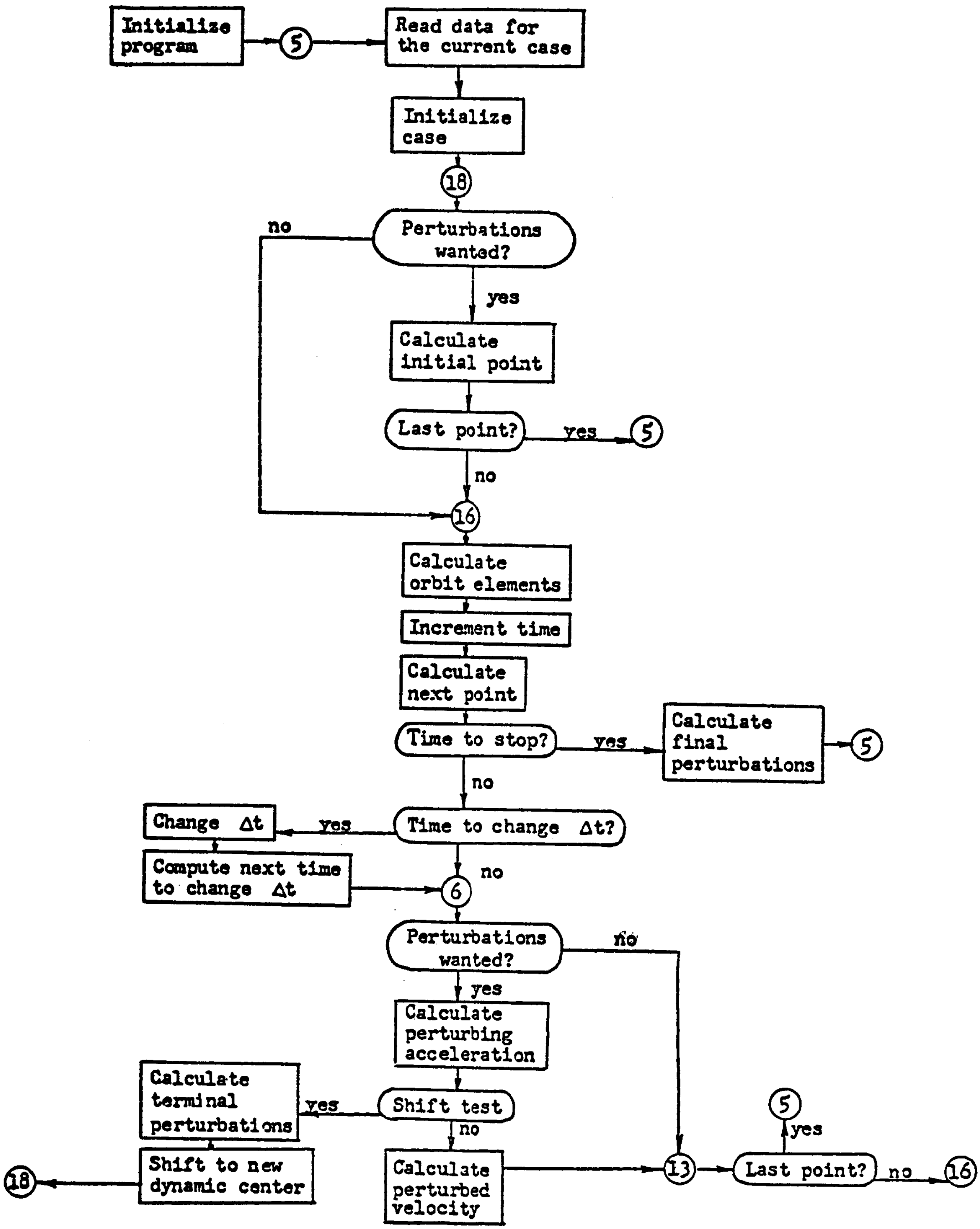

Fig. 4-1 Approximate Flow Chart for the High-Accuracy Program

Section 5

NONSTOP TRIPS PASSING BOTH MARS AND VENUS: THE INTERPLANETARY GRAND TOURS

The investigation of nonstop round trips to Mars or Venus quite naturally leads the analyst to inquire whether any orbits might be found which pass near both planets during an uninterrupted ballistic flight. Of course, any round-trip orbit whose aphelion exceeds the maximum orbital distance of Mars, and whose perihelion falls within the minimum distance of Venus is a likely candidate for such a mission, providing that the analyst is either patient enough or young enough to await the proper relative alignment of the three planets for that trip.

A somewhat more fruitful exercise, however, might involve the systematic search for all such trips which exist during any given calendar period, and the selection of those flights which show hope for execution, keeping in mind the realistic limitations of propulsion technology. At the outset, we are confronted with a paradox: Low-energy transfers to Mars seldom dip appreciably within the Earth's orbit while, on the other hand, low-energy transfers to Venus rarely stray outside the Earth's orbit. These contradictions make it painfully apparent that the trips presently sought will not likely be found among low-energy transfer orbits. Nevertheless, the problem is worth considering not only as an interesting academic pastime, but also because the velocity requirements required in some cases may actually be attainable using presently envisioned nuclear power plants.

By adopting a preliminary model for the solar system in which all planets move in coplanar circles, the relative geometry between any two planets is rendered strictly repetitive, permitting systematic generalizations of the dynamical phenomena involved. The results from this preliminary study are expected to lie reasonably close to their true values, and may be

used as first estimates in refinement procedures which later involve more realistic models for the planetary motions.

The desired orbits may be found graphically as follows: For every trip duration of reasonable length (say, 2 years or less) all ellipses which pass from Earth to Earth in the specified time may be generated, using Lambert's theorem in the manner outlined in Section 1. For the special case when the mission duration is an integral number of years, a complete family of ellipses (i. e. the nonsymmetric trips) exist for each trip time specified. All members of each such family may be found by employing the Earth-Sun-Mars angle, L, as the generating parameter, again using the technique described in Section 1.

The Earth-Mars transfer time, plus the transfer angle for each case then dictate the launch date, measured from opposition. Any three independent parameters, viz. major axis, launch date, and heliocentric flight-path angle at departure, ψ , (which has a unique correspondence with eccentricity), define the size, shape, and orientation of each Mars round trip. Similar considerations apply for Venus.

If p denotes the number of complete years in any trip, and m the number of complete orbital circuits, then for each set of flights with identical values of p and m, the angle ψ may be plotted against departure date, as in Figs. 5-1 to 5-3. By superimposing the corresponding Mars and Venus plots and aligning the conjunction and opposition marks to correspond in spacing to the calendar period of interest, points at which the two curves cross are acceptable orbits of the type sought. That is, these intersection points have associated values of major axis, eccentricity, and departure date which are identical for trips to both Mars and Venus; therefore, the orbits must be one and the same.

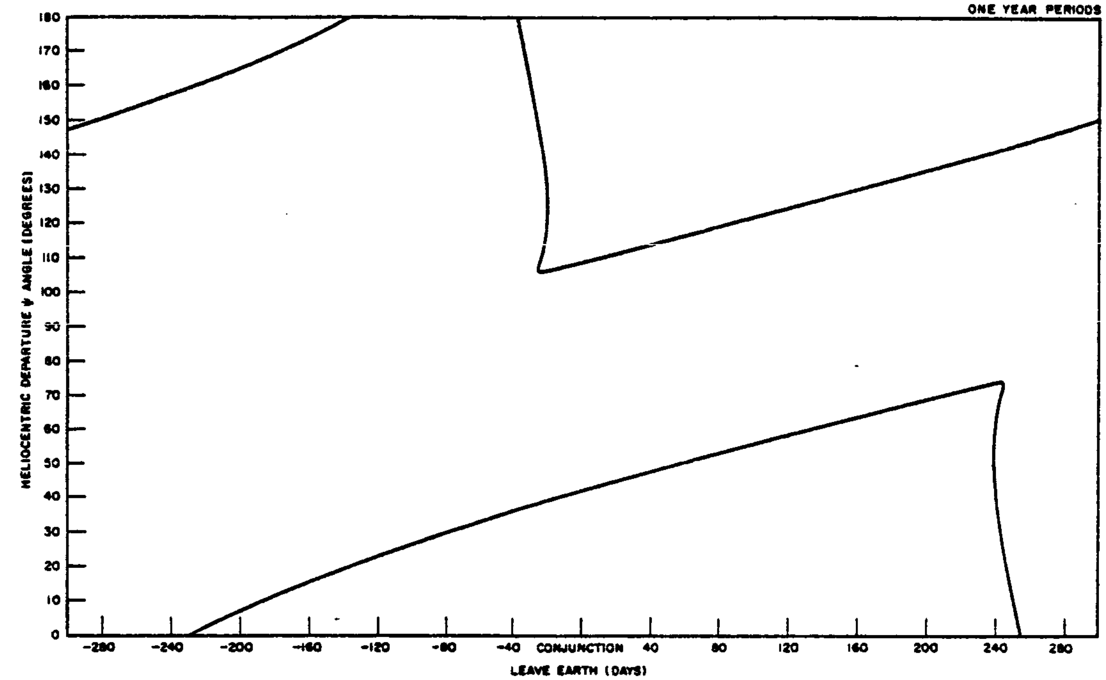

Fig. 5-1a Curves for Planning 3-Legged Nonstop Round Trips. One-year nonsymmetric curves past Venus

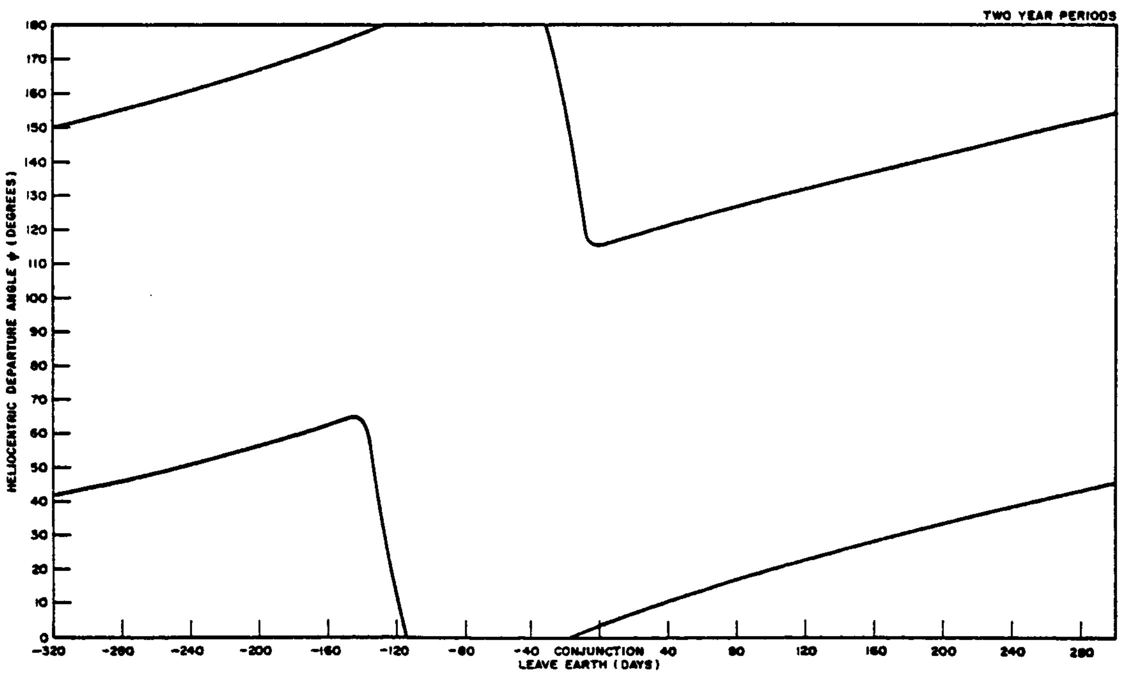

Fig. 5-1b Curves for Planning 3-Legged Nonstop Round Trips. Two-year nonsymmetric curves past Venus

Fig. 5-2a Curves for Planning 3-Legged Nonstop Round Trips. One-year nonsymmetric curves past Mars

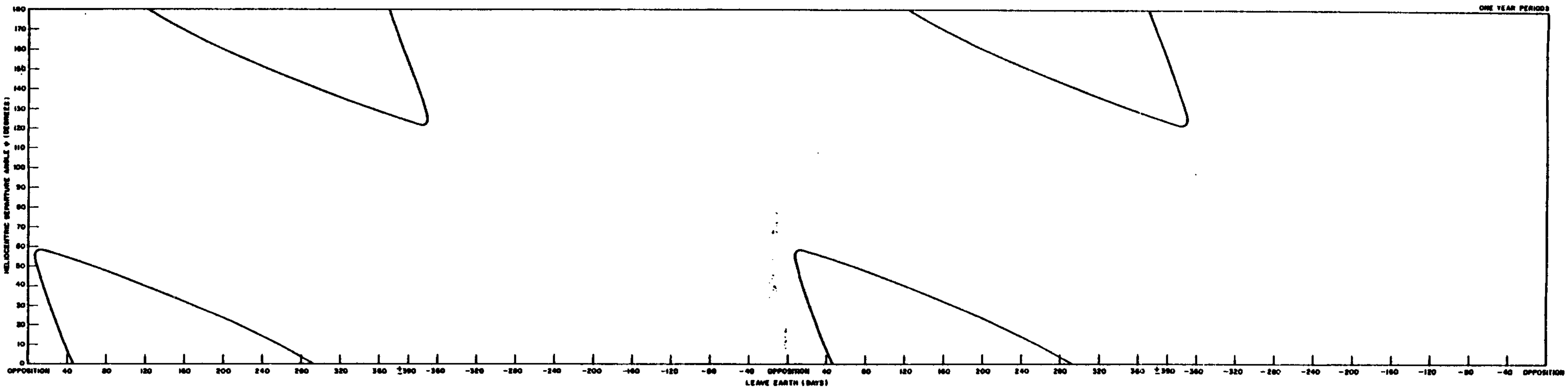

Fig. 5-2b Curves for Planning 3-Legged Nonstop Round Trips. Two-year nonsymmetric curves past Mars

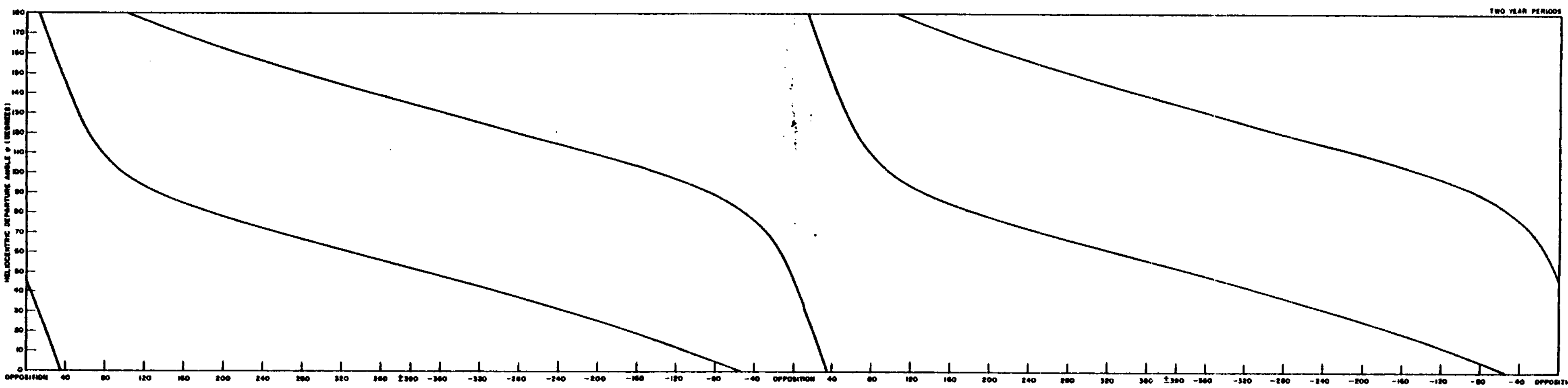

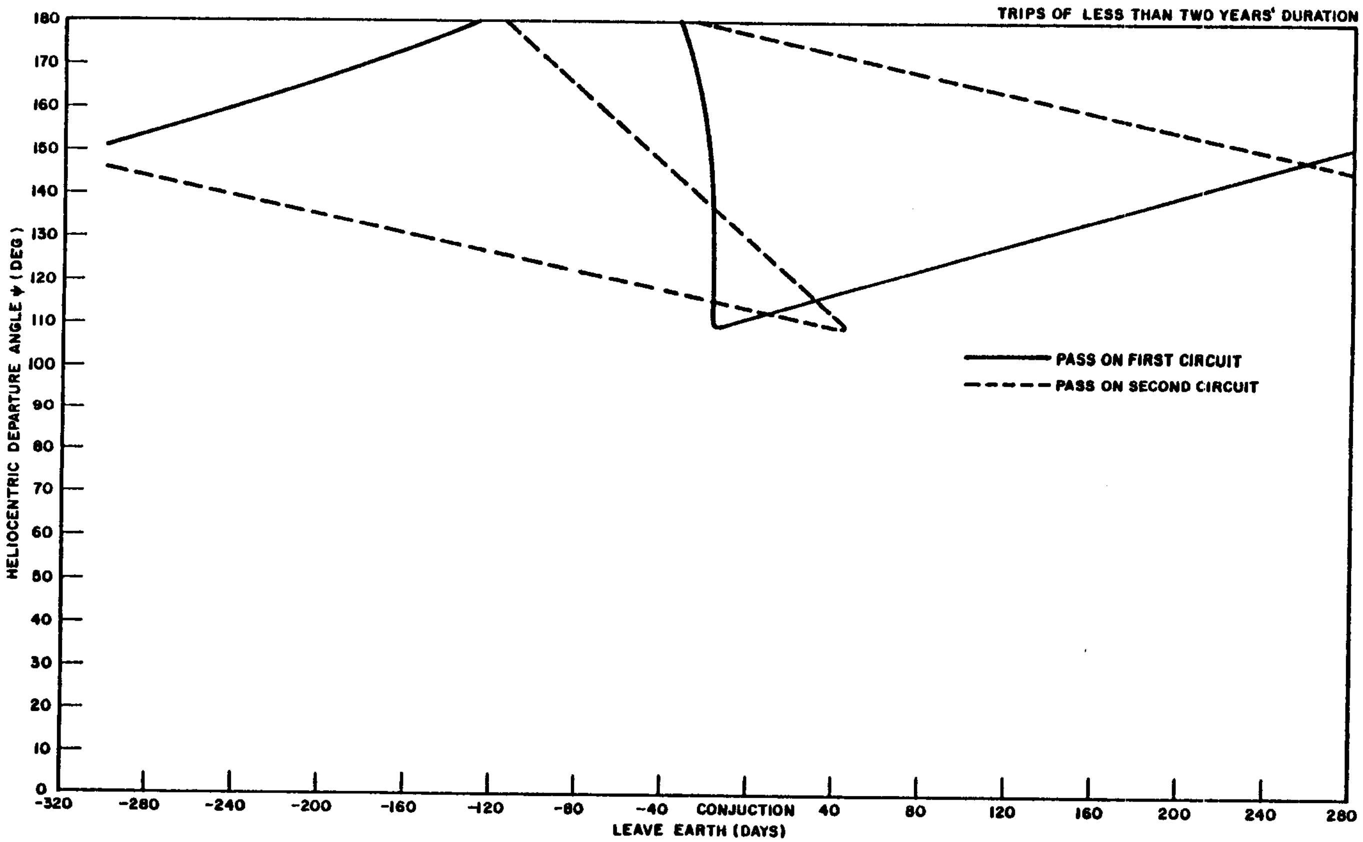

Fig. 5-3a Curves for Planning 3-Legged Nonstop Round Trips. One- to two-year symmetric trips past Venus

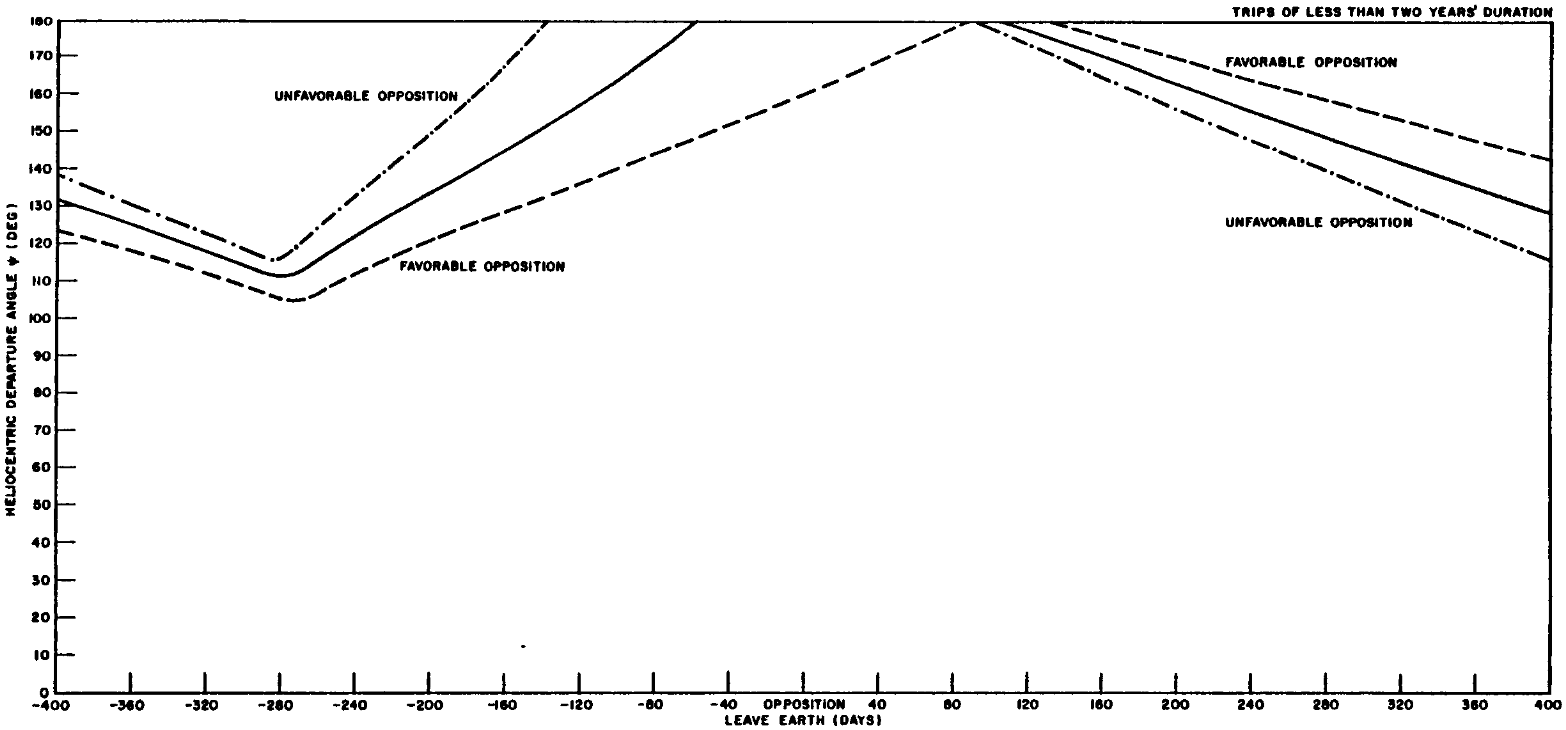

Fig. 5-3b Curves for Planning 3-Legged Nonstop Round Trips. One- to two-year symmetric trips past Mars

Figures 5-1 and 5-2 pertain to nonsymmetric orbits having periods of 1 and 2 years, respectively. Figure 5-3 pertains to symmetric trips of 1 and 2 years' duration.

Although brevity of time precluded a thorough study of these curves, the present investigation is expected to be continued and extended by refinement of promising cases, using more realistic planetary models.